USING ZEBRAFISH AS A MODEL SYSTEM FOR DYT1 DYSTONIA

by

Jonathan Sager

BS, University of Wisconsin - Oshkosh, 2006

Submitted to the Graduate Faculty of

Neurobiology in partial fulfillment

of the requirements for the degree of

Doctor of Philosophy

University of Pittsburgh

2012

UNIVERSITY OF PITTSBURGH

SCHOOL OF MEDICINE

This dissertation was presented

by

Jonathan Sager

It was defended on

June 12th, 2012

And approved by

A. Paula Monaghan-Nichols, PhD, Neurobiology

Neil A. Hukriede, PhD, Microbiology and Molecular genetics

Edward A. Burton, MD DPhil FRCP, Neurology

Laurie Ozelius, PhD, Genetics and Genomic Sciences, Mount Sinai Hospital

Committee Chair: Laura E. Lillien, PhD, Neurobiology

Dissertation Advisor: Gonzalo E. Torres, PhD, Neurobiology

USING ZEBRAFISH AS A MODEL SYSTEM FOR DYT1 DYSTONIA

Jonathan Sager

University of Pittsburgh, 2012

Dystonia is characterized by sustained involuntary muscle contractions producing repetitive twisting movements and abnormal postures. DYT1 dystonia, an early-onset primary dystonia, is caused by a trinucleotide deletion in the *TOR1A* gene, resulting in the loss of a single glutamic acid in the TorsinA protein. It is unknown how this mutation causes dysfunction of CNS motor circuits resulting in dystonia. The aims of this work were: (i) characterize the zebrafish homolog of human TOR1A in order to elucidate the functions of Torsins in vivo; (ii) generate transgenic zebrafish models of DYT1 dystonia suitable for mechanistic and drug discovery studies. An ancestral *tor1* gene found in the genomes of several fish species was duplicated at the root of the tetrapod lineage. In zebrafish, *tor1* is expressed as two isoforms with unique 5' exons. The amino acid sequences of both Torsin1 isoforms are 59% identical and 78% homologous to human TorsinA. A novel antibody was generated against Torsin1, and immunoreactivity was detected broadly in zebrafish CNS neurons. Introduction of ATP-hydrolysis abrogating mutations in the Walker B domain of Torsin1 caused a relocalization of the protein from the endoplasmic reticulum to the nuclear envelope in vitro, similar to findings with human TorsinA. Transient knockdown of tor1 expression during embryonic and early larval development did not produce a detectable cellular or behavioral phenotype, suggesting that essential functions of *tor1* occur later in development, or that compensatory functions are provided by other Torsin family proteins. Co-expression of Torsin1 and the dystonia-associated human mutant TorsinA caused Torsin1 to relocalize to the nuclear envelope, strongly suggesting that human TorsinA and

zebrafish Torsin1 interact. In view of this interaction, and the proposed dominant-negative mechanism whereby the DYT1 mutant causes clinical disease, we generated stable transgenic zebrafish in which the dystonia-related human TorsinA[ΔE] mutant was expressed in neurons of the zebrafish CNS. These transgenic animals exhibited a transient, juvenile-onset hypokinetic phenotype, beginning around one month of development and lasting for approximately one week. Future studies using these transgenic zebrafish will aim to elucidate the physiological and molecular basis of this phenotype and its relation to dystonia.

TABLE OF CONTENTS

LIST OF TABLES

LIST OF FIGURES

PREFACE

The completion of this thesis was dependent upon the contribution of time, knowledge and resources of many people, to whom I must express my gratitude. First off, many thanks is owed to both of my mentors: Edward Burton, MD DPhil, who has taught me all I know about molecular genetics and the secrets of RNA, and Gonzalo Torres, PhD, who has provided me with necessary encouragement and support. Both have been instrumental in my development as a scientist.

I would also like to thank many other scientists, including my committee members (Chair: Laura Lillien, PhD, Paula Monahan-Nichols, PhD, and Neil Hurkriede, PhD) and my external examiner (Laurie Ozelius, PhD), as well as past examination members (Cynthia Lance-Jones, PhD, Karl Kandler, PhD, and Susan Amara, PhD), who have all provided me with indispensible insights into the diversity of approach and appeal of science. A special thanks is owed to Willi Halfter, PhD, my first rotation advisor, a good man and good teacher.

Many thanks are also owed to past and present members of the Burton, Torres and Amara labs, especially Tracy Baust and Qing Bai, PhD. Without their help, this thesis would not have happened. Thanks are also due to the support staff of the CNUP, especially Patti Argenzio.

I also thank my friends, family, and Nick, for all they do.

This project would not have been possible without grants from both the Bachmann-Strauss Foundation and the Dystonia Medical Research Foundation.

1.0 INTRODUCTION

Dystonia is a group of movement disorders characterized by sustained, involuntary muscle contractions resulting in abnormal postures, repetitive and/or twisting movements (Watts and Koller, 2004). At the physiological level, these movements are the result of a decrease in reciprocal inhibition in the spinal cord, resulting in a co-contraction of agonist and antagonist muscle groups (Berardelli et al., 1998). To date, 19 different loci and 10 genes have been found to be responsible for inherited forms of dystonia (Fuchs and Ozelius, 2011), as well as several environmental factors, including brain lesions, heavy metals, and D2 dopamine receptor antagonist drugs. Although some forms of dystonia show varying degrees of symptomatic remission with current treatment, for many patients, these treatments have little to no efficacy. Because of this, there has been much interest in both understanding the diverse etiologies of dystonia, as well as developing model systems in which to discover new treatments. As a model system, zebrafish have unique advantages over other vertebrates because of their transparency during development, large clutch sizes, phylogenetic position, and genetic tractability. The aim of this thesis is to develop a zebrafish model for one of the genetic dystonias, mapped to the *DYT1* locus, which can be used for both hypothesis testing of gene function and large-scale novel compound screens.

1.1 DYSTONIA

Dystonia is a heterogeneous group of movement disorders, grouped together by the presentation of sustained, involuntary muscle contractions that result in abnormal postures, repetitive and/or twisting movements (Watts and Koller, 2004). It estimated that between 152 to 330 people per million are affected by this disorder (Nutt et al., 1988; Epidemiological Study of Dystonia in Europe (ESDE) Collaborative Group, 2000), making dystonia the third most common movement disorder, following Parkinson's disease and essential tremor. The clinical feature that distinguishes dystonia from other movement disorders is sustained and patterned involuntary muscle contractions. A common feature of these sustained movements is a co-contraction of agonist and antagonist muscle groups that are likely the result of reduced reciprocal inhibition within the spinal cord (Berardelli et al., 1998). There is large degree of heterogeneity in the severity of dystonic symptoms, ranging from focal or task-specific dystonias, such as writer's cramp or musician's dystonia, to more severe generalized dystonia, often causing disability. As a result, several key features have been used to define subclasses to aid distinguishing the dystonic state, including: age of onset (early-onset vs. adult), number of affected body parts (focal vs. generalized), and whether the dystonia manifests in the absence of other symptoms (primary vs. secondary). Although the most common form of dystonia is adult-onset, focal dystonia (Fuchs and Ozelius, 2011), the most severe is typically early-onset, which often begins as a focal dystonia and then becomes generalized to other body regions, sometimes leading to an inability to ambulate.

There is a large diversity in the etiology of different forms of dystonia, ranging from purely genetic to purely environmental factors. However, in all cases of primary dystonia, where

dystonia is the sole symptom, there is no noticeable neurodegeneration, suggesting that dystonia is the result of aberrant function or connectivity of the nervous system (Breakefield et al., 2008). Interestingly, the identification of focal lesions in secondary dystonia (where dystonia is the result of brain injury or other disease) post-mortem analysis of brain tissue has revealed that dystonic symptoms can result from injury to the basal ganglia, thalamus, brain stem, parietal lobe, or cerebellum, (Geyer and Bressman, 2006) suggesting that disruption of signaling in multiple processing nodes of motor circuits can result in dystonic symptology.

As a result of this diversity in dystonic etiologies, treatment options vary depending on subclass (Misbahuddin and Warner, 2001). However, for almost all cases of primary dystonia, treatment is based on alleviating symptoms rather than treating the cause. For patients with focal dystonia, the primary treatment is injection of botulinum toxin into the affected muscle. This treatment is less useful for patients with generalized dystonia. In generalized dystonia cases, a series of pharmacological treatments are first tried, including Levodopa, a precursor to dopamine, and trihexylphenidyl, an anticholinergic. If pharmacological treatments fail, deep brain stimulation of the globus pallidus is one of the few remaining options. The notable exception to this is dopa-responsive dystonia, named so because of the lasting and complete remission of symptoms after treatment with Levodopa. It was later discovered that the majority of these patients harbor mutations in the GCH1 gene, which encodes for the enzyme GTP cyclohydrolase. This enzyme is responsible for the production of the biopterin (BH4) cofactor, which is necessary for the rate-limiting enzyme (tyrosine hydroxylase) of dopamine synthesis.

1.1.1 Genetics of dystonia

Currently, there are 19 different presumed loci that have been identified as inherited dystonia, which have been given the prefix "DYT" (Fuchs and Ozelius, 2011). Although many of these loci have been mapped to chromosomal regions, two DYT loci (DYT2 and DYT4) are solely based on inheritance of the dystonic phenotype. The majority of genetic dystonias are inherited as autosomal dominant traits, often with reduced penetrance. Exceptions to this include DYT2, DYT17, and DYT16, which are inherited as an autosomal recessive trait, and DYT3, which is inherited as an X-linked recessive trait (Fuchs and Ozelius, 2011). Resolving these loci to the level of specific genes has been one of the first steps taken in understanding dystonia.

To date, mutations in 10 different genes have been identified as causing dystonia. Despite identification of dystonia-causing mutations, a clear mechanism of how these mutations result in dystonia has remained elusive. Mutations have been identified in genes encoding many different types of proteins, including transcription factors (THAP1 and TAF1) (Fuchs et al., 2009), ion pumps (ATP1A3) (Cannon, 2004), glucose transporters (SLC2A1) (Suls et al., 2008), protein kinases (PRKRA) (Camargos et al., 2008) as well as several proteins with unknown fuctions (TOR1A, SCGE, MR-1, and PRRT2) (Ozelius et al., 1997; Lee et al., 2004; Rainier et al., 2004; Makino et al., 2007; Kinugawa et al., 2009). Recently, it has been found that THAP1 acts as a repressor of TOR1A expression (Gavarini et al., 2010; Kaiser et al., 2010), suggesting a potential genetic convergence of disease mechanism, however, the variety of proteins identified has made the search for a common denominator for genetic dystonias more complicated.

1.1.2 DYT1 Dystonia

The most common and severe form of early onset, generalized dystonia is DYT1 dystonia, which has been mapped to mutations in the TOR1A gene (Ozelius et al., 1997). It is inherited as an autosomal dominant trait, although the dystonic phenotype has a reduced penetrance of 30-40% (Kramer et al., 1994). Typically, DYT1 dystonia manifests during adolesence (mean age = 13, range = 3-64) and begins in a single limb (Ozelius and Bressman, 2011). Over the next 2-5 years, the dystonic symptoms typically generalize to other body regions, though rarely affecting cranial muscles, after which the disease state stabilizes and persists throughout the patient's life. Interestingly, a correlation between age of onset and affected limbs has been noted; patients developing dystonia at younger ages are more likely to have symptoms start in the legs and generalize to the arms and trunk, whereas patients developing symptoms at older ages are more likely to have symptoms start in the arms, and experience less generalization of the dystonic symptoms (Breakefield et al., 2008).

1.1.3 TorsinA

The majority of DYT1 dystonia cases are caused by an in-frame, tri-nucleotide (GAG) deletion in exon 5 of the TOR1A gene, resulting in the loss of a single glutamic acid (ΔE) near the carboxyl terminus of the TorsinA protein (Ozelius et al., 1997). Three other mutations have been associated with DYT1 dystonia, including an 18 base pair deletion (Δ323-8) (Leung et al., 2001), identified in a single family, and two missense mutation, R288Q (Zirn et al., 2008) and F205I (Calakos et al., 2010), each identified in a single patient.

TorsinA is a member of the AAA^+ family of proteins (ATPase associated with various cellular activities), and is part of the Torsin family, found only in metazoan animals, with a total of four members in the vertebrate lineage (Breakefield et al., 2001). Members of the AAA+ family have roles in a diverse array of cellular functions (Hanson and Whiteheart, 2005), and *in vitro* studies have implicated human TorsinA in numerous cellular processes including cytoskeletal dynamics (Hewett et al., 2006), synaptic vesicle cycling and the secretory pathway (Torres et al., 2004; Hewett et al., 2007). TorsinA is expressed in a wide variety of cell types (Augood et al., 1998) and is found to predominately colocalize with markers for the endoplasmic reticulum (ER) (Hewett et al., 2000). Mutant TorsinA[ΔE] shows aberrant cellular localization, being redistributed from the ER to the nuclear envelope (NE) (Goodchild and Dauer, 2004), and in some cell lines, also forming membranous whorls (Hewett et al., 2000). Similar to mutant TorsinA[ΔE], disruption of the Walker B ATP hydrolysis domain of TorsinA by mutagenesis also caused relocalization to the NE (Goodchild and Dauer, 2004; Torres et al., 2004). Because comparable Walker B null mutations in other AAA+ family members exhibit a stabilization of substrate interactions (Babst, 1998; Weibezahn, 2003), the similar redistribution of TorsinA by Walker B and ΔE mutations led to the hypothesis that both mutations stabilize an interaction between TorsinA and a NE resident protein (Naismith et al., 2004). However, accumulating data suggest that the Walker B and ΔE mutants may not be mechanistically equivalent; differences in membranous whorl formation (Naismith et al., 2004) and the strength of co-immunoprecipiation with two NE substrate have been observed between Walker B and ΔE mutant TorsinA (Naismith et al., 2009).

TorsinA has been shown to interact with a variety of proteins including kinesin light chain 1 (Kamm et al., 2004), Snapin (Granata et al., 2008), lamina-associated polypeptide 1

(LAP1) (Goodchild and Dauer, 2005), luminal domain like LAP1 (LULL1) (Goodchild and Dauer, 2005), Printor (Giles et al., 2009), and Vimentin (Hewett et al., 2006). The relevance of these interactions to DYT1 dystonia, however, is unknown; given the variety of neuronal and somatic cell types that express TorsinA, it is difficult to translate protein-protein interactions, in tissue lysates, into disease causing mechanisms.

1.1.4 Animal models of DYT1 dystonia

Although in vitro studies have started to elucidate the cellular functions of Torsins, the mechanisms by which mutant TorsinA[ΔE] causes dystonia are not understood. Despite the dramatic clinical abnormalities, brain tissue from DYT1 dystonia patients is pathologically unaltered at autopsy, suggesting aberrant connectivity and/or activity of neural circuits might be the physiological cause of dystonia (Breakefield et al., 2008). Consequently, there has been significant interest in generating model systems to gain insights into the functions of TorsinA in neurons and motor circuits *in vivo*. In *C. elegans*, mutations in the Torsin-related *ooc-5* gene disrupted spindle orientation and PAR protein polarity at the 2-cell stage of development, thereby preventing asymmetric divisions and cell fate determination (Basham and Rose, 1999). Knockdown of the sole *D. melanogastor* Torsin family member, *dtorsin*, in the retina by RNA interference altered the cellular organization of pigment granules, suggesting a role in intracellular transport (Muraro and Moffat, 2006). Generation of a null *dtorsin* allele suggested that *dtorsin* may act as a postive-regulator of GTP cyclohydrolase, an enzyme important in the production of BH4, a limiting cofactor in dopamine synthesis (Noriko Wakabayashi-Ito, 2011).

In mice, multiple strategies have been employed to generate a transgenic model of dystonia, and while these models have yielded insights into the neuronal mechanisms perturbed

by expression of TorsinA[ΔE], none of these models exhibit overt dystonia (Dang et al., 2005; Goodchild et al., 2005; Sharma et al., 2005; Shashidharan et al., 2005; Grundmann et al., 2007; Yokoi et al., 2007; Page et al., 2010). The first attempts to model DYT1 dystonia in mice used overexpression of the human TorsinA[ΔE] protein as a strategy. The most characterized of these mouse models is the transgenic line overexpressing TorsinA[ΔE] under control of the CMV promoter. These animals preformed similarly to wildtype animals on intial rotarod trials, but fell off more quickly than non-transgenic littermates and animals overexpression wildtype TorsinA in subsequent trials, suggesting an impairment in motor learning (Sharma et al., 2005). Although no changes in subcellular localization between the human wildtype and TorsinA[ΔE] were observed in any brain regions, and the nuclear envelope morphological appeared normal, small increases were observed in striatal DOPAC, HVA, and epinephrine mice in this line (Zhao et al., 2008). Despite no differences in dopamine at basal levels, a reduced release of dopamine was observed in response to amphetamine (Balcioglu et al., 2007). In line with this observation, mice overexpressing TorsinA[ΔE] also showed a decreased locomoter response to amphetamine (Hewett et al., 2010). Similar deficits were observed in transgenic mice overexpressing TorsinA[ΔE] under the control of the *th* promoter, suggesting that these deficits can be caused by changes in dopaminergic signaling in the striatum (Page et al., 2010).

A mouse model generated by knocking in the ΔGAG mutation into the endogenous mouse *tor1a* caused mice to slip more often on the beam walking test (Dang et al., 2005). These mice were also hyperactive when examined in the open-field analysis, although only male transgenics showed significantly more beam breaks and total distance traveled when compared to wildtype mice. No differences were observed in open-field, light-dark, tail suspension or forced swim tests, and no differences were detected in prepulse inhibition (Yokoi et al., 2009).

However, these animals made significantly fewer entries into the open arms of the elevated-plus maze test, and increased freezing in response to the cue, but not the context, following fear conditioning. An increased number of c-fos positive neurons were observed in the central nucleus of the amygdala. A decrease in striatal HVA, observed by HPLC, was also noted in this line. Similarly, transgenic knockdown of the mouse *tor1a* gene also caused an increase in beam slips and hyperactivity specifically in male animals (Dang et al., 2006). Aggregrates of TorsinA were found in the pontine nuclei, but not the cortex or midbrain regions, specifically in male transgenics.

Inactivation of the endogenous murine *tor1a* by homologous recombination caused perinatal lethality, despite the absence of overt developmental morphological abnormalities (Goodchild et al., 2005). Interestingly, both knockout and homozygous ΔGAG knockin resulted in perinatal lethality due to lack of feeding(Goodchild et al., 2005). No changes in the gross morphology of the animals or their brains were detected. However, transmission electron micrographs of post-mitotic neurons in the spinal cord and cortex showed altered nuclear envelope morphology and the presence of luminal vesicles that most likely formed from the inner nuclear membrane. Interestingly, this was not observed in migrating neurons or other cell types of the body, including glia. Conditional knock-out of the *tor1a* gene in the cortex, generated by crossing *tor1a loxP* mice to *Emx1-cre* knockin mice, did not result in perinatal lethality (Yokoi et al., 2007). Behaviorally, these mice exhibit similarities to TorsinA[ΔE] overexpressing mice: hyperactivity in an open field and an increased number of beam slips on a rotorod.

Recently, a transgenic rat model of DYT1 dystoia, generated by expressing the human TOR1A gene, either with or without the ΔGAG deletion, with a potential promoter and all

intronic regions, identified similar phenotypic abnormalities (Grundmann et al., 2012). In this model, TorsinA[ΔE] showed a strong redistribution to the nuclear envelope in neurons of several brain regions, including the cortex, hippocampus, striatum, olfactory bulb, and substaina nigra, although this was not detected in the brainstem or cerebellum. Behaviorally, transgenic rats overexpressing TorsinA[ΔE] were significantly more likely to fall during the first three days of rotorod training, exhibited irregularities in gait, and a similar hind limb clasping phenotype, seen in several of the mouse models, which worsened during the first year.

1.2 ZEBRAFISH

Since the initial introduction of the zebrafish as a model organism for the study of vertebrate development, an impressive toolbox of experimental techniques for their experimental manipulation and analysis has been developed. Zebrafish embryos develop externally and are optically transparent, allowing direct observation of development and the deployment of fluorescent reporters and indicators to visualize morphology and physiology of cell groups of interest. Transgenic expression of exogenous genes, and experimental knockdown of endogenous genes, can be carried out using relatively straightforward techniques. Zebrafish breed regularly, produce large clutches of offspring and can be housed in large numbers allowing for large-scale genetic and chemical screens. By exploiting these favorable properties, the zebrafish model has proved a useful means to test hypotheses concerning gene function in development, and has provided numerous novel insights into the molecular basis of embryogenesis through large-scale genetics screens (Solnica-Krezel et al., 1994; Brockerhoff et al., 1995; Driever et al., 1996; Malicki et al., 1996; Amsterdam et al., 1999; Guo et al., 1999).

More recently, in vivo chemical modifier screens have been carried out in order to identify new compounds that act specifically on biological pathways of interest (Zon and Peterson, 2005; Molina et al., 2009). The ability to house zebrafish larvae in 96-well plates and the use of automated assay end points make the zebrafish uniquely suitable, amongst current vertebrate models, for high throughput chemical library screening in vivo.

1.2.1 Zebrafish as a model for neurological disorders

Zebrafish models of neurological disorders will be useful for understanding human diseases only if the mechanisms underlying pathogenesis are sufficiently phylogenetically conserved that insights gained in zebrafish models can be applied to the human conditions. There is no way of knowing *a priori* that this will be the case. However, a variety of convergent lines of evidence suggest that aspects of the zebrafish CNS, pertinent to human diseases, are conserved with respect to human, offering some support to the prediction that observations made in zebrafish models will be clinically applicable. The following sections with discuss the degree to which the molecular, cellular and tissue environment of the zebrafish brain mirrors that of the human, particularly with respect to systems potentially involved in dystonia.

1.2.2 Zebrafish neuroanatomy

The zebrafish CNS is organized similarly to that of other vertebrates, and is conventionally divided into the spinal cord, hindbrain, midbrain and forebrain (Kimmel, 1993; Wullimann et al., 1996). In terms of gross morphology, there are significant differences in scale and complexity between the human and zebrafish brain, and the identification of homologous brain regions has

been complicated by both eversion of the developing telencephalon (in contrast to the evagination seen in mammals) and the smaller less well-developed nature of the zebrafish forebrain in comparison with other brain regions. Despite these differences, several regions of the zebrafish CNS, such as the medulla, hypothalamus, optic tracts and tectum, olfactory system, spinal cord and cranial nerves show easily recognizable structural homology to the relevant areas of the human brain. However, with relevance to modeling dystonia, it should be stressed that key areas of the CNS show remarkably conserved structure to their human counterparts, including the basal ganglia, spinal cord and cerebellum.

Similar to human cerebellar cortex, the zebrafish cerebellum has molecular, Purkinje cell and granule cell layers; cell types present in the each of these laminae are similar to those found in the human brain, show similar inputs and synaptic connections, and express similar genes and specialized markers (Bae et al., 2009). The main difference between zebrafish and mammalian cerebellum is that cell bodies of output projection neurons in the zebrafish cerebellum (eurydendroid cells) are located in the cortex rather than the deep nuclei found in mammals.

Areas of the zebrafish telencephalon that are thought homologous to regions of the basal ganglia involved in human motor dysfunction have been identified through studies of gene expression, neurochemistry and axonal projections (Rink and Wullimann, 2001; Wullimann and Rink, 2002; Rink and Wullimann, 2004). The dorsal nucleus of the ventral telencephalic area, arising from the embryonic subpallium, is thought to be the zebrafish homologue of the mammalian striatum (Rink and Wullimann, 2004). Similar to the projection neurons of the mammalian striatum, neurons of the fish ventral telencephalic area are GABAergic, and cells in the region express substance P (Sharma et al., 1989), enkephalin (Reiner and Northcutt, 1992), and D1 (Kapsimali et al., 2000) and D2 (Boehmler et al., 2004) dopamine receptors in a variety

of different fish species. Furthermore, this area is rich in dopaminergic nerve terminals, derived from a major ascending dopaminergic projection, further corroborating the proposed homology of the region to the striatum. Another division of the dorsal telencephalon is proposed to be homologous to the nucleus basalis of Meynert, on account of prominent choline acetyltransferase-expressing neurons and projections to the dorsal telencephalic area (Mueller et al., 2004; Rink and Wullimann, 2004).

The dopaminergic system of zebrafish has been of significant interest to the development of models of human movement disorders, and is important to the study of dystonia as at least one form, dopa-responsive dystonia, has been clearly linked to dysfunction of the dopamine system. The zebrafish brain contains increasingly well-characterized groups of dopaminergic neurons, located in the olfactory bulbs, telencephalon, pretectal area and ventral diencephalon (Rink and Wullimann, 2002; Ma, 2003; Ryu et al., 2006). Much of the current understanding of the anatomy of the zebrafish dopaminergic system is based on expression patterns of tyrosine hydroxylase (the enzyme catalyzing the rate-limiting step in dopamine biosynthesis). The recent discovery of a gene duplication event in the zebrafish resulted in two separate *th* genes (Candy and Collet, 2005) with different expression patterns (Chen et al., 2009) may necessitate amending the current picture, since it is unclear at present which of the commonly used TH antibodies recognizes one or both isoenzymes and whether a divergence or subfractionalization of function has occurred between these two paralogs. Regardless, one of the diencephalic groups of TH-immunoreactive neurons, located in the posterior tuberculum of the hypothalamus, sends axonal projections that terminate in the dorsal telencephalic area. This is thought to be the zebrafish homologue of the mammalian nigrostriatal tract (Rink and Wullimann, 2001).

Similar to the situation in mammals, dopaminergic function is important in the regulation of locomotor behavior in zebrafish. Lesions of the dopaminergic system, induced by exposure to the dopamine neuron-specific toxin MPP^+ are associated with reduction in spontaneous movement of zebrafish larvae (Bretaud et al., 2004; Lam et al., 2005; McKinley et al., 2005; Sallinen et al., 2009b; Farrell et al., 2011). Similarly, exposure to agents that antagonize the actions of dopamine at its receptors also leads to decreased spontaneous larval movement (Giacomini et al., 2006; Boehmler et al., 2007; Farrell et al., 2011). In addition, dopamine function is important in the regulation of adult spontaneous movement. Although systemic exposure to MPTP or 6-OHDA did not seem to produce robust loss of dopamine neurons in the adult zebrafish posterior tuberculum, significant losses of dopamine and noradrenaline were noted, along with a reduction in mean velocity and increase in turn angles during spontaneous swimming (Anichtchik et al., 2004). Interestingly, dopamine also seems to modulate the development of motor behavior during embryogenesis; at 3 days post-fertilization, forebrain dopaminergic function inhibits swimming movements, but this response is lost by 5 days post-fertilization (Thirumalai and Cline, 2008). This is the opposite effect to that observed in older animals following manipulation of dopaminergic signaling and the mechanisms are not yet certain. However, this observation raises the possibility that functional abnormalities of dopaminergic neurotransmission provoked in transgenic models of motor disorders may manifest in unexpected ways if the models are evaluated very early during development. It is also recognized that manipulation of other neurotransmitter systems of relevance to human disease can modulate the spontaneous locomotor behavior of larval zebrafish. For example, recent work has shown that inhibition of monoamine oxidase B in larvae resulted in elevated levels of serotonin, but not of other monoamine neurotransmitters, accompanied by dose-dependent

reductions in movement of 7-day old larval zebrafish (Sallinen et al., 2009a). This is compatible with earlier studies showing that serotonin-specific reuptake inhibitors impair locomotor activity in zebrafish (Airhart et al., 2007) and that serotonin stimulates swimming behavior in larval zebrafish (Brustein et al., 2003).

One striking difference between mammalian and zebrafish brain is that the zebrafish CNS undergoes continued growth and acquisition of new neurons throughout life, and shows impressive capacity for regeneration of axons and neurons following focal lesions (Becker and Becker, 2008). The ability of zebrafish CNS to reform functional neural circuits after injury to fiber tracts is dependent both on properties of neurons that favor axonal re-growth, and also on the CNS environment, in which glia promote axonal growth and pathfinding, in contrast to the mammalian CNS, which presents an inhibitory environment to axonal regeneration. It is unclear at present whether this capacity for ongoing growth and repair will hamper attempts at modeling neurological diseases, although the first reports suggest that this is not the case (see below).

1.2.3 Phylogenetic conservation of genes implicated in human neurological disorders

Overall, there is significant genetic similarity between zebrafish and other vertebrates, including mammals. The degree of phylogenetic conservation is perhaps most prominent in pathways governing basic aspects of cellular homeostasis. Many of the genes known to cause hereditary neurological disease have highly conserved homologues in the zebrafish. The striking degree of phylogenetic conservation suggests the relevant cellular processes are of fundamental importance to the health and function of neurons and glia throughout vertebrate evolution.

A common method to study the function of endogenous zebrafish genes has been the use of chemically modified morpholino antisense oligonucleotides, which can be designed to target

either translation of a specific mRNA transcript, or prevent splicing of the relevant pre-mRNA, through complementarity to the sequence surrounding the translational initiation codon or splice signals (Nasevicius and Ekker, 2000). Morpholino oligonucleotides are stable *in vivo*, diffuse throughout embryos following microinjection and allow graded suppression of gene expression during the first few days after fertilization.

Not including this thesis, two zebrafish homologs to human dystonia-related genes have been identified: *glut1* (*slc2a1*) (Jensen et al., 2006; Zheng et al., 2010; 2012) and *atp1a3* (Sun et al., 2012). At the amino acid level, zebrafish Glut1 is 74% homologous to the human protein. Knockdown of *glut1* in zebrafish was leathal by 4dpf, and beginning around 2dpf, the developing nervous system showed enlarged ventricles, loss of the midbrain/hindbrain boundary, and an increase in apoptotic cell death (Jensen et al., 2006). Interestingly, overexpression of the human *GLUT1* in the morphant larvae rescued these phenotypes, demonstrating a conservation of gene function between humans and zebrafish. Further analysis revealed that knockdown of *glut1* resulted in a loss of cerebral endothelial cells and a downregulation of adherens and tight junctions in the developing blood brain barrier (Zheng et al., 2010). Due to the early effects of *glut1* knockdown, it remains unknown if mutations associated with DYT18 dystonia, linked to mutations in *GLUT1* (Suls et al., 2008), would provoke a similar phenotype to humans.

During a small molecule screen of >5,000 compounds, the zebrafish ATP1A3 protein was identified as being important in dopamine neuron survival (Sun et al., 2012). In this screen, a cardiac glycoside, Neriifolin, at low concentrations, was found to specifically influence the survival of dopamine neurons in the ventral forebrain. The zebrafish *atp1a3* gene was found to be strongly expressed in this group of cells. To determine the involvement of *atp1a3* in dopamine neuron survival, the researchers overexpressed a mutated human version of *ATP1A3*

that is largely resistant to the effects of cardiac glycosides. In larvae overexpressing this human version of *ATP1A3*, Neriifolin did not induce death of dopamine neurons, suggesting that the endogenous zebrafish *atp1a3* is not only the site of action for Neriifolin, but also that *atp1a3* plays an important role in the survival of dopamine neurons. Interestingly, this form of dystonia is often accompanied with parkinsonism-like symptoms, and a role for *atp1a3* in dopamine neuron survival may provide a potential mechanism for the presentation of these symptoms.

The presence of conserved zebrafish homologues of genes involved in human neurodegeneration suggests that it might be possible to provoke neuronal dysfunction or loss through cellular mechanisms similar to those involved in the pathogenesis of human diseases, supporting the notion that zebrafish might be an appropriate model in which to study the functions of the genes and the pathophysiology of the disorders. Several orthologues of genes involved in Parkinsonism, Alzheimer's disease and Huntington's disease have been identified in zebrafish, including *dj-1* (Bai et al., 2006), *parkin* (Flinn et al., 2009) and *pink1* (Anichtchik et al., 2008). Further review of the homology and function of these genes in zebrafish can be found in Sager et al., 2010.

Together, these studies provide evidence of phylogenetic conservation of selected aspects of structure and function of key brain regions, cell types, genes, proteins and biochemical pathways involved in neurodegeneration in humans. These observations support the argument that mechanisms relevant to neurological disease in humans may be conserved sufficiently to allow appropriate and relevant mechanistic insights be gained into human diseases, through construction and study of zebrafish models.

1.2.4 Zebrafish models of neurological disease

Recent publications have described the first proof-of-principle experiments showing that transgenic expression of genes triggering neurological disease in humans can provoke relevant phenotypes in zebrafish. Although there no current zebrafish models for dystonia outside of this thesis, several models of human Tauopathies, polyglutamine disorders and motor neuron disease have recently been published.

1.2.4.1 Tauopathy models

Abnormal forms of the microtubule associated protein Tau are deposited in neurofibrillary tangles in a number of sporadic human neurodegenerative diseases, including Alzheimer's disease, progressive supranuclear palsy and Pick's disease (Lee et al., 2001). In the adult human brain, the pre-mRNA from the *MAPT* gene encoding Tau is alternatively spliced, giving rise to six protein isoforms that contain either 3 or 4 microtubule binding domains (Goedert et al., 1989). In AD, neurofibrillary tangles contain 3- and 4-reapeat Tau, whereas 4-repeat Tau predominates in the tangles of PSP, and 3-repeat Tau in Pick's disease (Lee et al., 2001). In the majority of cases of these diseases, no abnormality has been identified in the *MAPT* gene. However, some cases of fronto-temporal dementia and parkinsonism, are caused by *MAPT* mutations that alter the primary sequence of Tau or the ratio of 3- to 4-repeat isoforms (Hutton et al., 1998). Since individual FTDP17 cases may show clinical and pathological similarity to PSP or Pick's disease, it is thought that abnormalities of Tau metabolism may be central to the pathogenesis of the sporadic diseases.

Given the proposed central role of Tau in a number of important neurodegenerative conditions, there has been interest in the construction of zebrafish Tauopathy models. The first publication reported a transient model, in which a Tau-GFP fusion protein was over-expressed in

zebrafish larvae using the GATA-2 promoter (Tomasiewicz et al., 2002). The fusion protein was phosphorylated similar to native Tau *in vitro* and showed an expression pattern in tissue culture suggesting interaction with the cytoskeleton. In zebrafish embryos, neurons expressed the fusion protein in a mosaic pattern, some examples showing fibrillar fluorescence in the cell body and proximal axon, resembling neurofibrillary tangles. The human Tau-GFP fusion was phosphorylated in the zebrafish brain. This initial study validated the use of a GFP fusion protein to monitor evolution of tangle pathology *in vivo*, and showed that a biochemical change relevant to human disease, phosphorylation, occurs in larval zebrafish. This suggests there is sufficient phylogenetic conservation of endogenous zebrafish kinases to modify the human protein. Stable transgenic zebrafish expressing human 4-repeat Tau were subsequently constructed using the newly-described *eno2* promoter (Bai et al., 2007). The phenotype of these transgenic fish has not yet been fully reported. The initial report showed evidence of refractile Tau accumulations within neuronal cell bodies and proximal axons, resembling neurofibrillary tangles. These accumulations were present in neurons throughout the brain, including regions of pathological relevance to PSP, such as the optic tectum. More recently, the Gal4-UAS system has been exploited in order to generate a Tauopathy model that shows a larval phenotype, with potential application to high throughput screening. Expression of the FTDP-17 Tau mutant P301L was driven from a novel bidirectional UAS promoter, allowing simultaneous expression of a separate red fluorescent protein in Tau-expressing cells (Paquet et al., 2009). The high levels of mutant Tau expression provoked by the *huc:gal4-vp16* driver were sufficient to induce a transient motor phenotype during embryogenesis, caused by a motor axonal outgrowth delay. At later time points, the Tau mutant caused enhanced cell death and protein aggregation in the spinal cord. In addition, rapid progression from early to late pathological Tau phosphorylation

was seen over the first few days of life. This hyperphosphorylation of Tau was insensitive to application of methylene blue, however, treatment with GSK3β inhibitors were able to reduce Tau phosphorylation. Taken together, these results suggest that the model may be used to identify other similar pharmacological inhibitors from chemical libraries. Unfortunately, loss of promoter activity prevented the examination of later pathological changes, and so it is unclear whether the phenotype was progressive and age-dependent, or transient. In addition, the *huc* promoter fragment used in this model only induced robust transgene expression in the spinal cord, which is not a prominent site of Tauopathy changes in human disease. However, this valuable study showed the utility of the Gal4-UAS system for modeling neurodegeneration in transgenic zebrafish and demonstrated evidence that biochemical changes characteristic of Tauopathy, including an orderly acquisition of abnormal phospho-epitopes and conformers, can be recapitulated in larval zebrafish.

1.2.4.2 Polyglutamine models

A number of autosomal dominant neurodegenerative diseases, including Huntington's disease (HDCRG, 1993) and several of the spinocerebellar ataxias (Orr et al., 1993; Kawaguchi et al., 1994; Imbert et al., 1996), are caused by pathological expansion of a tandem trinucelotide CAG repeat in the relevant gene, resulting in an elongated stretch of glutamine residues in the resulting protein. It is thought that the mechanism of pathogenesis involves a toxic gain of function mediated by the expanded polyglutamine tract, rather than loss of function of the affected gene (Landles and Bates, 2004; Zoghbi and Orr, 2009). Since this general pathogenic mechanism may be shared by these diseases, a polyQ toxicity model in zebrafish would present a possible means to elucidate pathogenesis and perhaps isolate a common treatment for the whole group of conditions. In the first report of a zebrafish polyQ model, transient expression of GFP-polyQ

fusion proteins was achieved by microinjection of plasmids, encoding the fluorescent fusion with polyQ tracts of differing lengths, under transcriptional control of a strong viral promoter (Miller et al., 2005). In human polyQ diseases, there is correlation between the length of the polyQ expansion and the severity of the phenotype, as measured by age of onset or rate of clinical progression. Expression of GFP-polyQ fusion proteins in zebrafish caused a decrease in embryo length and loss of tissue differentiation, resulting in gross morphological deficits and reduced viability. Although this acute response does not reflect the chronic neurological diseases seen in patients with polyQ expansion mutations, significant over-expression of these artificial proteins would be expected to provoke acute and severe phenotypes. Importantly, however, the model recapitulated two key features of polyQ diseases: first, there was correlation between the polyQ repeat length and the severity of the morphological phenotype. Second, GFP-positive inclusion bodies were formed, suggesting the formation of aggregates dependent on the polyQ tract (Miller et al., 2005). C-terminal Hsp70 (heat shock protein 70)-interacting protein (CHIP), which functions both as a co-chaperone and ubiquitin ligase, was shown to suppress aggregation of the PolyQ-GFP fusion, and the resulting toxicity, in this transient zebrafish model. The role of CHIP was then confirmed in a chronic mammalian model of Huntington's disease: N171-Q82 mice, in which the prion promoter drives expression of a Huntingtin fragment with a pathologically expanded polyQ tract, develop a neurobehavioral phenotype consisting of abnormal clasping movements, gait disturbance and tremor, associated with inclusion body neuropathology and loss of DARRP-32 immunoreactivity in the striatum. This phenotype was exacerbated when the mice were bred onto a CHIP haplo-insufficient background, resulting in accelerated clinical deterioration and premature death (Miller et al., 2005). These novel findings indicate that the acute, transient zebrafish model was predictive of at least one key biochemical event underlying

the pathogenesis of the chronic mammalian model, demonstrating that an appropriate mechanistic insights into disease pathogenesis was gained by studying the zebrafish model. A similar transient study, using mRNA injection to express GFP-polyQ(4, 25 or 102) confirmed that the expanded polyQ tract induced aggregation of the GFP fusion reporter *in vivo* (Schiffer et al., 2007). Time lapse photomicrography allowed direct visualization of the polyQ fusion protein being depleted from the cytoplasm as it was incorporated into growing aggregates. Interestingly, visualization of apoptotic cells relative to aggregates showed an unexpected dissociation, suggesting that aggregation was cytoprotective and that the toxic species may be pre-fibrillar GFP-polyQ (Schiffer et al., 2007). This report was remarkable for the first use of a zebrafish polyQ model to test possible chemical inhibitors of polyQ aggregation *in vivo*; some differences in the anti-aggregate activity of compounds were seen between cell culture and zebrafish and it is possible that the *in vivo* setting of the zebrafish model will provide a more representative environment for identification of compounds with relevant properties. A more recent study used a cell culture model in order to screen for enhancers of autophagy that might be efficacious in clearing aggregated Huntingtin and other substrates from cells (Williams et al., 2008). The indentified compounds were then subjected to verification in a novel stable transgenic zebrafish line, expressing a GFP-Huntingtin71Q fusion protein under control of the rhodopsin promoter, leading to aggregation of the fusion protein and loss of rod outer segments and rhodopsin expression from the retina. Several of the compounds identified as reducing aggregation in the cell culture model also prevented formation of aggregates in the zebrafish model, providing validation of the cell culture system, and suggesting that zebrafish models might be useful in the future for primary screens of therapeutic compounds.

1.2.4.3 ALS model

Familial amyotrophic lateral sclerosis is uncommon, but a fifth of such cases arise from mutations in the gene encoding superoxide dismutase (SOD) (Deng et al., 1993; Rosen et al., 1993). The mutations are thought to provoke degeneration of upper and lower motor neurons by a gain of function mechanism (Turner and Talbot, 2008), although the details remain uncertain. In order to evaluate the validity of a zebrafish model of ALS, a recent study used mRNA microinjection to effect transient over-expression of SOD mutants (Lemmens et al., 2007). The microinjected animals showed normal morphology and normal development of Mauthner neurons, Rohan-Beard sensory neurons and lateral line sensory neurons, despite robust expression of the mutant SOD protein. However a motor axonopathy was observed, manifest as shortened length and abnormal branching, suggesting that, similar to the human diseases, ubiquitous expression of the mutant protein had evoked motor neuron-specific neuropathology (Lemmens et al., 2007). This important finding is the first example of pathology specific to relevant neuronal populations being provoked by ubiquitous expression of a pathogenic protein, suggesting that this model may be useful to elucidate the mechanisms underlying specific vulnerability of motor neurons to this mutation. The pathological axonal changes were rescued by simultaneous over-expression of VEGF and were exacerbated by morpholino knockdown of VEGF expression (Lemmens et al., 2007). These findings are similar to those observed in SOD transgenic mice, and suggest that at least some of the biochemical mechanisms underlying the axonopathy in the zebrafish model may be shared with a mammalian model.

Together, these emerging lines of evidence indicate that relevant phenotypic abnormalities, mediated by conserved mechanisms, can be provoked in zebrafish models by transgenic expression of mutant human proteins involved in the pathogenesis of

neurodegenerative diseases. These findings are therefore encouraging that mechanistic insights and putative interventions identified in zebrafish models will be applicable to the human diseases.

The primary hypothesis of this thesis is that zebrafish will be a suitable model system to study DYT1 dystonia. Following this hypothesis, I aimed to first identify and characterize the endogenous zebrafish homolog of the human *TOR1A* gene. Second, I set out to generate transgenic zebrafish overexpressing either the wildtype or TorsinA[ΔE] to develop a zebrafish model of DYT1 dystonia. The following chapters will describe the results of the experiments designed to address these aims. First, the methods for all experiments described in this thesis will be presented in Chapter 2. Chapter 3 will discuss the identification and characterization of the endogenous zebrafish homolog to the human *TOR1A*, and will be followed in Chapter 4 by a characterization of the protein product transcribed from this homolog. Chapters 5&6 will discuss the creation and characterization (respectively) of transgenic zebrafish overexpressing either wildtype or TorsinA[ΔE]. The final chapter of the thesis will conclude with a broader discussion of the results and propose potential future directions for the use of zebrafish in modeling DYT1 dystonia.

2.0 METHODS AND MATERIALS

2.1 ANIMALS

Experiments were carried out in accordance with NIH guidelines and Institutional Animal Care and Use Committee approvals. Adult strain AB zebrafish were maintained at 28.5°C and euthanized by deep tricaine anesthesia followed by exposure to ice-cold water. Embryos were raised in E3 buffer (5mM NaCl, 0.17mM KCl, 0.33 mM $CaCl_2$, 0.33 mM $MgSO_4$), and supplemented, where necessary, with 0.003% 1-phenyl 2-thiourea (PTU) to inhibit pigmentation.

2.2 RACE

RACE was carried out as previously described (Bai et al., 2006; 2007; 2009). Briefly, total RNA was extracted from adult Zebrafish brain using *RNAqueous* (Ambion, Austin, TX) and reverse transcribed using *SuperScript III* (Invitrogen, Carlsbad, CA). 5' and 3' RACE was preformed using *FirstChoice RACE* (Ambion, Austin, TX) with zebrafish *tor1* primers: *tor1* exon2 reverse for 5' RACE and *tor1* exon4 forward for3' RACE. PCR products were cloned into pGEM-T (Promega, Madison, WI) and sequenced. The coding sequence for each isoform was also amplified from the RACE cDNA library, using PCR with PFX Platinum (Invitrogen, Carlsbad, CA), isoform specific 5' primers (*tor1_tv1* 5' UTR forward and *tor1_tv2* 5' UTR forward) and a

shared 3' primer (*tor1* 3' UTR reverse). Terminal deoxyadenosine were added to the 3' ends of the PCR products by addition of GoTaq (Promega, Madison, WI) to the PCR mixture, followed by incubation at 70°C for 30 minutes. PCR product was subsequently ligated into pGEM-T. Multiple sequences were aligned and digital full-length cDNA files were constructed using *VectorNTI Suite* (Invitrogen, Carlsbad, CA). All primer sequences are listed in table 2.1.

2.3 NORTHERN BLOTS

Northern blots were carried out as described (Bai et al., 2007; 2009). Briefly, total RNA, extracted from adult zebrafish brain using *RNAqueous* (Ambion, Austin, TX), was resolved through a 1% agarose fomaldehyde/MOPS gel, and transferred to a Nytran-N membrane (Schleicher and Schuell BioScience, Keene, NH). A DIG-labeled *tor1* antisense probe, containing the entire *tor1_tv1* open reading frame, was made using *in vitro* transcription from a plasmid template with DIG conjugated UTP (Roche, Indianapolis, IN). Membrane was pre-hybridized in Ultra-Hyp (Ambion, Austin, TX) containing Torula RNA (Sigma, St. Louis, MO) at a final concentration of 1mg/ml. The *tor1*a probe was added to the pre-hybridization buffer to a final concentration of 25ng/ml and incubated overnight at 68°C. Blots were washed sequentially with 2x SSC (150mM NaCl, 15mM $Na_3C_6H_5O_7 \bullet 2H_2O$)/0.1% SDS and 0.1x SC/0.1% SDS. Probe was detected using a 1:12500 dilution of an anti-DIG antibody conjugated to alkaline phosphatase (Roche, Indianapolis, IN) in 1% blocking buffer. *CDP-star* (Roche, Indianapolis, IN) was added to the blots and light-emission was detected by exposure to photographic film.

2.4 WHOLE MOUNT *IN SITU* HYBRIDIZATION

Whole mount in situ hybridization was carried out as previously described (Bai et al., 2007; 2009). Briefly, embryos were collected and allowed to develop to various ages in E3 buffer (5mM NaCl, 0.17mM KCl, 0.33mM $Cacl_2$ 0.33mM $MgSO_4$) containing 0.003% 1-phenyl-2-thiourea to inhibit melanogensis. At various ages, embryos were placed in 4% paraformaldyde and allowed to fix overnight at 4°C. The following day, embryos were washed in PBS, dehydrated with methanol and stored at -20°C. Embryos were first washed in acetone at -20°C, then hydrated with 50%, 30% methanol and then PBS. Room temperature incubation (5-60 minutes) with Protease-K (10µg/µl) permeabilized embryos (protease treatment was skipped for embryos under 24h), which were then post-fixed in 4% PFA for 20min and washed in filtered PBTw (PBS, 0.1% Tween, 0.2% BSA). Embryos were incubated in UltraHyb Buffer (Ambion) containing 1mg/ml Torula RNA and 50µg/ml heparin for 1h at 68°C before 150µg of the *tor1_tv1*, or *DAT*, probe (used for Northern blot) was added and embryos were allowed to incubated overnight. The following day embryos were washed in 50% formamide, 2x SSC, 0.3% CHAPS, then 2x SSC, 0.3% CHAPS, followed by 0.2x SSC, 0.3% CHAPS. Embryos were blocked for 1h in 1x MAB (100mM Maleic acid, 150mM NaCl, pH 7.5) containing 1% blocking serum, and probe was detected by incubation with an anti-DIG antibody conjugated to alkaline phosphatase for 3 hours at 37°C. Following washing in PBS, antibody hybridization was detected with BM Purple (Roche, Indianapolis, IN). Embryos were washed in PBS to stop the reaction and post-fixed in 4% PFA.

2.5 REVERSE TRANSCRIPTASE PCR

Total RNA was extracted from various tissues using RNAqueous, except muscle, which was processed with Trizol Reagent (Invitrogen). RNA was reverse transcribed with the Superscript III kit according to manufacturers protocol with random hexamer primers (Invitrogen) and the resulting cDNA was amplified with isoform specific 5' primers (*tor1_tv1* and *tor1_tv2* RT-PCR forward) and a common 3' primer (*tor1* exon2 Reverse) using PCR (60°C annealing temperature; 35 cycles). Products were resolved and visualized on a 2.5% agarose gel containing ethidium bromide. As a loading control, *bactin1* cDNA was amplified, using *bactin1* forward and reverse primers. All primer sequences are listed in table 2.1.

2.6 CELL CULTURE AND TRANSFECTION

HEK cells were maintained in DMEM supplemented with 10% FBS and 50µg/mL of each penicillin and streptomycin and maintained at 37°C in a humidified, 5% CO_2 incubator. MN9D cells (provided by Dr. Alfred Heller, University of Chicago) were maintained in DMEM high glucose, supplemented with 10% FBS and 50µg/mL of each penicillin and streptomycin and maintained at 37°C in a humidified, 5% CO_2 incubator (Choi et al., 1991). Cells were grown to 80% confluence and transfected with 2µg plasmid using Lipofectamine 2000 (Invitrogen, Carlsbad, CA). The following day, cells were transferred to Poly-D coated glass coverslips and allowed to adhere overnight. Cells were fixed in 4% PFA, washed in 1X PBS, counterstained with DAPI and mounted to slides for imaging. To visualize the ER compartment, cells were immunostained with a rabbit anti-PDI antibody (Assay Desgins, Ann Arbor, MI) at a 1:500

dilution, washed with PBS, and primary antibody was detected with a Cy-5-conjugated, goat anti-rabbit secondary (Santa Cruz Biotechnologies, Santa Cruz, CA) at a 1:1000 dilution.

2.7 WESTERN BLOTS

Transfected cells and adult fish brains were sonicated in RIPA buffer (10 mM Tris, 150 mM NaCl, 1 mM EDTA, 0.1% SDS, 1% Triton X-100, and 1% sodium deoxycholate, pH 7.4) and protein concentrations were measured using BCA assay (Biorad, Hercules, CA). Equal amounts of protein were resolved on a 10% poly-acrylamide gel, transferred to nitrocellulose, and blocked with 10% milk in TBS (50 mM Tris-HCl, 150 mM NaCl, 0.2% Tween 20). Torsin1 antibody was generated by peptide (CPDKEVVEKMAHD) inoculation of rabbits (New England Peptide). Serum was subsequently column purified against the peptide using a SulfoLink immobilization kit (Pierce). Affinity-purified antibody was used at a dilution of 1:1000, and allowed to hybridize overnight at 4°C. Protein A conjugated to HRP (1:4000) was used to detect primary antibody, and HRP was visualized by addition of chemilumenesent substrate and exposure to photographic film. For blocking experiments, antibody was pre-incubated with 760 µM peptide in PBS for 2.5 hours at 37°C.

2.8 IMMUNOHISTOCHEMISTRY

Adult zebrafish were transcadially perfused with PBS before brains and spinal cord were dissected, fixed in 4% PFA overnight, and cryoprotected in PBS containing 30% sucrose. 14µM

cryosections were post-fixed with 4% PFA, and were incubated overnight at 4°C with Torsin1 antibody (1:500) in carrier buffer (PBS, 1% goat serum, 1% BSA). Primary antibody was detected with an anti-rabbit HRP-conjugated antibody (Pierce, Rockford, IL) at 1:1000 in carrier buffer. HRP was detected using NovaRed (Vector Laboratories, Burlingame, CA) and sections were countered stained with Mayer hematoxylin (Sigma, St. Louis, MO).

2.9 SUBCLONING AND CONSTRUCTS

To create expression vectors for the *tor1* isoforms introduced into pGEM-T, described in section 2.2 were used as template. From pGEM-T, the coding sequence was amplified with the addition of 5' BamHI and 3' NcoI sites for introduction into CS2+eGFP, resulting in the fusion of eGFP to the carboxyl terminus of the Torsin1 protein, and the coding sequence was amplified with the addition of 5' BamH1 and 3' XhoI restriction sites for introduction into pcDNA3.1. Mutations were introduced into the coding sequence (CDS) of the *tor1-eGFP* fusion construct using the QuikChange® Site-Directed Mutagenesis Kit (Stratagene) and *tor1* K114T forward and reverse, or *tor1* E177Q forward and reverse, primers. The *tor1* CDS of all constructs were verified by sequencing at GENEWIZ, and all primers are listed in table 2.1.

Previously described vectors containing the coding sequence of human *TOR1A* and *TOR1A*[ΔE] in the pcDNA3.1 plasmid were used as the PCR template for insertion into pCS2+eGFP and pCS2+mRFP plasmids. For both the creation of pCS2+eGFP, *TOR1A* and *TOR1A*[ΔE] coding sequences were amplified with the addition of 5' BamH1 and 3' Nco1 restriction sites, resulting in fusion of eGFP to the carboxyl terminus of TorsinA. In order to create pCS2+mRFP vectors containing either the *TOR1A* or *TOR1A*[ΔE] coding sequence was

amplified with the addition of 5' and 3' BamHI sites. After digestion of pCS2+mRFP with BamHI, 5' phosphate groups were removed incubation of the linear plasmid with calf intestine phosphatase to prevent recircularization of the vector. The TorsinA coding sequence of all constructs were verified by sequencing at GENEWIZ, and all primers are listed in table 2.1.

2.10 BAC RECOMBINATION

TOR1A-eGFP-SV40 and *TOR1A[ΔE]*-eGFP-SV40 fragments were subcloned, using PO_4-G-*TOR1A* forward and PacI-SV40 reverse primers, from pCS2+ plasmids into a previously described intermediate construct, digested with StuI and PacI, containing the 5' and 3' arms of a 12 kb fragment of the eno2 gene (Bai et al., 2007). The resulting intermediate construct was linearized between the 5' and 3' arms by restriction digest with HindIII. Previously generated DY380-BACzC51M24 (Bai et al., 2007) bacteria were grown at 32°C to OD590 = 0.5 prior to induction at 42°C for 15 minutes. Linearized plasmid was introduced by electroporation. Recombinants were identified by ampicillin resistance, and verified by restriction digest and direct DNA sequencing.

2.11 MORPHOLINO INJECTIONS

Two splice-blocking morpholino oligionucleotides (MOs) covering exon2/intron2 (E2I2) and exon3/intron3 boundaries (E3/I3) (E2/I2: 5'-ATATGAAGTCAGCTTACCTTGTAGG-3' and E3/I3: 5'-TGTTAGTAGACACTGACCTGAGGAA-3'), along with two different control

morpholinos (Standard: 5'-CCTCTTACCTCAgTTACAATTTATA-3' and Random 5'-NNNNNNNNNNNNNNNNNNNNNNNNN-3') were ordered from Genetools, Inc. Embryos were injected with 6ng of both Tor1 MOs between the 1- to 2-cell stages to achieve almost 100% knockdown at 24 hours post fertilization (hpf). The level of *tor1* knockdown was examined using the same reverse transcriptase PCR protocol described in section 2.5, with either *tor1_tv1* or *tor1_tv2* RT-PCR forward and *tor1* exon4 reverse primers (sequences are in table 2.1). To control for non-specific effects, a set of control embryos were injected with 6ng of both Control MOs. Embryos were dechorionated at 24 hpf and raised in an incubator set at 28.5°C and fixed with an internal light source programmed to a 14:10 light:dark cycle.

2.12 mRNA INJECTIONS

Human *TOR1A*-eGFP and *TOR1A*[ΔE]-eGFP mRNA was created using pCS2+ plasmids described above. Plasmids were transformed in SCS110 bacteria to remove DNA methylation, and were subsequently linearized at the Asp718I site, 3' to the poly(A) signal. After linearization, mRNA was transcribed from the Sp6 promoter using the mMessage Machine kit (Ambion, Austin, TX). Intracellular injection of 1–2 nl of mRNA solution (500 pg/nl mRNA, 0.25% phenol red, 120 mM KCl, 20 mM HEPES, pH 7.4) was carried out at the single cell stage, and embryos were raised in an incubator set at 28.5°C and fixed with an internal light source programmed to a 14:10 light:dark cycle. Larvae were collected at 4 days post fertilization (dpf), fixed in 4% PFA overnight at 4°C, washed in PBS and cryoprotected in 30% sucrose in PBS. Sections of microinjection embryos were counterstained with DAPI to provide relative localization of the fluorescently tagged protein encoded by the injected mRNA.

2.13 I-SCE1 TRANSGENESIS

A restriction digest containing 0.6μg of plasmid DNA (pBS-I-Sce1-*eno2*:TOR1A-eGFP, or pBS-I-Sce1-*eno2*:TOR1A[ΔE]-GFP), 1μl injection dye (0.5% phenol red, 240mM KCl, 40mM HEPES pH 7.4), 1μl I-Sce1 buffer (100mM Tris–HCl, 100 mM $MgCl_2$,10 mM Dithiothreitol, pH 8.8), 1μl (5U) I-Sce1 (New England Biolabs), and nuclease-free H2O (Ambion, Austin, TX) to 10 μl total was prepared on ice, and 0.5nl of the restriction digest reaction, containing 30pg DNA, was microinjected into one-cell stage embryos using a glass micropipette. All surviving fish were raised to sexual maturity and crossed to wildtype AB strain fish to permit identification of germline chimeras by visual expression of GFP. F1 progeny, from outcrossing each germline-transgenic F0 fish, were raised to adulthood. Epifluorescense microscopy was used to divide transgene-positive F2 generation embryos from non-transgenic clutchmates after outcrossing F1 transgene positive fish to wild-type AB strain fish. Each line of transgenic fish was derived from a single F1 founder, and each F1 founder was derived from a single F0 germline chimera, with one exception: Tg(*eno2*:TOR1A[ΔE]-eGFP)^{pt454} and Tg(*eno2*:TOR1A[ΔE]-eGFP)^{pt455} were derived from separate F1 transgene-positive fish that were derived from the same F0 germline chimera. Stocks were maintained by visually identifying GFP expression in embryos. The data reported in this thesis are derived from F2 and F3 generation zebrafish.

2.14 HPLC

Neurotransmitter measurements were performed by adapting a previously reported method (Milanese et al., 2012). Adult zebrafish brains were sonicated in 200 μl of 4 M perchloric acid,

0.1% $Na_2S_2O_5$, 0.1% EDTA on ice, and centrifuged at 17,000 X g for one hour at 4 °C. The supernatant was removed and filtered through a 0.22-μm nylon membrane (Spin-X, Corning Glass). The pellet was dissolved in 100 μl of 1M NaOH for measurement of protein concentration. A Waters 2695 HPLC separation module (Waters, Milford, MA) was loaded with 25 μl of filtrate. The HPLC mobile phase consisted of 0.06 M sodium phosphate monobasic, 0.03 M citric acid, 8% methanol, 1.1 mM 1-octanesulfonic acid, 0.1 mM EDTA, 2 mM sodium chloride, pH 3.5. Neurotransmitters were separated on a Waters XBridge C18 4.6 X 150-mm column, particle size 3.5 μm, at 34 °C, and detected using a Waters 2465 electrochemical detector with a glassy carbon electrode set at 750 mV, referenced to an ISAAC electrode. Neurotransmitters levels were normalized to protein levels, using a standard curve generated from injection of high purity standards.

2.15 SPONTANEOUS LOCOMOTOR BEHAVIOR

Larvae and adult recordings of spontaneous locomotion of transgenic, MO injected and control fish were collected by recording using either the Zebrabox system (5-45dpf) or our previously described video collection system (Cario et al., 2011; Farrell et al., 2011). Briefly, embryos and larvae were transferred to individual wells of a multi-well plate (96 well for 5-14dpf, 48-wells for 21 – 45dpf, and 6-well for 60+ dpf) and filmed for 1 to 3 hours at 2 frames per second. Videos were analyzed using custom matlab software to quantify spontaneous propulsive movements. Both parametric (ANOVA) and non-parametric (Kruskal-Wallis) statistics were used to analyze data sets between 4-7 dpf because at least one group per data set did not pass the D'Agostino & Pearson omnibus normality test. Because accumulated data sets of uninjected

larvae at 5 days post fertilization (dpf) are normally distributed, data sets are reported as mean +/- SEM. After 14dpf, all data sets were normally distributed and significance was determined by one-way ANOVA. Although data sets for both control morphoino and *tor1* morpholino differ in the variance of average active and rest durations compared to uninjected larvae using the Bartlett test for equal variances, control and *tor1* morpholino injected larvae do not differ in their variance when these two groups are compared using an F test.

2.16 ACOUSTIC STARTLE BEHAVIOR

To measure startle responsiveness and locomoter response, 35 dpf larvae were placed in an individual 10cm X 10cm square well of a 9 well grid and stimulated using a small vibration exciter (4810, Bruel and Kjaer, Norcross, GA), controlled by an digital-analogue card (PCI-6221, National Instruments, Austin, TX) which also triggered the camera to collect a 120 frame (120 ms) window. The startle stimulus was a 6 ms duration, 500 Hz waveform generated by custom software. Each group of larvae were recorded for 20 trials, separated by 15 seconds to avoid habituation. Bend angles, duration and maximal angular velocity were measured using the previously described software Flote software package (Burgess and Granato, 2007).

Table 2.1 – Primer Sequences. This table contains the sequences for primers used in this thesis. All primers were purchased from Sigma-Aldrich.

Primer Name	**Purpose**	**Sequence (5' to 3')**
tor1 exon2 Reverse	5' RACE and RT-PCR	GGCTTTCAGGATGACTTGACCT
tor1 exon4 Forward	3' RACE	TTCAGGTGGCTCTGGATTTC
tor1_tv1 5' UTR Forward	mRNA cloning	CGGAAGTGGGTCGTCATTAT
tor1_tv2 5' UTR Forward	mRNA cloning	CCACCCTGTTTCCGACTAAA
tor1 3' UTR Reverse	mRNA cloning	CCCTTTAAAACAGGGACACG
tor1_tv1 RT-PCR Forward	RT-PCR, MO RT-PCR	TTCTTTTGGCTCCGTTTACGG
tor1_tv2 RT-PCR Forward	RT-PCR, MO RT-PCR	AAGCAGGAAGTGGCGGCTGT
bactin1 Forward	RT-PCR	CCAACTGGGATGATATGGAGAAGA
bactin1 Reverse	RT-PCR	CAATGGTGATGACCTGTCCGTC
Tor1 exon4 Reverse	MO RT-PCR	TCTTTGCCGTCCTTCCAGAAA
BamH1-*tor1_tv1* Forward	Subcloning into pcDNA3.1 & pCS2+eGFP	TATAGGATCCACCATGCGCTCGGCCTGGCTG
BamH1-*tor1_tv2* Forward	Subcloning into pcDNA3.1 & pCS2+eGFP	TATAGGATCCACCATGAACGCTCGGCCTCCT
Xho1-*tor1* Reverse	Subcloning into pcDNA3.1	TATACTCGAGTCAGATATAGAAGTCCAGTCT
Nco1-*tor1* Reverse	Subcloning into pCS2+eGFP	TATACCATGGCATAGAAGTCCAGTCTGCT
tor1 K114T Forward	Walker A Mutagenesis	CTGGACCGGCACCGGTACCAACTTTGTGAGCCAACTATTGGC
tor1 K114T	Walker A	GCCAATAGTTGGCTCACAAAGTTGGTACCGGTGCCGGTCCAG

Reverse	Mutagenesis	
tor1 E177Q Forward	Walker B Mutagenesis	CGTTCCATGTTCATTTTTGATCAAATGGATAAAATGCATCCTGGG
tor1 E177Q Reverse	Walker B Mutagenesis	CCCAGGATGCATTTTATCCATTTGATCAAAAATGAACATGGAACG
BamH1-*TOR1A* Forward	Subcloning into pCS2+eGFP	TATAGGATCCATGAAGCTGGGCCGG
Nco1-*TOR1A* Reverse	Subcloning into pCS2+eGFP	TATACCATGGCATCATCGTAGTAATAAT
BamH1-*TOR1A Reverse*	Subcloning into pCS2+mRFP	TATAGGATCCATCATCGTAGTAATAATCT
PO_4-G-TOR1A Forward	Subcloning into pBS-eno2arms-I-Sce1	GATGAAGCTGGGCCGGGCCGT
PacI-SV40 Reverse	Subcloning into pBS-eno2arms-I-Sce1	ACATTTAATTAAGAATTAAAAAACCTCCCAC

3.0 CHARACTERIZATION OF THE ZEBRAFISH *TOR1A* HOMOLOG

3.1 INTRODUCTION

The most prevalent form of hereditary dystonia is linked to the DYT1 locus and most often manifests clinically during late childhood and adolescence (Kramer et al., 1994). DYT1 dystonia is caused by mutations in the *TOR1A* gene encoding TorsinA (Ozelius et al., 1997). Nearly all patients harbor an in-frame trinucleotide GAG deletion in exon 5 of *TOR1A*, resulting in the loss of a single glutamic acid (ΔE) near the carboxy terminal of TorsinA. The mutant allele gives rise to dystonia that is inherited as an autosomal dominant trait, although only approximately 40% of mutation carriers manifest dystonia (Kramer et al., 1994).

As a first step toward generating a zebrafish model of DYT1 dystonia, we identified the zebrafish homolog of TorsinA. Here, we show that the zebrafish genome contains a single *tor1* gene, expressed as two splice variants, in contrast to the dual *TOR1A* and *TOR1B* paralogues found in tetrapod genomes.

3.2 IDENTIFICATION OF THE ZEBRAFISH *TOR1A* HOMOLOG, *TOR1*

To identify zebrafish proteins with homology to human TorsinA, the zebrafish RefSeq mRNA database (www.ncbi.nlm.nih.gov final accession date: August, 11, 2011) was interrogated by

TBLASTN using the human TorsinA protein sequence as a probe. Ten sequences with homology to human TorsinA were further analyzed. The predicted translations of the zebrafish sequences were aligned with Torsin protein sequences derived from human, chicken and xenopus, as well as the nearest *C. elegans* and drosophila homologs, using the ClustalX 2.1 algorithm (Larkin et al., 2007), and a dendrogram was constructed to illustrate the inferred evolutionary relationships between the proteins, using the BEAST program (Drummond and Rambaut, 2007) (Figure 3.1).

Two putative zebrafish proteins appeared most closely related to TorsinA proteins from other vertebrate species. Comparison of the mRNA and genomic sequences showed that the two transcripts encoding these putative proteins are derived from a single gene by inclusion of alternative 5' exons (Figure 3.2). We refer to the gene (si:ch73-178d14.1) as *tor1*, and its two transcript variants as *tor1_tv1* (NM_001200015) and *tor1_tv2* (BC_050957). The resulting proteins are referred to as Torsin1a and Torsin1b respectively. The *tor1* gene maps to zebrafish chromosome 21, and spans approximately 11.78kb of sequence.

The zebrafish genome contains an additional cluster of four adjacent genes on chromosome 23 predicted to encode Torsin-like proteins. Sequence comparison suggests that these putative proteins are most closely related to Torsin1 and Torsin3 family proteins, although they show less homology than either Torsin1a or Torsin1b to human TorsinA. We found evidence that two of these genes (NP_001124104 and NP_957150) are transcribed. Each of these genes shows divergent exon structure with respect to human TOR1A, suggesting that they are more distantly related than *tor1* to TOR1A (see below). The Torsin-like gene cluster was not found in other teleosts and was located in a region of chromosome 23 with little conservation of

synteny with respect to other teleosts (not shown), suggesting that this region has undergone substantial rearrangement in zebrafish.

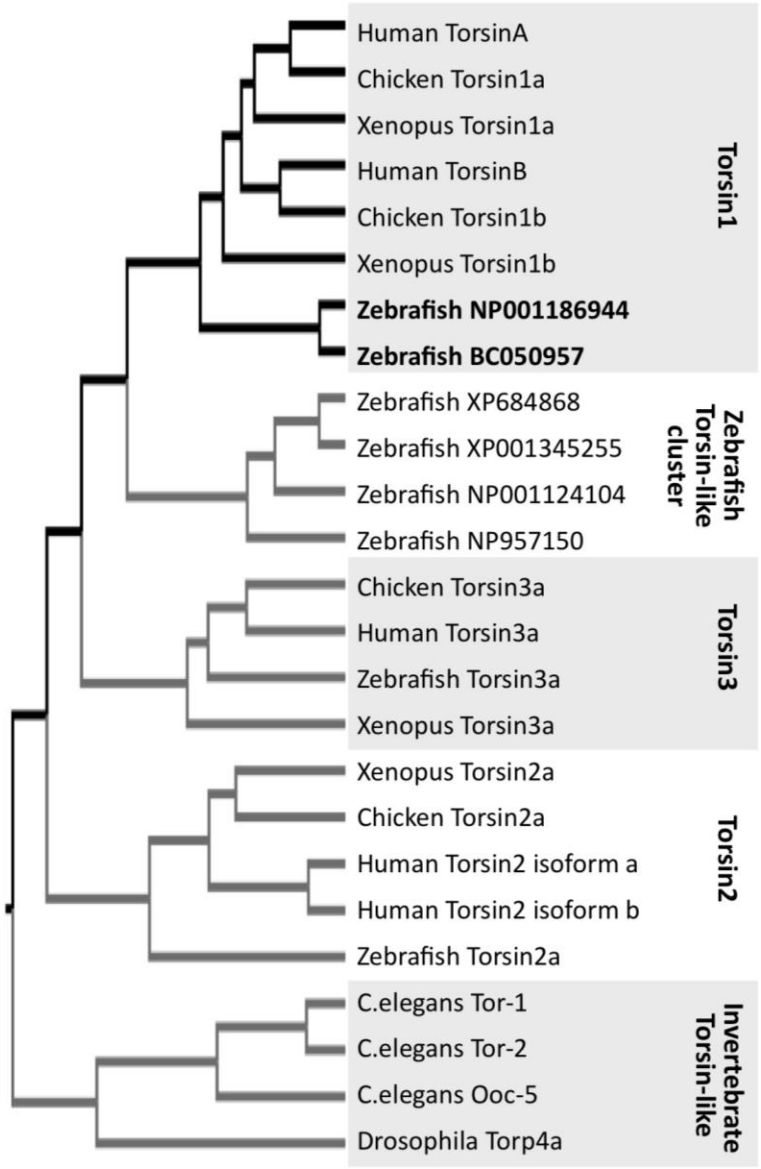

Figure 3.1 – Identification of zebrafish Torsins

Human TorsinA was used as a probe to interrogate the NCBI zebrafish RefSeq RNA database by TBLASTN. Eight different zebrafish mRNA sequences with homology to TorsinA were translated and aligned with Torsins from *C. elegans*, *D. melanogaster*, Xenopus, Chicken, and Human. A dendrogram was constructed to illustrate the inferred evolutionary relationships between Torsin family proteins from different species.

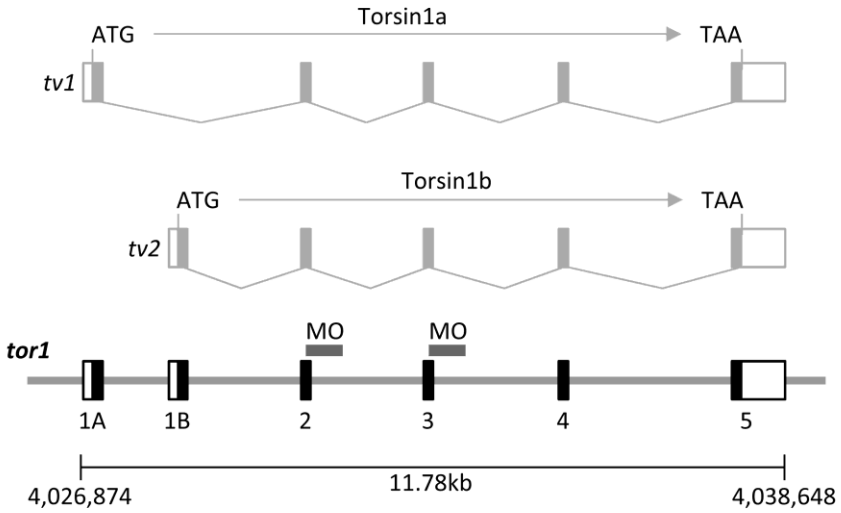

Figure 3.2 – Zebrafish *tor1* is expressed as two different transcript variants

The two zebrafish transcripts most closely related to human *TOR1A* were found to be transcribed from a single gene by inclusion of alternative 5' exons. *tor1* transcript variants 1 and 2 encode Torsin1 isoforms a and b, which differ at their N termini. The two transcripts are depicted above the genomic sequence. The splice boundaries targeted by morpholino oligonucleotides in figure 4.4 are labeled 'MO'.

3.3 SYNTENY BETWEEN TOR1 AND TOR1A

In order to better understand the relationships between zebrafish and human Torsins, we next examined the genomic context of Torsin1 family genes in the human, and how this is conserved in other vertebrate species (Figure 3.3). In human, the dual torsin1 family members TOR1A and TOR1B are adjacent and inverted with respect to one another. The order of the flanking genes PRRX2 – PTGES – TOR1A – TOR1B – C9orf78 – USP20 – FNBP1 is conserved from mammals to amphibians.

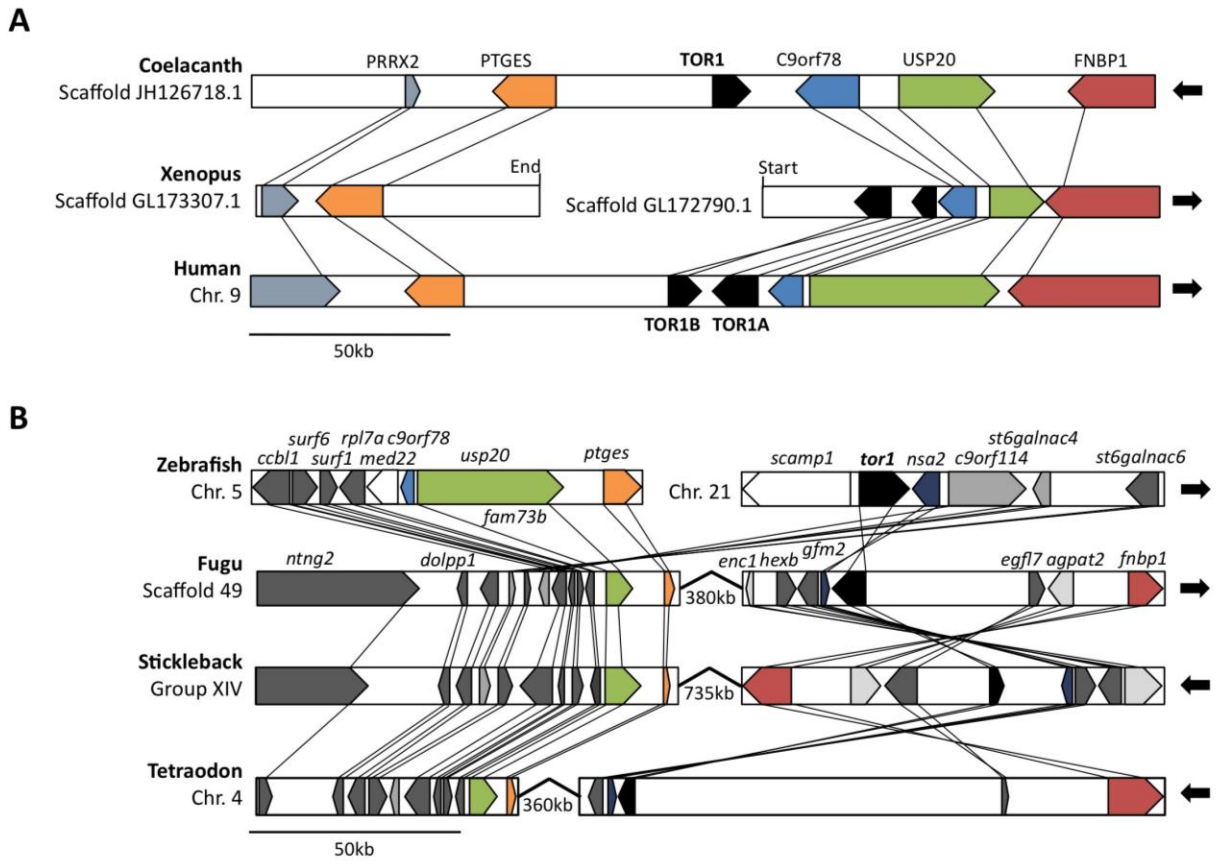

Figure 3.3 – Syntenic relationships of *tor1*, TOR1A and TOR1B

(A) The diagram shows the order and orientation of genes flanking TOR1A and TOR1B in the human and xenopus genomes, and *tor1* in the coelacanth genome. The map is shown to scale; large arrows show direction of telomere. TOR1A, TOR1B and *tor1* are colored black. The flanking genes are colored green (USP20), red (FNBP1), blue (C9orf78), orange (PTGES) and lilac (PRRX2). Orthologous genes are connected by solid lines. **(B)** The diagram shows the order and orientation of genes flanking *tor1* in the zebrafish, fugu, stickleback, and tetraodon genomes. The color scheme is identical to panel A; additional flanking genes are colored as follows: dark grey - conserved chromosomal positions in all four fish species; light grey - conserved chromosomal positions in two or three fish species; white - chromosomal position not conserved.

In coelacanth, a later diverging fish species, this gene order is also conserved. However, similar to other fish species, coelacanth has a single *tor1* gene instead of the dual TOR1A and TOR1B genes found in xenopus and human. This suggests that *tor1* was duplicated at the root of the tetrapod lineage. In earlier diverging fish species, substantial genomic rearrangements with respect to tetrapods and coelacanth disrupt the conservation of synteny surrounding the Torsin1 family genes. *fnbp1* is found in close proximity to *tor1* in fugu, stickleback and tetraodon, but appears ~2 megabases upstream of *tor1* in the zebrafish genome. Interestingly, the genes immediately flanking TOR1A and TOR1B in human are found in syntenic blocks separated from *tor1* in earlier-diverging fish species. Thus *ptges* and *usp20* are adjacent to one another, but located >350kb from *tor1*, in fugu, stickleback and tetraodon; in zebrafish, these genes and *c9orf78* are located on a different chromosome to *tor1*. However, *tor1* in all four fish species shows conserved syntenic relationships. Given the proximity of *tor1* and *fnbp1* in three of the species, and the single *tor1* gene in coelacanth despite conservation of synteny with human TOR1A and TOR1B, these data suggest that zebrafish *tor1* and human TOR1A and TOR1B share a common genomic origin.

3.4 CLONING OF THE *TOR1* mRNA

We cloned *tor1* cDNA and mapped its transcriptional start sites by rapid amplification of cDNA ends (RACE), using RNA isolated from adult zebrafish brain tissue (Figure 3.4). 5'RACE was carried out as previously reported using the tobacco acid pyrophosphatase (TAP) method to allow specific ligation of the RACE adapter to the 5' end of mRNA transcripts (Figure 3.4A). *tor1* cDNA was amplified using a 3' primer complementary to exon 2 of the *tor1* mRNA (which

is shared by both transcript variants) and a 5' RACE adaptor primer, yielding a single PCR product. TAP^- controls confirmed that amplification of this product was dependent on hydrolysis of the 7-methylguanylate mRNA cap prior to adapter ligation; RT-PCR controls confirmed that reverse transcription was equivalent in both TAP^- and TAP^+ samples. These controls show that the boundary between the RACE adapter and the cDNA sequence corresponds to the 5' end of the transcript and hence the transcriptional start site in the genomic sequence. 5'RACE products were cloned and sequenced: *tor1_tv1* and *tor1_tv2* were found to initiate transcription from different promoters located at the 5' end of the gene; the unique first exons in each transcript splice into a common mRNA at exon 2 (Figure 3.4B,C). A single major transcriptional start site was found in *tor1_tv1*, whereas *tor1_tv2* showed two different 5' termini. As is commonly found in ubiquitously-expressed genes, neither promoter region contained a consensus TATA box or initiator motif (Schug et al., 2005).

The 3' end of the *tor1* transcript was cloned by 3'RACE (Figure 3.4D). A single GATAAA polyadenylation signal at position 1862 (with respect to the first nucleotide of *tor1_tv1*), located 24bp upstream of the poly(A) tail, is shared by both transcript variants. After allowing for addition of the poly(A) tail, the sizes of the complete *tor1_tv1* (1881bp) and *tor1_tv2* (1886bp) cDNA sequences are compatible with the single ≈2.1kb *tor1*-hybridizing band found on northern blot analysis of brain RNA (Figure 3.4E).

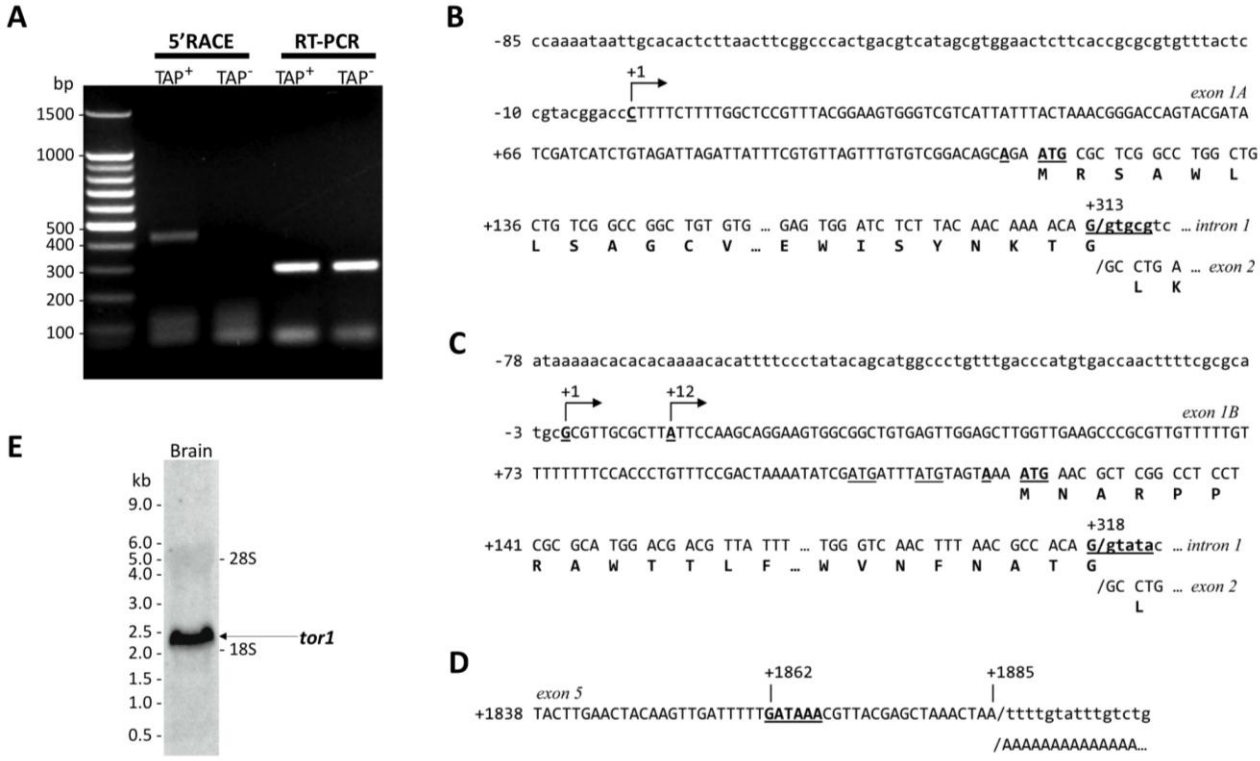

Figure 3.4 - *tor1* promoters and transcripts

(A) Zebrafish brain total RNA was treated with tobacco acid pyrophosphatase (TAP^+; lanes 2 and 4) or untreated (TAP^-; lanes 3 and 5) prior to RACE adapter ligation and reverse transcription. *tor1* was amplified by 5'RACE using a *tor1* exon 2 reverse primer and a RACE adapter primer (lanes 2 and 3) or by RT-PCR using *tor1* primers (lanes 4 and 5). **(B, C)** The transcriptional start sites of *tor1_tv1* **(B)** and *tor1_tv2* **(C)** were determined by comparing the genomic sequence with sequences of the 5' RACE products shown in panel A. The transcriptional start sites are shown underlined with arrows; bases are numbered such that +1 represents the first nucleotide of the most 5' transcriptional start site. The open reading frames of exons 1a and 1b and their 3' splice sites are shown. The consensus **A**NN**AUG** translational initiation signals are indicated in bold and underlined; non-consensus AUG sequences in the

5'UTR of *tor1_tv2* are underlined. **(D)** 3'RACE was employed to determine the 3' terminus of the transcript. The polyadenylation signal within exon 5 is underlined in bold. The position of the poly(A) tail in the mRNA is indicated. **(E)** Brain total RNA was separated electrophoretically and the resulting northern blot was probed using a cRNA probe to *tor1*. The positions of molecular size standards and the 28S and 18S rRNA bands are shown.

3.5 ORGANIZATION OF THE *TOR1* GENE

The *tor1* cDNA sequences were next mapped to the Zv9 assembly of the zebrafish genomic sequence and the exon boundaries and splice sites determined (Table 3.1). Both zebrafish *tor1* and human TOR1A transcripts contain 5 exons. The phases of all splice boundaries are conserved between TOR1A and *tor1*; in addition, exons 2, 3, and 4 share identical lengths between the human and zebrafish sequences. This striking conservation of genomic organization between the human TOR1A and zebrafish *tor1* genes provides further evidence that they descend from a common ancestral gene.

Table 3.1 – Genomic organization of zebrafish *tor1* compared with human TOR1A. The splice acceptor and donor sequence for each exon and intron boundary of the zebrafish *tor1* gene is shown, as well as the length and phase of each exon. The exon length and phase are compared to the human TOR1A gene.

	Zebrafish				Human		
Exon	**Splice acceptor**	**Splice donor**	**Exon Length ***	**Phase**	**Exon**	**Exon Length ***	**Phase**
1	-	tv1= AAA ACA G /gtgcgtca **K T G**	tv1= 313 (1-66)	tv1= 1	1	255 (1-60)	1
		tv2= GCC ACA G /gtatacag **A T G**	tv2= 318 (1-66)	tv2= 1			
2	ctccttcccgcag /GC CTG AAG **L K**	TAC AAG /gtaagctg **Y K**	266 (67-154)	0	2	266 (61-148)	0
3	ctgcggggtttag /ACG CAG **T Q**	TTC CTC AG /gtcagtgt **F L S**	176 (155-213)	2	3	176 (149-207)	2
4	tgtgtttatgtag /T AAC GCC **N A**	AAC AGT / acgtcaca **N S**	128 (214-256)	1	4	128 (208-250)	1
5	tgttcccgcaggc /GGT TTC	-	996 (257-336)	-	5	1281 (251-332)	-

3.6 EXPRESSION OF *TOR1* mRNA

We next determined the temporal and spatial expression patterns of *tor1*. mRNA for both *tv1* and *tv2* was detected by RT-PCR during early embryonic development. However, isoform-specific probes complementary to the short exon sequences unique to each transcript gave insufficient signal in whole mount RNA *in situ* hybridization assays to localize *tor1* transcripts. Consequently, we employed a larger cRNA probe complementary to the entire *tor1* open reading frame shared by both transcripts. At 12 hours post fertilization (hpf), *tor1* was expressed throughout the entire embryo (Figure 3.5A). A sense control did not show hybridization at this time point, suggesting that the observed staining pattern was not attributable to non-specific hybridization. At later developmental points, the pattern appeared unaltered, but the expression level progressively reduced and was barely detectable by 96hpf. In the adult, both *tor1_tv1* and *tor1_tv2* were detected by RT-PCR in several tissues including brain, foregut, hindgut, muscle, and gonad (Figure 3.5B). Relative to β-actin, expression of both isoforms was lower in brain and muscle compared to gut and gonad, suggesting reduced expression of *tor1* in post-mitotic tissues. In addition, the relative expression of the two transcripts differed between tissues. For example, *tor1_tv1* was more abundant in foregut, whereas *tor1_tv2* was expressed more strongly in the hindgut. These data suggest that expression of the two transcripts is regulated independently by distinct *cis*-regulatory elements.

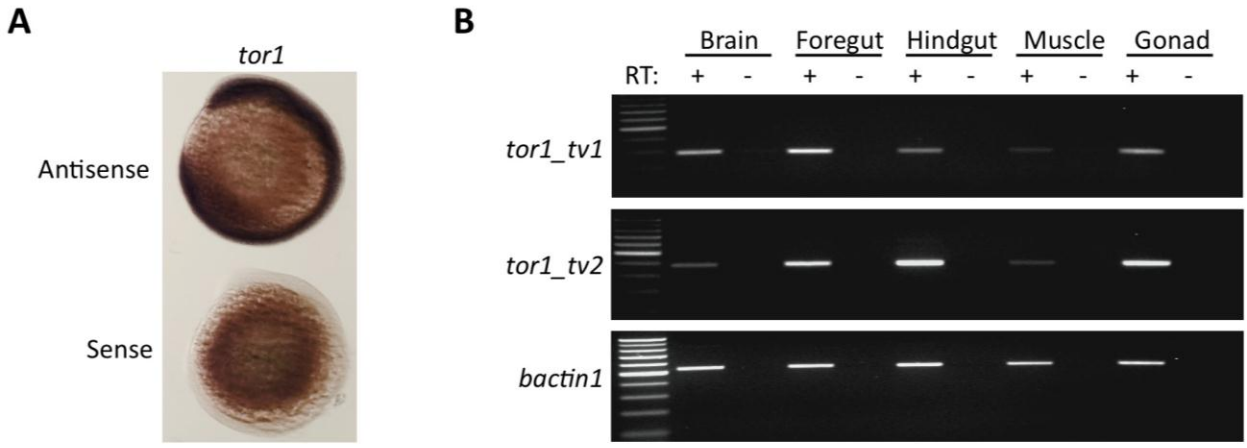

Figure 3.5 – Larval and adult expression of *tor1*

(A) RNA i*n situ* hybridization was employed to detect the *tor1* transcript during development. Hybridized probe was detected using a histochemical reaction with a blue/purple product. The photomicrograph shows embryos at 12 hpf; the upper of the pair was hybridized with a *tor1* antisense probe and the lower with a *tor1* sense control probe. **(B)** Reverse transcriptase PCR was employed to detect *tor1_tv1* (upper panel) or *tor1_tv2* (middle panel) mRNA in brain, foregut, hindgut, muscle, and gonads of adult zebrafish. Total RNA was treated with reverse transcriptase (RT^+); controls lacking reverse transcriptase (RT^-) excluded amplification of genomic DNA sequences. *bactin1* was amplified as a ubiquitously expressed control mRNA (lower panel).

3.7 DISCUSSION

The data presented here suggest that a novel zebrafish gene, *tor1,* is a single zebrafish homolog of the mammalian *TOR1A* and *TOR1B* genes. Conservation of sequence and genomic organization provide strong evidence that the zebrafish and human genes share a common ancestor, and we found notable similarities between the expression patterns of the human and zebrafish mRNAs, and the domain organization and subcellular localization of the proteins. There is limited conservation of synteny between teleost and tetrapod genomes in the immediate vicinity of the *tor1* genes, suggesting that substantial genomic reorganizations occurred in this region during evolution. One of the more striking differences is the presence of adjacent *TOR1A* and *TOR1B* genes in tetrapods, whereas the genomes of zebrafish, fugu, stickleback, tetraodon and coelacanth all contain a single *tor1* gene. These data strongly suggest that an ancestral *tor1* locus was duplicated during the fin-to-limb transition, resulting in distinct *TOR1A* and *TOR1B* genes before the emergence of amphibious tetrapods. The functional divergence of TorsinA and TorsinB remain to be determined; TorsinA and TorsinB show complementary expression patterns (Kim et al., 2010), though it is possible that they mediate similar cellular functions in different groups of cells, as many paralogous proteins with distinct expression patterns show redundant functions (Kafri et al., 2009). In support of the possibility that TorsinA and TorsinB have partially redundant functions, there is evidence that TorsinB may partially compensate for the functional effects of mutations in TorsinA: morphological abnormalities of the nuclear envelope in fibroblasts derived from ΔE/ΔE knockin mice were exacerbated by loss of TorsinB (Kim et al., 2010). It is possible that the single *tor1* gene in zebrafish will prove advantageous for determining the role of Torsin1 in neurons, since loss of function phenotypes are unlikely to

be mitigated by compensatory functions provided by closely related proteins. It is also possible that discrete functions of TorsinA and TorsinB are distributed between the Torsin1A and Torsin1B isoforms encoded by *tor1* transcript variants in zebrafish, as TorsinA and TorsinB are most divergent at the N-terminal region. Compatible with this idea, the expression pattern of *tor1* showed similarities to both *TOR1A* and *TOR1B*. The relatively weak expression of both *tor1_tv1* and *tor1_tv2* in the brain, compared to gut and gonads resembles the expression of mammalian *TOR1B*, which is more abundantly expressed in somatic cells than neurons (Kim et al., 2010). Conversely, expression of Torsin1 in the zebrafish nervous system appeared to closely resemble the expression of TorsinA in the mammalian nervous system, with prominent localization in the cell body and processes of neurons and absence from white matter tracts (Shashidharan et al., 2000). The development of isoform-specific antibodies to zebrafish Torsin1a and Torsin1b will allow clarification of whether the expression patterns of these two proteins are complementary and similar to mammalian TorsinA and TorsinB.

4.0 CHARACTERIZATION OF THE TORSIN1 PROTEIN

4.1 INTRODUCTION

Torsins are a metazoan-specific group of proteins belonging to AAA^+ superfamily of proteins (ATPase associated with various cellular activities) (Breakefield et al., 2001). AAA^+ family proteins participate in a diverse array of cellular functions (Hanson and Whiteheart, 2005), however, the functions of Torsins largely remain to be determined. Human TorsinA is expressed in a wide variety of cell types, and is found to primarily colocalize with markers for the endoplasmic reticulum (Hewett et al., 2000). The primary cellular phentoype observed with mutant TorsinA[ΔE] is a redistribution from the ER to the nuclear envelope (NE) (Goodchild and Dauer, 2004), although in some cell lines, the formation of membranous whorls can also be observed (Hewett et al., 2000). Similar to mutant TorsinA[ΔE], non-fuctional mutations introduced into the Walker B ATP hydrolysis domain of TorsinA also caused relocalization to the NE (Goodchild and Dauer, 2004; Torres et al., 2004).

Here I report that the zebrafish Torsin1 shares a similar protein domain structure with human TorsinA, and mutations in the ATP hydrolysis domain of Torsin1 resulted in redistribution of the protein to the nuclear envelope. Similar to murine *TOR1A*, loss of *tor1* during early development did not cause morphological defects in the nervous system, loss of dopamine neurons or deficits in spontaneous movement. Taken together, the findings provide an

essential basis for further studies to elucidate the functions of Torsin proteins in CNS function and for future development of a zebrafish DYT1 dystonia model.

4.2 SEQUENCE HOMOLOGY BETWEEN TORSINA AND TORSIN1

The amino termini of Torsin1a and Torsin1b, encoded by exons 1A and 1B, are divergent; however, both are predicted to contain a cleavable ER retention signal, followed by an alpha-helical domain and both proteins are 336 amino acids in length. Alignment of zebrafish Torsin1a and Torsin1b with human TorsinA and TorsinB revealed conservation of key functional domains, including consensus sequences for the ATP-binding Walker A domain, the ATP-hydrolysis Walker B domain, and the Sensor 1, and Sensor 2 domains (Figure 4.1A). Both zebrafish isoforms are 59% identical and 78% similar to TorsinA and 57% identical and 77% similar to TorsinB, whereas TorsinA and TorsinB share 66% identity and 77% similarity at the amino acid level. The highest degree of divergence between zebrafish Torsin1 and human TorsinA was observed within the amino terminus: the amino acid sequence encoded by the first exon of Torsin1a protein shares 23% and 28% identity, and 34% and 43% similarity, with human TorsinA and TorsinB, respectively; and Torsin1b shares 20% and 21% identity, and 39% and 35% similarity, with human TorsinA and TorsinB, respectively (Figure 4.1B). Similarly, maximal divergence between Human TorsinA and TorsinB (38.5% identity and 51% similarity) was also within the amino terminus.

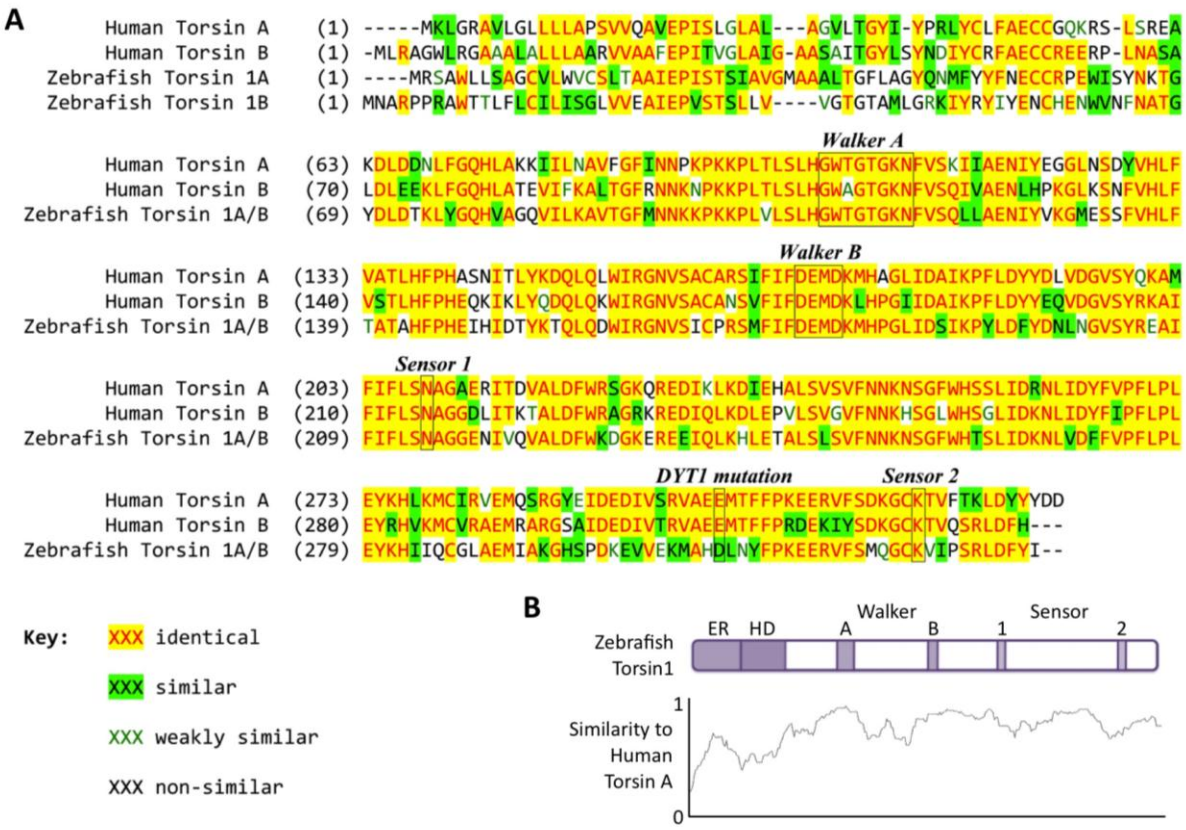

Figure 4.1 – Homology between zebrafish and human Torsin1 family proteins

(A) The AlignX implementation of the ClustalW algorithm was used to align the amino acid sequences of zebrafish Torsin1a and 1b, and human TorsinA and TorsinB. The Walker A (ATP binding), Walker B (ATP hydrolysis), Sensor 1 and Sensor 2 domains are labeled. The position of the glutamic acid deletion associated with DYT1 dystonia is indicated. Identical and similar amino acids at each position of the alignment are colored as shown. **(B)** Zebrafish Torsin 1a is depicted schematically showing the functional domains discussed in the text. Key: ER, endoplasmic reticulum signal; HD, hydrophobic domain. The graph below shows similarity between zebrafish Torsin1A and human TorsinA at each position of a sliding 15-amino acid window of comparison, corresponding to the schematic drawing of Torsin 1 (0=no homology, 1=identity).

4.3 DEVELOPMENT OF AN ANTIBODY AGAINST TORSIN1

In order to better characterize Tosin1, we next developed a polyclonal antibody against a peptide sequence near the carboxyl terminal, which is divergent between Torsin1 and other zebrafish Torsins (Figure 4.2A). Polyclonal antisera to this antigen were raised in rabbits, and affinity-purified against the peptide. The purified antibody was initially tested by probing western blots of protein lysates from HEK293 cells, which were transfected with a construct expressing *tor1_tv2* under the CMV immediate-early promoter, or empty vector as a negative control. A single immunoreactive species of 32kDa was detected in cells expressing *tor1_tv2*, whereas no immunoreactive proteins were present in the cells transfected with empty vector (Figure 4.2B). This demonstrates that the antibody can recognize Torsin1 expressed in cultured cells. Next, we analyzed adult zebrafish brain lysate by western blot (Figure 4.2C). Two bands were detected with apparent molecular weights of 47kDa and 45kDa. Detection of both bands was prevented by pre-incubation of the antibody with the cognate peptide, and neither band was present when blots were probed with pre-immune serum. This result confirms that the 45kDa and 47kDa species contain the cognate peptide sequence, and therefore most likely represent Torsin1. *tor1* is expressed at low levels in embryos, and we did not detect convincing Torsin1-immunoreactive signal during early development. Consequently we were not able to further confirm specificity of the antibody for Torsin1 *in vivo* by showing loss of immunoreactive signal after morpholino knockdown of *tor1* expression (see below).

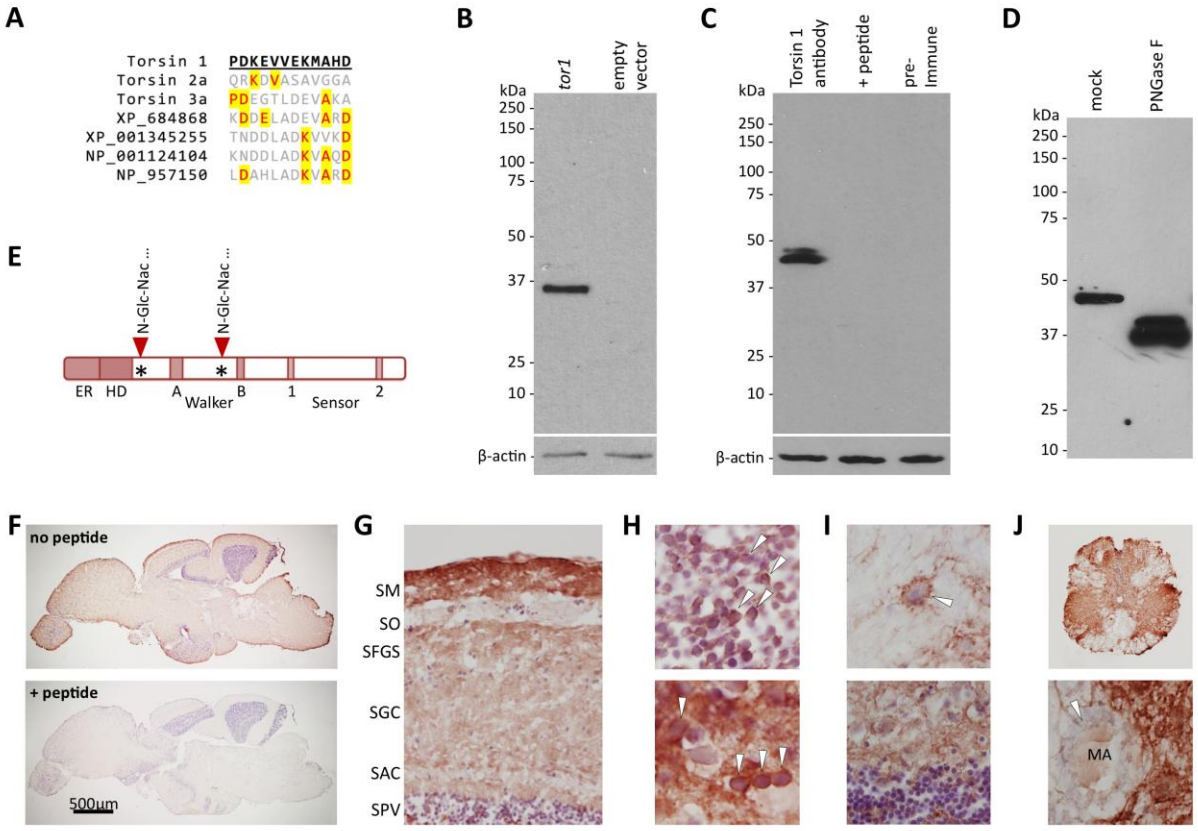

Figure 4.2 – Characterization of a putative Torsin1 antibody

(A) The peptide sequence used to raise polyclonal antibodies to zebrafish Torsin1 is shown underlined in bold. An alignment between torsin1 and the homologous regions of other zebrafish Torsin-like proteins is shown to illustrate the lack of potentially cross-reacting sequences in other Torsins. Amino acids that are identical to Torsin1 at each position are highlighted in yellow. **(B)** HEK cells were transfected with a plasmid encoding Torsin1b (lane 1) or with empty vector (lane 2). A western blot made with lysates from transfected cells was probed with affinity-purified Torsin1 antibody. The blot was then re-probed with an antibody to β-actin as a control for equal protein loading (lower panel). **(C)** Identical samples of zebrafish whole brain lysate were resolved by SDS-PAGE in adjacent lanes of a gel and the resulting

western blot was divided into strips each containing a single lane. The strips were probed with either affinity-purified Torsin1 antibody (lane 1), affinity-purified Torsin1 antibody pre-incubated with the peptide immunogen shown in panel A (lane 2), or pre-immune serum (lane 3). The blots were then re-probed with an antibody to β-actin as a control for equal protein loading (lower panel). **(D)** Whole brain lysate was either treated with PNGase F (lane 2) to remove N-linked carbohydrate moieties, or mock treated without addition of PNGase F (lane 1), prior to SDS-PAGE and immunoblotting with Torsin1 antibody. **(E)** The schematic representation of Torsin1 shows the positions of the consensus N-glycosylation sites. **(F–K)** Adult zebrafish CNS sections were labeled with Torsin1 antibody; immunoreactive structures were revealed by chromogenic histochemistry with a red reaction product. Sections were counterstained with Mayer's hematoxylin so that nuclei appear blue. **(F)** Parasagittal sections of the whole zebrafish brain are shown labeled with Torsin1 antibody. In the lower panel, the antibody was pre-incubated with the peptide immunogen. **(G)** Optic tectum. Key: SM, stratum marginale; SO, stratum opticum; SFGS, stratum fibrosum griseum superficiale; SGC, stratum griseum centrale; SAC, stratum album central; SPV, stratum periventriculare. **(H)** Periventricular lamina of optic tectum (upper panel) and medulla oblongata (lower image), showing cytoplasmic Torsin1 expression in neurons (arrowheads). **(I)** Thalamus (upper panel) and cerebellum (lower panel) showing expression of Torsin1 in neuropil; arrowhead in upper panel shows a neuron surrounded by punctate Torsin1 immunoreactivity that may be present in nerve terminals. **(J)** Spinal cord at low magnification (upper panel) and high magnification (lower panel) showing robust Torsin1 signal in gray matter, but absence of Torsin1 in white matter. The arrowhead in the lower panel shows the myelin sheath surrounding the Mauthner axon (MA).

4.4 GLYCOSYLATION OF TORSIN1 IN THE ZEBRAFISH BRAIN

The apparent molecular weight of the Torsin1 differed between cultured cells and the zebrafish brain *in vivo*. It is known that Torsins are subjected to post-translational modifications, including signal peptide cleavage and N-glycosylation (Hewett et al., 2000; Callan et al., 2007). Pre-incubation of brain lysate with peptide:N-glycosidase F (PNGase F), an amidase that cleaves between asparagine and the innermost N-acetyl-glucosamine (GlcNAc) residue of the oligosaccharide chain of N-linked glycoproteins, altered the electrophoretic mobility of Torsin1, which migrated at 36-38kDa following PNGaseF treatment (Figure 4.2D). This mobility shift demonstrates the presence of N-linked carbohydrate chains totaling approximately 9kDa. The consensus 'sequon' or target sequence for N-glycosylation is N-X-S or N-X-T, where X is any residue except for proline. There are two predicted N-glycosylation sites in Torsin1, at residues 63 and 164 (Figure 4.2E). The lower apparent molecular weight observed in cultured cells suggests that Torsin1 is processed differently in transformed human kidney cells to the physiological processing that occurs in the zebrafish brain *in vivo*.

4.5 EXPRESSION OF TORSIN1 IN THE ZEBRAFISH BRAIN

Sections from adult zebrafish brain were labeled with Torsin1 antibody and processed for immunohistochemistry. Immunoreactive signal was seen in multiple different brain regions and was abolished by pre-incubation of the antibody with the cognate peptide (Figure 4.2F), indicating that the tissue epitope recognized by the antibody is shared by the peptide, and is therefore likely to represent Torsin1. Expression of Torsin1 was abundant in grey matter

regions, such as the optic tectum, cerebellum, brainstem nuclei and central grey matter of the spinal cord (Figures 4.2G-K). Immunoreactivity was especially prominent in the neuropil of the stratum marginale of the optic tectum, the molecular layer of the cerebellum and the dorsal telencephalon. In addition, cytoplasmic labeling was apparent in some larger neurons of the brainstem and diencephalon. White matter tracts, including the optic nerves and tracts, the medial longitudinal fasciculus and long descending tracts of the spinal cord, did not show immunoreactivity for Torsin1. These data suggest that Torsin1 is expressed in the cell body and dendrites of neurons in multiple CNS regions, but is not expressed in myelinated fibers.

4.6 SUBCELLULAR LOCALIZATION OF TORSIN1

The DYT1 dystonia mutation in TOR1A causes deletion of one glutamate residue from an EE motif in the carboxyl terminal of TorsinA. Although the pathophysiological properties of this mutation are yet to be fully elucidated, one striking property of the mutant is relocalization of the protein from the endoplasmic reticulum to the nuclear envelope (Hewett et al., 2000). The homologous region in zebrafish Torsin1 contains the amino acids HD (boxed sequence in Figure 4.1A), precluding mutagenesis studies to determine whether the zebrafish protein undergoes similar relocalization following introduction of the same mutation. However, redistribution of human TorsinA to the nuclear envelope is also observed when null mutations are introduced into the ATP hydrolysis domains of TorsinA (Goodchild and Dauer, 2004). To investigate whether the subcellular localization of Torsin1a and Torsin1b can be altered by similar mutations, zebrafish Torsin1-eGFP fusion proteins were constructed because the antibody described above detected cross-reactive bands when immunoblotting lysates of several cell lines. Both Torsin1a

and Torsin1b isoforms were localized to the cytosol (Figures 4.3A,B) in the mouse dopaminergic MN9D cell line. This distribution pattern is consistent with the diffuse intracellular localization observed with human TorsinA (Hewett et al., 2000). Next, we examined whether null mutations in the conserved ATP binding (Walker a) and ATP hydrolysis domains (Walker B) of Torsin1 altered the cellular redistribution of Torsin1. Similar to human TorsinA, a null mutation (K114T; (Whiteheart et al., 1994; Babst, 1998)) in the ATP binding domain of Torsin1 did not alter the localization of the Torsin1-GFP fusion proteins. However, the E177Q mutation (Whiteheart et al., 1994; Babst, 1998) in the ATP hydrolysis domain resulted in the accumulation of Torsin1-GFP in the nuclear envelope. These results show that zebrafish Torsin1, similar to human TorsinA, can enter the nuclear envelope and a null mutation of the ATP hydrolysis domain results in its sequestration in this location. Zebrafish Torsin1 proteins thus share key aspects of dynamic cellular localization with human TorsinA, and this depends on at least some of the same functional domains. This suggests that zebrafish Torsin1 and human TorsinA, may share a common set of interacting proteins and cellular functions.

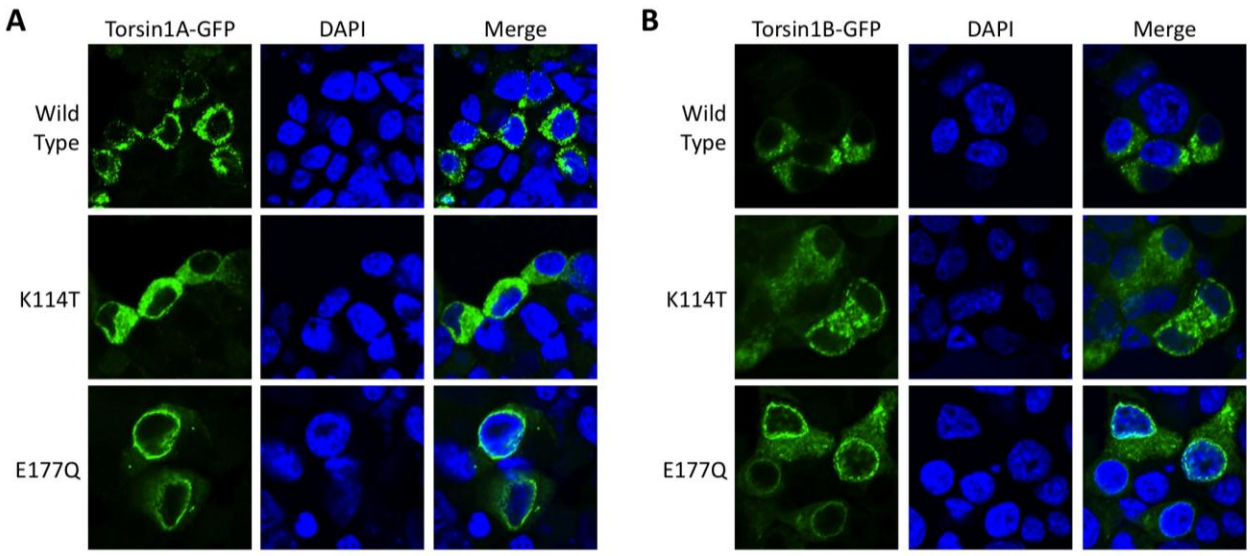

Figure 4.3 - ATP-binding and ATP-hydrolysis mutations in Torsin1 alter cellular localization

MN9D cells were transfected with expression plasmids encoding either **(A)** Torsin1a-eGFP or **(B)** Torsin1b-eGFP fusion proteins. The images show single confocal planes through transfected cells demonstrating GFP fusion protein localization (green, left column) relative to the nucleus (DAPI counterstain, blue, center column). For each panel, the top row of images shows wild type Torsin1, the middle row of images shows a Torsin1[K114T] mutant, which disrupts the Walker A (ATP-binding) domain, and the bottom row shows a Torsin1[E177Q] mutant, which disrupts the Walker B (ATP hydrolysis) domain.

4.7 *TOR1* IS NOT ESSENTIAL FOR EARLY LARVAL DEVELOPMENT

To determine the function of *tor1* during larval development, we targeted its expression by using morpholino antisense oligonucleotides (MOs). Since we could not reliably detect Torsin1 protein in embryos using the antibody described above, we opted to use splice site MOs to

inhibit pre-mRNA processing, because knockdown could be verified readily by RT-PCR. Initial studies showed that a combination of two MOs targeting the exon2/intron2 and exon3/intron3 splice donor consensus sequences caused both exons 2 and 3 to be excluded from the transcript (Figure 4.4A). This resulted in a frame shift and formation of a premature stop codon, which abrogated expression of the Walker B domain and both Sensor domains (Figure 4.4B). This combination of MOs efficiently disrupted expression of *tor1* mRNA up to 5 days post fertilization (dpf) (Figure 4.4A). To exclude phenotypes attributable to adverse effects from microinjection, and non-specific toxicity of MOs, we compared *tor1* knockdown zebrafish with wild-type animals, and with animals injected with control non-targeting MO.

There were no differences in survival between uninjected, control MO injected, or *tor1* MO injected embryos. Zebrafish from all three experimental groups showed normal morphological development through day 7 (not shown). We next evaluated development of dopaminergic neurons, because the function of the dopamine system is disrupted in some patients with dystonia. Whole mount RNA in situ hybridization was employed to label developing dopaminergic neurons using a probe specific to the *slc6a3* transcript encoding the dopamine transporter, which is expressed exclusively in dopamine neurons (Holzschuh et al., 2001; Bai and Burton, 2009). We did not observe any differences between wild type larvae and larvae lacking Torsin1 in the position of dopaminergic neurons or in the intensity of *slc6a3* expression at 48hpf or 72hpf (Figure 4.4C and data not shown). The total number of diencephalic *slc6a3* $^{+}$ neurons was determined in each population of zebrafish; loss of Torsin1 did not affect the number of dopamine neurons at these developmental points (Figure 4.4D). We conclude that, similar to murine *TOR1A*$^{-/-}$ lines, loss of Torsin1 in zebrafish did not give rise to morphological abnormalities of the dopamine system during development.

Finally, we asked whether loss of Torsin1 provoked abnormalities of motor function by employing a previously described assay (Cario et al., 2011; Farrell et al., 2011) to quantify spontaneous propulsive movements in uninjected larvae, control MO injected larvae, and larvae lacking Torsin1. Compared with controls, larvae lacking Torsin1 did not show statistically significant differences in mean velocity, percent time moving, active velocity, mean duration of movement bursts, or mean rest duration between movements at 4 – 6 dpf (Figures 4.4E-I show data at 5 dpf). At earlier developmental time points before 4dpf, when *tor1* knockdown was most prominent, larval propulsive movements are relatively infrequent and somewhat variable, making it difficult to detect differences between experimental groups (Farrell et al., 2011). To evaluate zebrafish between 1 – 4 dpf, we employed a second method that examines propulsive and non-propulsive movements by determining changes in pixel grayscale values from frame to frame of a video stream, rather than detecting displacement of the larval centroid. The pixel quantification method is sensitive to both propulsive and non-propulsive movements, such as coiling and re-orientation movements, and consequently has previously allowed us to detect differences in motor activity between experimental groups at early developmental points (Milanese et al., 2012). However, even using this method, we did not detect differences between the motor activity of controls animals lacking Torsin1 between 1-4dpf (data not shown). Taken together, these findings show that Torsin1 is not critical for early morphological development and early development of motor function.

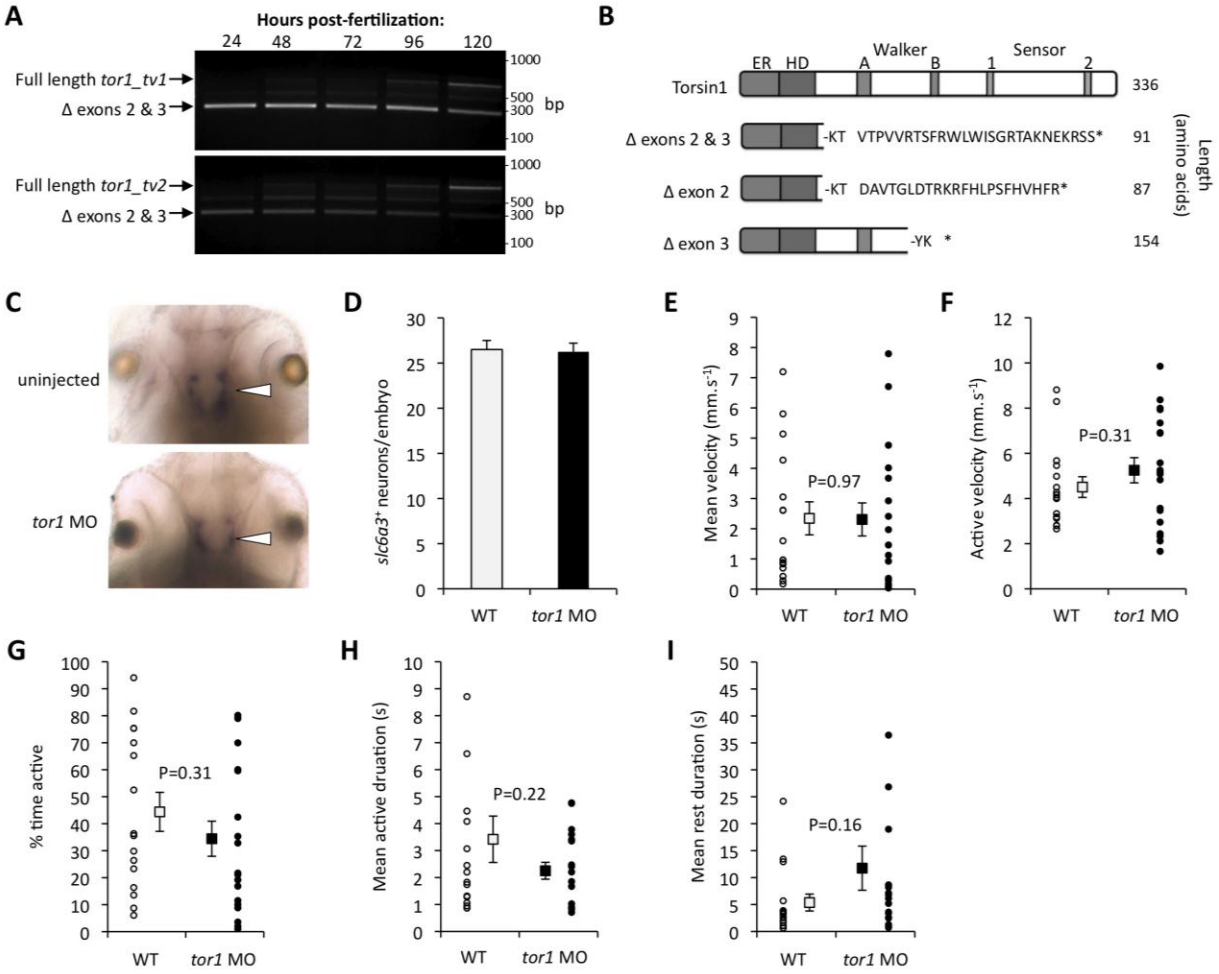

Figure 4.4 – Torsin1 is dispensable for early development of the motor system

(A) Single-cell zebrafish embryos were microinjected with morpholino oligonucleotides designed to block splicing of *tor1* exons 2 and 3 (see figure 2). At the times indicated between 24 and 120 hours post-fertilization, RNA was harvested from developing zebrafish and subjected to RT-PCR using primers specific for *tor1_tv1* (upper panel) and *tor1_tv2* (lower panel). The pictures show ethidium bromide stained agarose gels after the RT-PCR products were resolved by electrophoresis. The positions of PCR products corresponding to wild-type *tor1* mRNA and the transcript lacking exons 2 and 3 are shown. **(B)** A schematic representation of the predicted protein products produced by transcripts lacking exons 2, 3 or both exons. It is not known if any

of these truncated products is stable. **(C)** Whole mount RNA *in situ* hybridization was carried out using a cRNA probe for *slc6a3* (‘*dat*’) to localize dopaminergic neurons. Representative dorsal views are shown of the brains of an uninjected control embryo (upper panel) and an embryo lacking Torsin1 (lower panel) at 48 hours post-fertilization. The diencephalic group of developing dopaminergic neurons is indicated by an arrowhead. **(D)** The total number of slc6a3^{+} cells in the diencephalon was counted in zebrafish lacking Torsin1 and control zebrafish at 48hpf. Graphs show mean + standard error. **(E–I)** Spontaneous movements of uninjected wild-type zebrafish (n=16) and zebrafish injected with MO targeting *tor1* (n=19) were recorded at 5dpf in 96-well plates using a video camera. Recordings were analyzed to determine: **(E)** mean velocity (total displacement/total time of recording); **(F)** active velocity (displacement/time spent moving); **(G)** % time moving; **(H)** mean duration of active episodes; and **(I)** mean duration of rest episodes. For each graph, values for each individual larva are shown as small circles and the mean for the group shown as a filled square. Error bars shown standard error.

4.8 DISCUSSION

In order to characterize the Torsin1 protein, we developed a novel antibody directed towards its C-terminus. We showed that: (i) the antibody recognizes a protein produced by expression of *tor1* in cultured cells; and (ii) pre-incubation of the antibody with its cognate peptide prevented it from detecting epitopes on either western blot or tissue sections. These controls support the conclusion that the antibody specifically detected Torsin1 in zebrafish brain. However, loss of immunoreactive signal in genetic knockout tissue is generally considered a 'gold standard' for proving antibody specificity (Saper, 2005); in this case, the absence of clearly demonstrable Torsin1 immunoreactivity during early development precluded confirmation of specificity by MO-mediated knockdown of the *tor1* transcript. Formal proof that the antibody specifically detects Torsin1 in the zebrafish brain therefore awaits the development of stable *tor1*$^{-/-}$ lines. Nonetheless, the availability of this antibody allowed some initial conclusions to be drawn about the nature of Torsin1: it is expressed as two species in CNS, a major 47kDa form and a minor 45kDa form; both species are heavily N-glycosylated, showing loss of 9kDa carbohydrates after deglycosylation; and the protein localizes to neuronal somatic cytoplasm and neuropil, but was not detected in mylinated fibers. These properties are similar to those previously reported for human TorsinA, and are compatible with an endoplasmic reticulum subcellular localization in neurons. The origin of the two protein species is unclear; the predicted molecular weight of both Torsin1a and Torsin1b is similar (38.2 and 38.4 kD, respectively) and approximately the size of the major protein isoform found after

deglycosylation. It is possible that different post-translational modifications are responsible for the two forms, or that signal peptide cleavage is directed to a different site in the nascent protein by each of the unique N-termini.

Relocalization of TorsinA from the endoplasmic reticulum to the nuclear envelope is a hallmark of the dystonia-associated ΔE mutation. This relocalization can also be induced by mutations in the ATP-hydrolysis domains of TorsinA. Although we were not able to introduce the ΔE mutation into Torsin1, because of lack of sequence conservation in this region of the C-terminus, we have demonstrated that zebrafish Torsin1 can be made to accumulate in the nuclear envelope by the introduction of an ATP-hydrolysis null mutation in the Walker B domain. Interestingly, this relocalization was observed in a heterologous murine cell line. Trafficking of Torsins between nuclear envelope and endoplasmic reticulum is thought to depend on their interactions with specific substrates and with other Torsin molecules in homohexameric complexes. This raises the possibilities that the zebrafish protein may interact with (i) one or more mammalian nuclear envelope proteins, possibly some of the same proteins that interact with endogenous mammalian torsins; or (ii) endogenous mammalian TorsinA to form complexes. These possibilities are not mutually exclusive and both are equally compatible with the data presented. For example, even if zebrafish Torsin1 did not recognize murine nuclear envelope substrates, disruption of its ATPase domain may have prevented a Torsin1/TorsinA heterohexamer from disengaging the substrate. These data show an intriguing degree of functional interaction between the heterologous proteins and imply that at least some of the cellular roles may be phylogenetically conserved. It will be of interest to determine whether TorsinA behave similarly in zebrafish cells, since this will have significant implications for

generating a zebrafish model of DYT1 dystonia based on transgenic expression of human TorsinA[ΔE].

We did not identify any morphological or neurobehavioral abnormalities resulting from loss of Torsin1 early in development. This result is consistent with findings in murine *TOR1A*$^{-/-}$ lines, in which the first observed phenotypic abnormality was perinatal lethality due to lack of feeding. In the zebrafish, the analogous developmental point occurs around 5dpf, when patterning of the nervous system is nearly complete and larvae begin actively pursuing food. Unfortunately, by this time point, the expression of both *tor1* transcripts had largely recovered from transient MO-mediated knockdown; consequently it remains unclear whether loss of *tor1* in zebrafish at this developmental point would provoke similar abnormalities to the mouse. DYT1 dystonia patients usually first show symptoms during late childhood or adolescence. Consequently, it is expected that critical CNS functions of TorsinA, of relevance to the pathogenesis of dystonia, could occur much later during development. In order to address this possibility and to elucidate the role of Torsin1 during later development, it will be necessary to develop a stable *tor1*$^{-/-}$ allele. This would not only allow unambiguous evaluation of Torsin1 functions during later time points, but will also facilitate validation of Torsin1 antibodies for further biochemical studies.

In conclusion, the zebrafish may provide a powerful model system to study the neuronal functions of Torsin1 *in vivo*, and an opportunity to study how the functions of Torsin1s have evolved. This work provides essential background for future studies on gene function and raises the intriguing possibility of a transgenic zebrafish model of DYT1 dystonia, with potential applications in understanding pathogenesis and developing novel treatments. The possibility of generating a zebrafish model of DYT1 dystonia will be discuss in the following chapters.

5.0 GENERATION OF TRANSGENIC ZEBRAFISH OVEREXPRESSING WILD TYPE, OR THE DYSONTIA-ASSOCIATED MUTANT, TORSINA

5.1 INTRODUCTION

Following the characterization of the endogenous zebrafish Torsin1, I set out to develop a zebrafish model for DYT1 dystonia by creating stable transgenic lines overexpressing either the human TorsinA or the TorsinA[ΔE]. Several lines of evidence suggests that TorsinA[ΔE] is a loss-of-function allele (Torres et al., 2004), as opposed to a toxic gain-of-function, which exerts a dominant-negative effect through oligomerization with the wild-type TorsinA, possibly decreasing or abolishing the functional activity of TorsinA hexamers. In line with this hypothesis, overexpression of TorsinA[ΔE] in several different mouse models of DYT1 dystonia has produced behavioral, neurochemical, and electrophysiological phenotypes (Dang et al., 2005; Goodchild et al., 2005; Sharma et al., 2005; Shashidharan et al., 2005; Grundmann et al., 2007; Yokoi et al., 2007; Page et al., 2010).

Several methods exist to create stable transgenic zebrafish. The first transgenic zebrafish were generated by microinjecting linearized plasmid DNA into the cytoplasm of one-cell stage embryos (Stuart et al., 1988). This results in concatermerization of DNA, which remains episomal and is distributed in a mosaic manner during subsequent cell divisions. Inefficient integration of concatemers during late cell divisions results in single integration events of many

tandem copies of the transgene and significant mosaicism. Consequently, the technique is very inefficient, necessitating screening many fish to identify germline transgenic founders. Two technical advances, meaganucleases and transposons, have substantially improved the efficiency by which foreign DNA can become inserted into the genome for the generation of transgenic models (Figure 5.1).

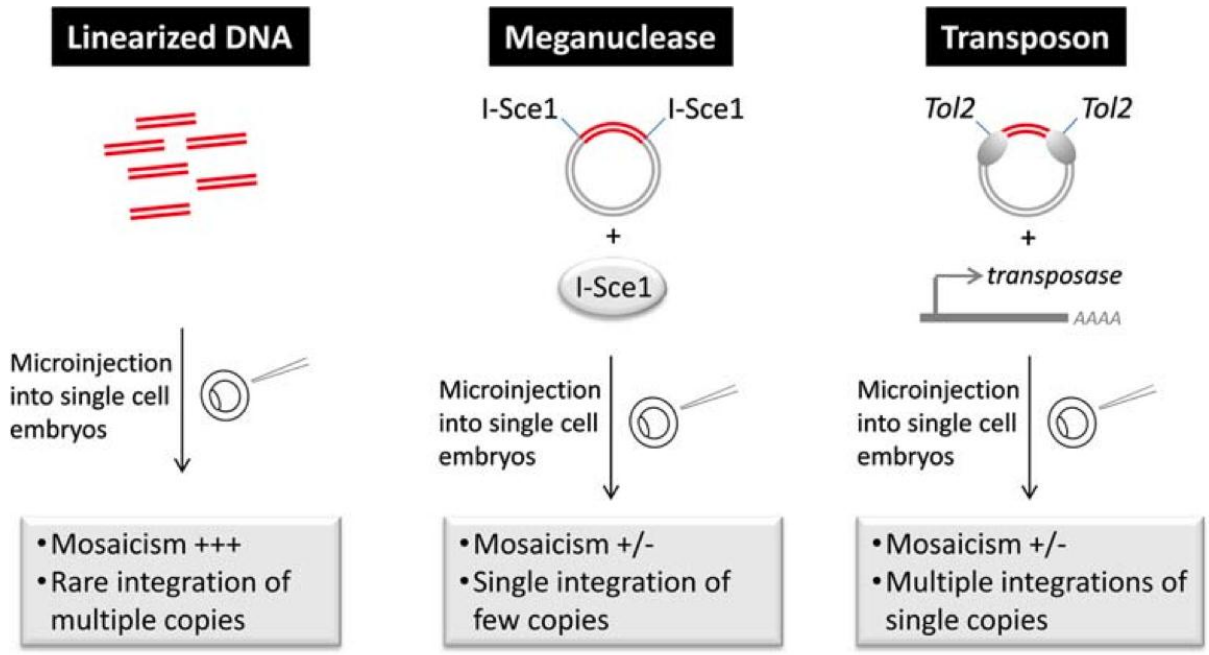

Figure 5.1 Methods for the construction of stable transgenic zebrafish.

The summary schematic illustrates the three major techniques used for generating stable lines of transgenic zebrafish .

The meganuclease I-sce1 is an intron-encoded endonuclease from saccharomyces cerevisiae (Jacquier and Dujon, 1985). I-Sce1 cleaves DNA at an 18 bp sequence-specific recognition site that is not present within the zebrafish genome. Co-injection of I-sce1 with a

transgene plasmid, in which the transgene expression cassette is flanked by I-sce1 sites, into zebrafish embryos substantially reduces mosaicism, allowing more efficient examination of the expression pattern of reporter constructs in transient assays, and improving the rate of transmission of the transgene from germline F0 mosaics to their progeny, F1 transgenic founders (Thermes et al., 2002). In addition, the single site of integration usually contains a low number of copies of the transgene (Thermes et al., 2002). The mechanisms underlying these observations are uncertain. I-sce1 shows slow enzymatic turnover, because the monomeric enzyme has high affinity for one of the cleavage products (Grabher and Wittbrodt, 2008). I-Sce1 may prevent concatemerisation that usually occurs after microinjection of linearized DNA, by limiting access of ligases to cut ends and by digesting concatemers that do occur. The efficiency of recombination may involve enhanced nuclear import of cleaved DNA and interaction of I-Sce1 with the double strand break repair system. It has been reported that careful optimization of parameters using this technique almost completely eliminates mosaicism in animals with genomic integration, and allows transmission of the transgene from F0 to F1 fish with a near-Mendelian rate (Thermes et al., 2002; Soroldoni et al., 2009). Within the Burton laboratory, the rate seldom approaches this level, but is substantially better than linearized plasmid injection. In addition, the single site of integration has resulted in simple Mendelian transmission of a variety of transgenes in subsequent outcrosses, facilitating the generation of double transgenic reporter zebrafish (Bai et al., 2009).

Transposons are mobile DNA elements; type 2 transposons encode an enzyme, transposase, which mediates excision of the transposon from the genome and its re- insertion at another location. Transposons have been used extensively in Drosophila genetics, but their application is species specific and until recently no vertebrate transposons had been identified.

The discovery of a transposon, Tol2, in the genome of the freshwater fish medaka (Koga et al., 1996) allowed subsequent development of a powerful genetic tool for zebrafish transgenesis (Kawakami et al., 2000). By deletion of the open reading frame of the transposase from Tol2, a non-autonomous element was generated, which could insert into the genome when the transposase was supplied *in trans*. By generating a transgene plasmid, in which the transgene expression cassette is flanked by the non-autonomous transposon elements, and co-injecting the plasmid into zebrafish embryos along with mRNA encoding transposase, highly efficient integration of the transgene into the genome occurs. This approach most frequently yields multiple single copy integration events, although it is possible to select single copy integrants if necessary, by southern blot. The technique is efficient and has been used increasingly since its introduction and subsequent refinement (Kawakami, 2004), because it is necessary to inject and screen a smaller number of fish than other techniques in order to identify stable transgenic lines. Despite this advantage of Tol2-mediated transgenesis, I decided to use meganuclease-mediated transgenesis because single integration events would facilitate characterization of the transgenic lines, and produce more stable levels of transgene expression during subsequent outcrosses.

I was then faced with the decision of which promoter to use to drive transgene expression. In order to generate transgenic models of neurological disorders in zebrafish, appropriate cis-acting regulatory elements must be used to drive transgene expression in a suitable temporal and spatial expression pattern, and at appropriate levels, to model pathology. The first transgenic zebrafish suffered from inactivation of transgenes, possibly because of use of non-zebrafish promoter elements, and the use of zebrafish cis-acting regulatory regions has allowed development of stable lines with reliable expression of transgenes (Higashijima et al., 1997; Long et al., 1997). In the case of DYT1 dystonia, the *TOR1A* gene is expressed ubiquitously in

neurons throughout the nervous system (Augood et al., 1999), and the specific neuronal circuits disrupted by TorsinA[ΔE] expression are unknown. For this reason, expression of TorsinA[ΔE] in many different neuronal types, widely distributed throughout the neuraxis, would be desirable. Three such promoter elements have been described, and two have been used to develop stable transgenic zebrafish models for other neurological disorders.

Deletion analysis showed that a fragment of the upstream sequence of *gata2*, lacking hematopoietic regulatory elements and containing a neuronal enhancer, was able to drive robust expression of GFP in developing neurons (Meng et al., 1997). This element was subsequently used to express a Tau-GFP fusion protein in a transient zebrafish model of Tauopathy (Tomasiewicz et al., 2002). However, stable transgenic lines using this element to drive transcription have not yet been described, and its activity in the adult zebrafish CNS is unknown.

The second pan-neuronal promoter element reported was derived from the zebrafish *huc* gene, which is the homologue of the *Drosophila elav* gene, and encodes an RNA binding protein, HuC/D, commonly used as an early neuronal marker (Kim et al., 1996). A 2.8 kb fragment of the proximal flanking region was sufficient to drive robust pan-neuronal expression in embryos (Park et al., 2000), and the promoter has subsequently been used to generate a stable model of Tauopathy (Paquet et al., 2009). Both the *huc* and *gata2* promoter elements are active in neurons, however, the early time points at which they become transcriptionally active are a potential source of concern for model construction; expression of TorsinA[ΔE] early in embryogenesis could provoke developmental anomalies or result in lethality, as knocking out *tor1* homologs in other species inhibits development (Basham and Rose, 1999; Goodchild et al., 2005; Wakabayashi-Ito et al., 2011), and would make the creation of stable transgenic lines impossible.

In view of this concern, I decided to use a promoter element derived from the *eno2* gene, which encodes the neuron-specific γ-enolase isoenzyme, and was identified as a marker of differentiated neurons (Bai et al., 2007).

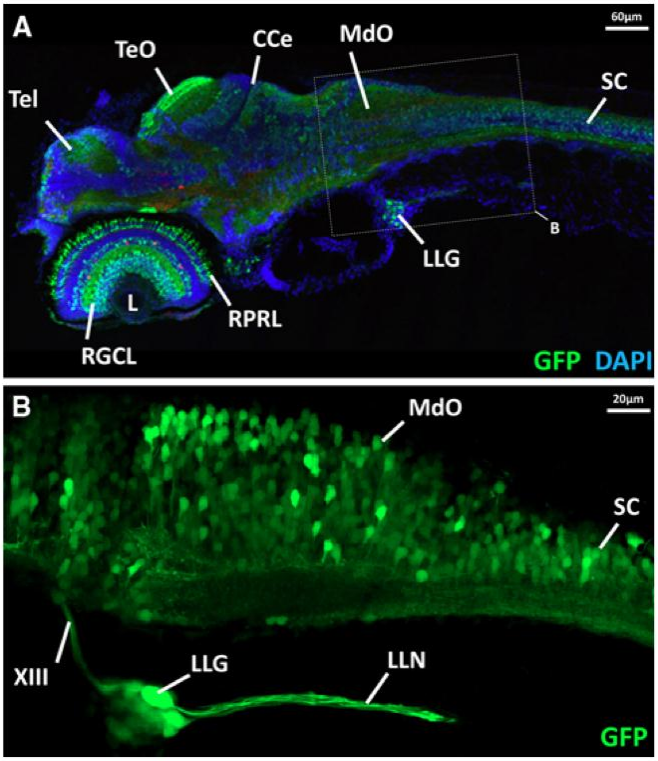

Figure 5.2 Zebrafish eno2 promoter construct.

The pictures show micrographs of Tg(*eno2*:egfp) zebrafish larvae in order to demonstrate widespread neuronal expression of a GFP transgene under control of the 12 kb *eno2* element that was developed for generation of transgenic models of neurological disease. **(A)** The oblique sagittal section is labeled for transgene expression (GFP; green) and a nuclear counterstain (blue: DAPI) to facilitate identification of anatomical landmarks. GFP expression is seen throughout the neuraxis, and is particularly prominent in the retina and optic tectum. *Tel* telencephalon, *TeO*

optic tectum, *CCe* cerebellum, *MdO* medulla oblongata, *SC* spinal cord, *RCGL* retinal ganglion cell layer, *L* ocular lens, *RPRL* retinal photoreceptor layer, *LLG* lateral line ganglion. The boxed area marks the approximate region shown at higher magnification in (B). **(B)** A Z-projection is shown of multiple confocal planes imaged from a live intact Tg(*eno2*:GFP) zebrafish, illustrating GFP expression in neurons of the CNS and PNS. *LLN* lateral line nerve, *XIII* eighth cranial nerve, otherwise same as (A) (Sager et al., 2010).

Expression of eno2 was detected at low levels by 24hpf, but the abundance of the mRNA increased substantially in the brain and spinal cord between 60 and 72 h post-fertilization, and expression persisted at high levels into adulthood, in a pan-neuronal pattern. The regulatory region of eno2 is complex; there is an untranslated first exon, and the first intron contains a CpG island that appears important for promoter activity. A 12 kb fragment of the promoter, including the first intron, was active in driving reporter gene expression in neurons throughout the brain and spinal cord from 48 h post-fertilization through adulthood, including neuronal types relevant to neurodegenerative diseases, such as cerebellar Purkinje cells and cholinergic neurons (Figure 5.2) (Bai et al., 2007). The eno2 construct was also highly active in the retina and visual pathways (Bai et al., 2009). This element was used to generate a transgenic zebrafish Tauopathy model (Bai et al., 2007) and is currently being used by a number of groups for a variety of applications.

Because morpholino experiments, and mRNA microinjections (described below) did not produce a detectable motor phenotype, potentially as a result of mosaicism and/or the transient nature of the experiments, the pan-neuronal *eno2* promoter was also used to maximize the

possibility of identifying a phenotype relevant to DYT1 dystonia. In this chapter I report that co-expression of the zebrafish Torsin1 and the human TorsinA[ΔE] proteins resulted in the relocalization of Torsin1 to the NE *in vitro*, and transient overexpression of TorsinA[ΔE] in zebrafish larvae resulted in accumulation of the protein to cytoplasmic aggregates. Furthermore, I present the creation of stable transgenic zebrafish overexpressing either wildtype or TorsinA[ΔE] under control of the *eno2* promoter. These transgenic zebrafish develop normally and show no differences in survival rates. Inhereitance of the transgene in each of these lines follows a Mendelian pattern, demonstrating that each line contains a single site of transgene integration. Expression of the transgene can be detected by epifluorescent microscopy beginning at 3dpf, and in adult transgenic by immunoblotting whole brain lysate.

5.2 CO-EXPRESSION OF HUMAN TORSINA AND ZEBRAFISH TORSIN1 IN VITRO

As a first step to examine the feasibility of overexpressing TorsinA[ΔE] in the zebrafish, it was therefore necessary to determine if zebrafish Torsin1 is capable of interacting with human TorsinA. Because the antibody presented in Chapter 4 cannot be used to confirm immunoprecipitation of the Torsin1 protein (data not shown), I addressed this question be exploiting the observation that human TorsinA[ΔE] relocalizes wildtype human TorsinA to the nuclear envelope (Goodchild and Dauer, 2004). In line with this observation, I first asked whether human TorsinA[ΔE] would similarly relocalize zebrafish Torsin1 to the NE when both proteins were co-expressed. MN9D cells were first transfected with either Torsin1 isoform fused

to eGFP (Figure 5.3A). Both Torsin1 isoforms appeared to localize to cytoplasmic puncta, which co-localized with protein disulfide-isomerase (PDI), a marker for the endoplasmic reticulum. Next, cells were co-transfected with a single Torsin1 isoform and wildtype human TorsinA fused to mRFP (Figure 5.3B). Coexpression of Torsin1 and the human TorsinA did not change the localization compared to when either protein was expressed alone, and both proteins colocalized with PDI. Interestingly, co-expression of either Torsin1 isoform with the human TorsinA[ΔE] caused both proteins to accumulate in the nuclear envelope of MN9D cells (Figure 5.3C), similar to what was observed when the human wildtype and TorsinA[ΔE] were co-expressed. This result suggests that human TorsinA and zebrafish Torsin1 are able to interact and that human TorsinA[ΔE] is able to trap zebrafish Torsin1 in the nuclear envelope, mostly likely by the formation of interspecies hexamers.

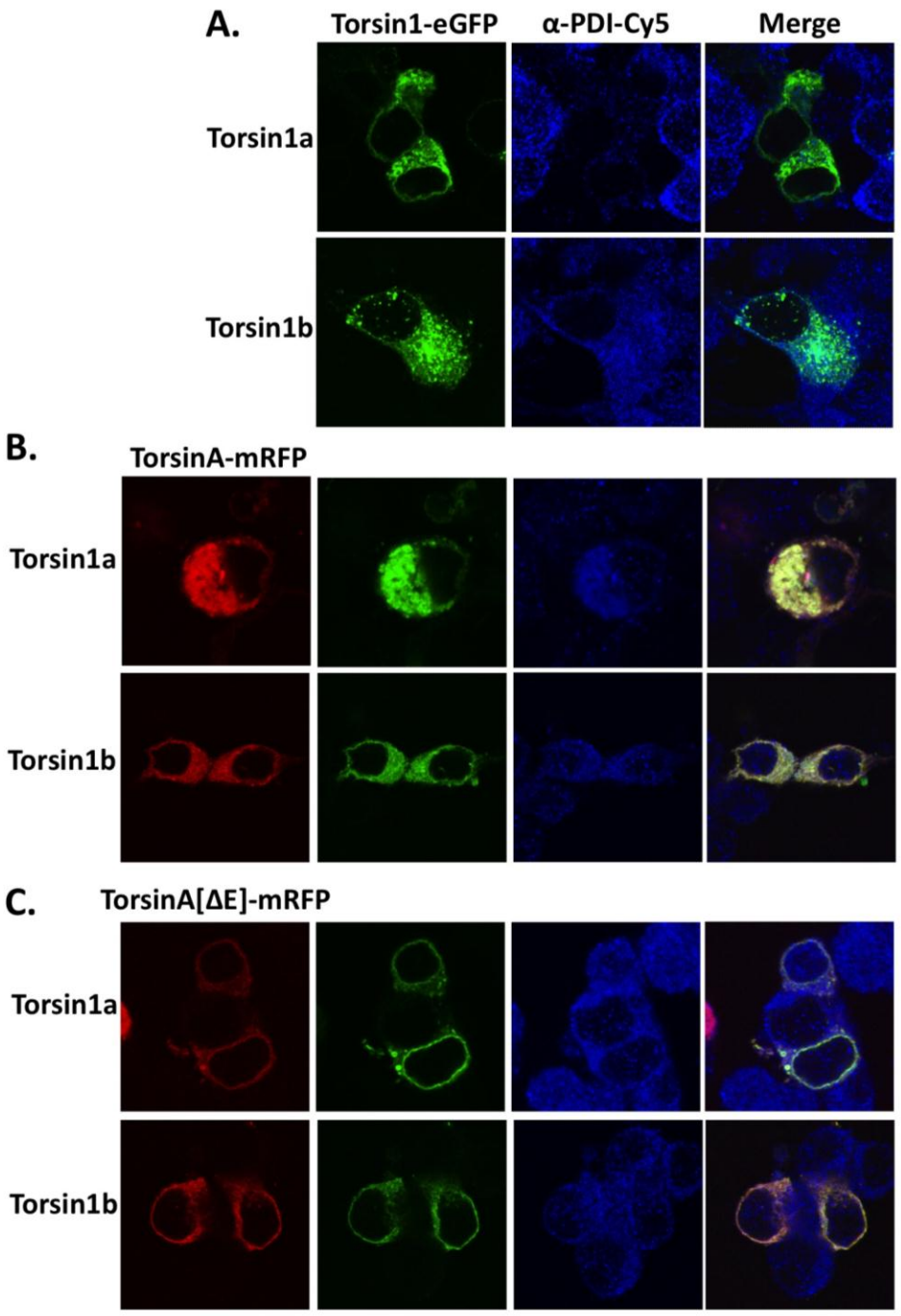

Figure 5.3 Co-expression of zebrafish Torsin1 and human TorsinA in vitro

(A) Both Torsin1 isoforms were fused to eGFP, expressed in MN9D cells (A, first column), and immunostained for PDI (middle column). Co-localization is presented in the merge image (last

column). Cells were then cotransfected with both Torsin1 isoforms and either the wild type TorsinA **(B)** or TorsinA[ΔE] **(C)** fused to mRFP. In both (B) and (C), the first column shows the localization of human TorsinA-mRFP fusion protein, the second column shows the localization of zebrafish Torsin1-eGFP fusion protein, the third column shows the immunostaining for PDI, and the final column presents a merged image of the first three columns.

5.3 EXPRESSION OF HUMAN TORSINA IN ZEBRAFISH LARVAE

I next wanted to investigate if the distribution of human TorsinA would be altered by the [ΔE] mutation in the context of the cellular environment of the zebrafish CNS. To examine this, 1 ng of mRNA encoding either wildtype TorsinA or TorsinA[ΔE] fused to either mRFP or eGFP (respectively) was transcribed *in vitro* and injected into one-cell stage embryos. Expression of either fusion protein did not produce abnormalities in the gross morphological development or spontaneous movement of larval fish (data not shown). These results were similar to what was observed with morpholino knockdown of the endogenous *tor1* gene. Between 3-5 dpf, embryos were examined for localization of the TorsinA fusion protein. In all cell types of the developing larvae expressing wildtype TorsinA, the protein was found diffusely within the cytoplasm (Figure 5.3, neurons in the hindbrain). In contrast, TorsinA[ΔE] was found in large clusters of cytoplasmic fluorescence. Due to the relatively small ring of cytoplasm that surrounds the large nuclei of developing zebrafish neurons, it is difficult to determine whether the TorsinA[ΔE] is accumulating within the NE, as has been observed in the rat model of DYT1 dystonia (Grundmann et al., 2012). Interestingly, when both the wildtype and *TOR1A[ΔGAG]* mRNA

was co-injected into zebrafish embryos, the TorsinA[ΔE] was able to recruit the wildtype protein into these large cytoplasmic aggregates, possibly by the formation of hexamers containing both the wildtype and mutant protein. Notably, this did not occur in all neurons coexpressing both wildtype and TorsinA[ΔE], but was primarily observed in neurons which appeared to be more strongly expressing the mutant protein; conversely, neurons which appeared to be expressing the wildtype TorsinA at higher levels, showed a more diffuse localization of both the wildtype and TorsinA[ΔE]. Although I did not detect a strong NE ring of TorsinA[ΔE] in zebrafish neurons, as was observed in transfected MN9D cells, the formation of TorsinA[ΔE] inclusion bodies has been observed in several neuronal groups in the hindbrain of patients with DYT1 dystonia (McNaught et al., 2004), and suggests that zebrafish cellular environment is able to recapitulate aspects of TorsinA[ΔE] relocalization.

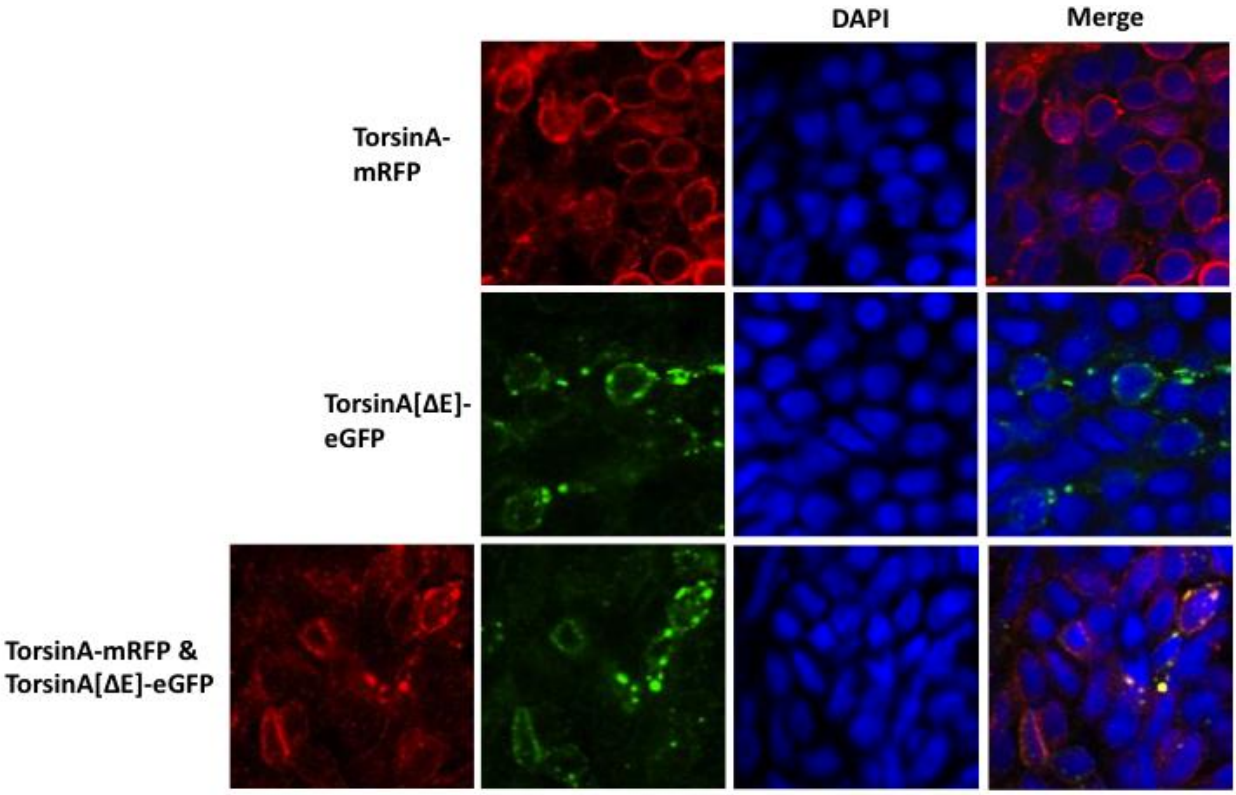

Figure 5.4 Co-expression of TorsinA and TorsinA[ΔE] in zebrafish larvae

Zebrafish embryos were injected with mRNA encoding TorsinA-mRFP (top row), TorsinA[ΔE]-eGFP (middle row), or both TorsinA-mRFP and TorsinA[ΔE]-eGFP (bottom row). All sets of images are from the hindbrain region of 4dpf larvae, counterstained with DAPI (second to last column).

5.4 CREATION AND IDENTIFICATION OF FOUNDER LINES AND PROPOGATION OF F1 AND F2 GENERATIONS

Although we were unable to identify a movement phenotype in mRNA injected larvae, we rationalized that this could be due to two potential confounding factors of the experimental technique: i) mRNA injection results in a mosaic expression pattern, and ii) expression of mRNA is transient and is no longer visible at 6 dpf, precluding identification of a phenotype that may occur later in development. To circumvent these confounding issues, I decided to develop stable transgenic lines which overexpress either the wildtype TorsinA or TorsinA[ΔE] pan-neuronally, under the control of the *eno2* promoter (Bai et al., 2007; 2009). A 12 kb fragment of the *eno2* gene, starting 8kb upstream of the transcriptional start site though the translational start site in exon 2, was previously determined to be sufficient to drive transgene expression in neurons of the zebrafish CNS, beginning between 2-3dpf and continuing through adulthood. This 12 kb fragment was captured from the zC51M24 genomic BAC clone by gap repair recombination into an acceptor plasmid encoding either wildtype or TorsinA[ΔE], in frame to the 3' *eno2* homologous arm at the 5' end of the TorsinA coding sequence and GFP-poly(A) at the 3' end. The resulting plasmids contained the 12 kb *eno2* fragment described above, with *TOR1A*-eGFP-PolyA inserted in frame with exon 2 of the *eno2* gene, as well as I-Sce1 meganuclease sites flanking the entire cassette. These plasmids were microinjected into one-cell stage zebrafish embryos, and ~60 embryos for each transgene were raised to adulthood. Germline transmission of the transgene was determined by outcrossing F0 fish to uninjected AB fish and examining embryos for GFP expression. Three F0 fish from the wildtype *TOR1A* injections, and two F0 fish from the *TOR1A*[ΔGAG] injections, were identified as being capable

of germline transmission of the transgene, suggesting a transgenesis rate of 3-4%, similar to what has been previously reported with I-Sce1 transgenesis with the eno2 promoter (Bai et al., 2007). Independent transgenic lines were established from each of the germline F0 fish, and a third TorsinA[ΔE] line was generated from one of the two F0 fish. The transgene alleles for the Tg(*eno2*:TOR1A-eGFP) fish were designated Pt450-452 inclusive, and the transgene alleles for the Tg(*eno2*:TOR1A[ΔE]-eGFP) were designated Pt453-455 inclusive. It is unknown whether the Pt454 and Pt455 lines represent independent germline integration events, or whether these two lines are representatives of the same integration event, as these two lines were derived from the same Tg(*eno2*:TOR1A[ΔE]-eGFP) F0 fish. For clarity, Pt450-454 will herein be referred to as wtTOR1A Lines 1-3 respectively, and Pt453-455 will be referred to as TOR1A[ΔE] Lines 1-3 respectively.

5.5 EXPRESSION OF TRANSGENE IN F2 GENERATION FISH

Expression of the transgene in the F2 generation was determined by resolving whole brain lysate of two fish from each line using SDS-PAGE, and probing for GFP expression by immunoblot (Figure 5.5). Whole brain lysate from AB and Tg(*eno2*:eGFP) fish was used as a negative and positive control (respectively) for GFP detection, and immunoblotting for ß-actin served as a loading control for each sample. Although only two fish were analyzed from each line, the expression the wtTorsinA-eGFP fusion protein varied between the individual, both between and within transgenic lines. wtTOR1A Line 2 showed the most variability between fish, while wtTOR1A Line 3 showed less variability, but weaker expression. Surprisingly, expression of the wtTorsinA-eGFP fusion protein in wtTOR1A Line 1 was below the detectable threshold of the

technique, suggesting silencing of the transgene between 5 dpf and adulthood. Expression of the TorsinA-eGFP fusion protein was significantly more stable in TOR1A[ΔE] transgenic lines. TOR1A[ΔE] Line 2 showed a slightly higher expression of the TorsinA[ΔE]-eGFP fusion protein, and was expressed at similar levels in both animals. TOR1A[ΔE] Line 3, also showed a similar expression level between animals, but expression was somewhat weaker when compared to TOR1A[ΔE] Line 2. Expression of the TorsinA[ΔE] -eGFP fusion protein was more variable between animals of TOR1A[ΔE] Line 1. Despite the variability in expression of the transgene between, and within, different transgenic lines, the ratio of GFP+ embryos to those lacking detectable GFP, at 3-4 dpf, was approximately 1:1 in all six transgenic lines (Table 5.1), suggesting that each of these lines are the product of a single integration event that is inherited following the rules of Mendelian genetics.

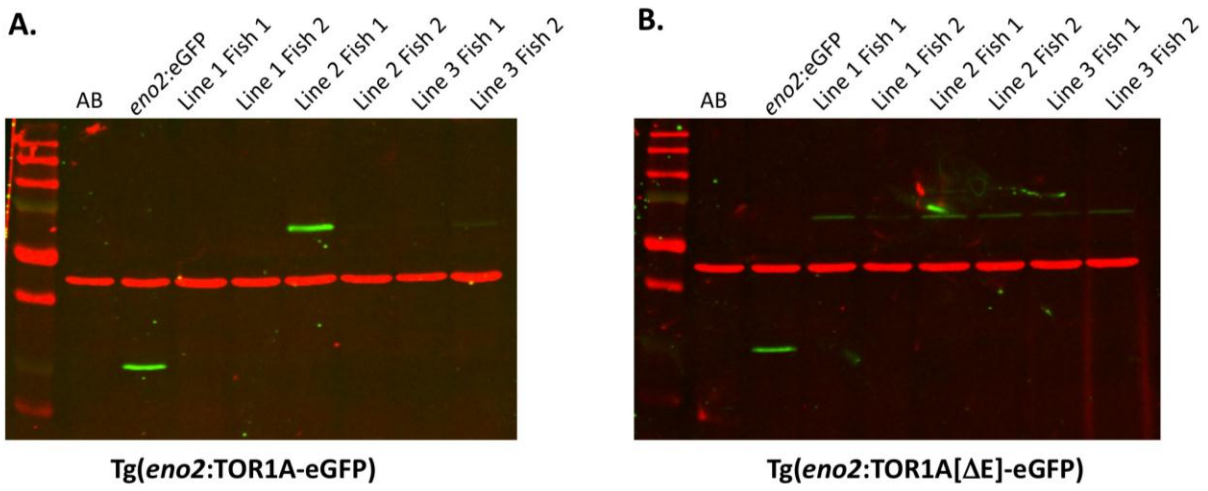

Figure 5.5 - Expression of Transgene in F2 Generation

(A) Whole brain lysate from two fish of each of the three wtTOR1A transgenic lines was resolved using SDS-PAGE and immunoblotted with GFP (green bands) and ß-actin (red bands) antibodies. **(B)** Whole brain lysate from two fish of each of the three TOR1A[ΔE] transgenic lines was resolved using SDS-PAGE and immunoblotted with GFP (green bands) and ß-actin (red bands) antibodies. For both (A) and (B), Lane 2 (AB fish) and Lane 3 (Tg(*eno2*:GFP) fish) represent negative and positive controls (respectively) for GFP immunoreactivity.

Table 5.1 - Inheritance of Transgene in Tg(*eno2*:TOR1A-eGFP) and Tg(*eno2*:TOR1A[ΔE]-eGFP) zebrafish. Embryos were examined for GFP expression between 3-5dpf, and the number of GFP positive and GFP negative embryos for each transgenic line were recorded.

Tg(*eno2*:TOR1A-eGFP)					
wtTOR1A Line 1		wtTOR1A Line 2		wtTOR1A Line 3	
GFP-positive	GFP-negative	GFP-positive	GFP-negative	GFP-positive	GFP-negative
113	148	141	168	91	83
Tg(*eno2*:TOR1A[ΔE]-eGFP)					
TOR1A[ΔE] Line 1		TOR1A[ΔE] Line 2		TOR1A[ΔE] Line 3	
GFP-positive	GFP-negative	GFP-positive	GFP-negative	GFP-positive	GFP-negative
119	111	104	96	119	114

5.6 DISCUSSION

This chapter examined the suitability and construction of transgenic zebrafish which pan-neuronally overexpress either wildtype or TorsinA[ΔE]. The relocalization of the zebrafish Torsin1 to the NE by co-expression with TorsinA[ΔE] *in vitro*, suggests that Torsin1 and TorsinA interact in a manner similar to wildtype and TorsinA[ΔE]. Whether this is due to interspecies Torsin1/TorsinA hexamer formation, or an unknown mechanism, remains to be

determined. However, it was of significant importance that expression of TorsinA[ΔE] was able to disrupt localization of zebrafish Torsin1, as developing a model based on overexpression of TorsinA[ΔE] would only be successful if the two proteins interact.

Of note, overexpression of TorsinA[ΔE] by mRNA injections in developing embryos, also resulted in an abberant localization of the TorsinA[ΔE] protein compared to wildtype TorsinA. Although the localization of TorsinA[ΔE] in the developing nervous system did not result in a clear perinuclear profile, indicative of NE accumulation, expression of TorsinA[ΔE] did result in the formation of large cytoplasmic aggregates. Furthermore, co-expression of TorsinA[ΔE] and wildtype TorsinA in zebrafish larvae resulted in the formation of large cytoplasmic aggregates containing both proteins. This discrepancy in TorsinA[ΔE] localization (NE vs. cytoplasmic aggregates) has been observed in several different cell lines and a clear explanation for this has not been identified (Hewett et al., 2000; Goodchild and Dauer, 2004). Although not demonstrated here, transmission electron micrographs of the cytoplasmic inclusion bodies have been shown to be the result of the formation of membranous whorls, posited to be derived from the NE due to colocalization with several NE proteins (Bragg et al., 2004). Furthermore, different tissue types from human patients diagnosed with DYT1 dystonia has been shown to reveal a similar dichotomous localization of TorsinA; cultured fibroblasts from DYT1 patients show a strong NE staining with a TorsinA antibody (Goodchild and Dauer, 2004), while post-mortem analysis of several brainstem nuclei show the formation of TorsinA immunoreactive inclusion bodies (McNaught et al., 2004). It is unknown which, if either, localization is important for the pathogenesis of dystonia. Given that several studies have suggested that TorsinA[ΔE] functions as a loss-of-function allele, rather than a toxic gain-of-function allele, the localization of TorsinA[ΔE] may be less relevant than the fact that

TorsinA[ΔE] can sequester the wildtype protein from its relevant site of action. Taken together, the results from these two experiments suggest expression of TorsinA[ΔE] in the zebrafish nervous system will result in the depletion of Torsin1 from its primary site of action by the formation of cytoplasmic aggregates containing both Torsin1 and TorsinA[ΔE].

Similar to the *tor1* morpholino results discussed in Chapter 4, mRNA injection of either *TOR1A[ΔGAG]* or wildtype *TOR1A* did not produce a phenotype in a spontaneous movement assay. This result does not completely negate the possibility that Torsin1 plays an early role in the development of motor behavior, as both techniques are limited by both mosaicism and transient effectiveness. Also, as previously discussed in Chapter 4, it is possible that a motor phenotype may not be detected until later in zebrafish development.

To provide for a more clear assessment of the role of Torsin1 in zebrafish development and nervous sytsem function, I decided to create transgenic lines that overexpress either wildtype or TorsinA[ΔE] in neurons of the zebrafish. Transgenic animals were readily identified by expression of the TorsinA-eGFP fusion protein in the retina at 3dpf. Over the next few days of development, GFP could be detected throughout the neuroaxis, including the retina, brain, and spinal cord, as well as the distal margins of the fin, consistent with the previously characterized expression pattern of the *eno2* gene. In the F2 and F3 generation of these transgenic lines, GFP expression was detectable in approximately 50% of animals, suggesting that each of these lines represents the integration of the transgene at a single locus within the zebrafish genome, that is passed to subsequent generations following Mendelian genetics. However, it is unknown whether this single integration site contains concatemers of the transgene, or if the integration site contains a single copy of the transgene.

Analysis of the expression levels of the transgene in adult F2 generation fish revealed a significant degree of variation, especially between the wtTOR1A lines. It is unknown why this is the case, as other transgenic animals using the same promoter and technique have yielded fairly consistent levels of expression between independent transgenic lines. It should be noted that in every transgenic line GFP expression was easily detected in F2 larvae, despite the lack of detection by immunoblotting whole brain lysate of adult animals. This suggests that in the case of wtTOR1A line 1, transgene expression was silenced during juvenile development, which could potentially be the result of the site of transgene integration. Alternatively, the differences in expression levels of the transgene could be exploited for dosage effects and/or developmental timing of expression. Further characterization of these transgenic lines will be presented in chapter 6 of this thesis.

6.0 CHARACTERIZAION OF TRANSGENIC ZEBRAFISH OVEREXPRESSING WILD TYPE OR DYSTONIA-ASSOCIATED MUTANT TORSINA

6.1 INTRODUCTION

Following the creation of multiple transgenic zebrafish lines overexpressing either wildtype or TorsinA[ΔE], I next sought to examine potential phenotypes associated with transgene expression. Although no animal model system has produced a dystonic phenotype, and the transgenic fish described here develop normally and do not display overt changes in locomotion, several movement abnormalities have been consistently identified, including hyperactivity in open field tests (Shashidharan et al., 2005; Dang et al., 2006) and impaired performance during rotorod trials (Dang et al., 2005; Sharma et al., 2005; Shashidharan et al., 2005; Grundmann et al., 2012). How overexpression of TorsinA[ΔE] causes these movement abnormalities is not known, although small changes in the dopamine metabolites, DOPAC and HVA, have been found in several of the models (Zhao et al., 2008) (Yokoi et al., 2009).

In zebrafish, the ontology of measurable behaviors begins before the end of the first day of development, and by the end of the first week, a variety of behaviors have become established. The ability of larval zebrafish to produce movement begins around 17 hpf, when motorneurons first contact muscle cells (Saint-Amant and Drapeau, 1998). At this time, movement is limited to spontaneous side-to-side contractions of the tail and is sensitive to

nicotinic acetylcholine receptor antagonists (Saint-Amant and Drapeau, 1998). By 21 hpf embryos are able to move in response to touch by coiling their tail, however, swimming in response to touch is not observed until 26 hpf (Saint-Amant and Drapeau, 1998). Ablation studies have shown that neurons in the hindbrain are necessary for touch responses, including both tail coiling and swimming (Saint-Amant and Drapeau, 1998). Under normal conditions, embryos hatch from their chorion around 48 hpf. Subsequently, infrequent, spontaneous swimming behavior larvae can be recorded. This form of movement is produced by high-frequency tail beats, generally lasting 1-2 seconds (Buss and Drapeau, 2001). Around 4 dpf, the frequency of tail beats begins to decrease and the swim bladder inflates, and over the next few days larvae begin to swim in a 'beat-and-glide' mode, similar to adult fish (Buss and Drapeau, 2001). The total time spent swimming and total distance moved increases over the next several weeks of development, and reaches a plateau around 2 months post fertilization (personal observation).

The relative simplicity of measuring total distance moved during a recording period makes this assay ideal for large-scale screens, and several reports exist on the development of the technological components necessary for, and the variables of, such a measure (Cahill, 2007; Creton, 2009; MacPhail et al., 2009; Cario et al., 2011; Farrell et al., 2011). Pharmacological modulation of dopamine transmission is capable of producing the robust changes in the amount of observed swimming necessary to screen behavioral changes, although it remains to be seen if this type of assay can be successfully employed with possibly more subtle changes induced by transgenes (Farrell et al., 2011).

Several more stereotyped, sensory induced behaviors have been characterized in zebrafish, and the control of many of these behaviors relies on different neuronal circuitry,

allowing for a dissection of affected neuronal populations measured by behavioral endpoints. Beginning around 4 dpf larvae are able to exhibit optokinetic responses (OKR) (Brockerhoff, 2006), and while the exact circuit controlling this behavior in zebrafish remains unknown, it has been demonstrated through laser ablation studies, that the optic tectum may serve to help regulate the saccadic rate of the OKR (Roeser and Baier, 2003). By 5 dpf, larvae exhibit acoustic startle responses (Zeddies and Fay, 2005), thought to be controlled by only three pairs of reticulospinal neurons, and by 7dpf, larvae are able to habituate to repeated exposure to acoustic stimuli (Best et al., 2008). Prepulse inhibition can be measured at 6 dpf using acoustic stimuli, and is sensitive to both dopaminergic and glutamateric modulation (Burgess and Granato, 2007). Reflex behaviors to both touch and auditory sensory modalities have also been well characterized around 7dpf, and result in a well-characterized C-bend of the larval body that can be measured in both timing and angle, and may prove useful for detecting more subtle movement deficits in larvae.

This chapter reports that similar to overexpession of TorsinA[ΔE] in rats (Grundmann et al., 2012), TorsinA[ΔE] presents a perinuclear localization in neurons of the adult zebrafish, contrasting with the more diffuse cytoplasmic localization of wildtype TorsinA. No significant differences were observed in the levels of dopamine or GABA as a result of wildtype or TorsinA[ΔE] expression. At the behavioral level, expression of TorsinA[ΔE] resulted in a transient reduction in spontaneous locomoter behavior, reaching significance at 33dpf and lasting for about one week. Further examination of kinesis during this time window did not reveal differences in the degrees, or angular velocity, of various body segments during the C-bend reflex, suggesting that the decrease in spontaneous locomotion, resulting from TorsinA[ΔE] overexpression, is likely due to dysregulation of swimming behavior.

6.2 TORSINA LOCALIZATION IN ZEBRAFISH BRAIN

Following the generation of the transgenic lines, I first examined the localization of the TorsinA and TorsinA[ΔE] in the adult zebrafish nervous system by immunostaining and confocal microscopy. Adult brains from TOR1A[ΔE] Line 2 and wtTOR1A Line 3 were sectioned and immunostained for both GFP and HuC, a neuronal marker. Co-localization of HuC and GFP was observed across all brain regions, as well as the spinal cord, confirming the proper spatial expression pattern attributed to the *eno2* promoter. I next examined these sections using confocal microscopy. In all neurons examined, the localization of wildtype TorsinA was found to be primarily cytoplasmic (Figure 6.1). In contrast, TorsinA[ΔE] localized to puncta primarily surrounding the nucleus of all neurons examined. Thus, overexpression of wildtype and TorsinA[ΔE] is the adult zebrafish recapitulates the cellular phenotype observed *in vitro* and in the rat model.

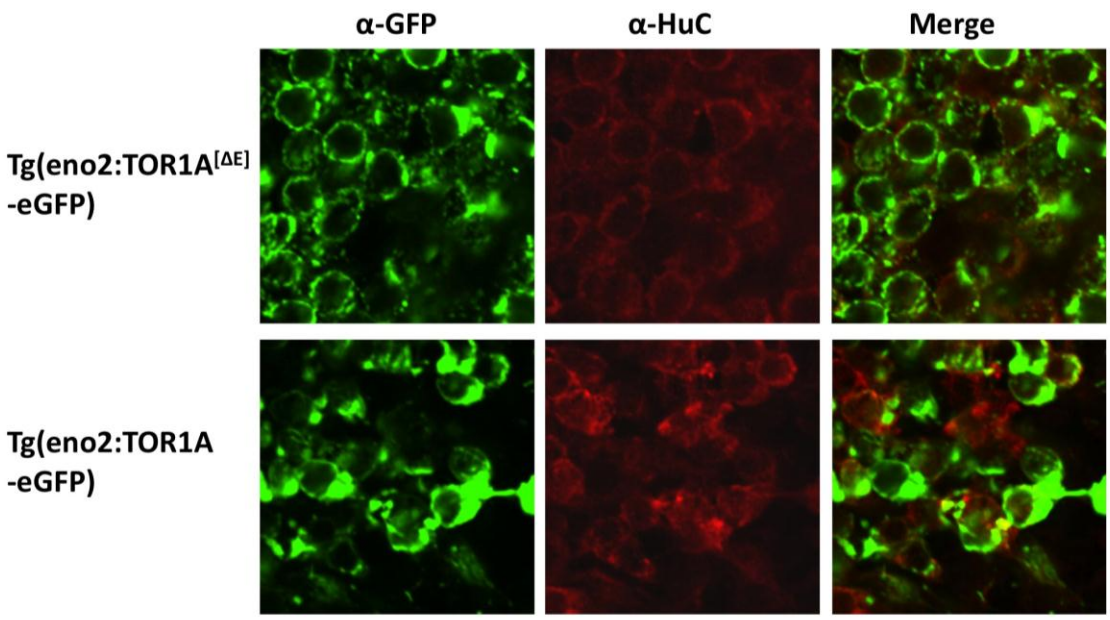

Figure 6.1 Localization of wildtype and TorsinA[ΔE] in the zebrafish brain

Sections of brain tissue from either TorsinA[ΔE] overexpressing (Top row) or wildtype TorsinA overexpressing (bottom row) were immunostained for both GFP (first column) and HuC (middle column), a neuronal marker. A merged image of GFP and HuC immunolabelling is presented in the final column.

6.3 DOPAMINE AND GABA CONTENT ARE UNALTERED BY MUTANT TORSINA

Next, I asked if the expression, or differential localization between, wildtype and TorsinA[ΔE] resulted in changes in the levels of dopamine and GABA in the adult brains of transgenic zebrafish. Several studies have reported changes in the levels of dopamine metabolites in

different mouse models for DYT1 dystonia (Zhao et al., 2008) (Yokoi et al., 2009), and it has also been suggested, from human studies, that decreases in GABA may also underlie the dystonic phenotype (Levy and Hallett, 2002). To address this question, whole brains were dissected from: wildtype AB strain zebrafish, TOR1A[ΔE] Line 2 and nontransgenic clutchmates, and wtTOR1A line 3 and nontransgenic clutchmates. These brains were rapidly sonicated, to avoid oxidation, and the samples were prepared for HPLC followed by electrochemical detection of neurotransmitters. Because brain weight varied significantly between animals, values from HPLC were normalized to protein concentrations for each sample. No significant differences were observed in the levels of both dopamine and GABA in the brains of zebrafish overexpressing either wildtype or TorsinA[ΔE] (Figure 6.2). Using this method, we were unable to reliably detect the presence of the dopamine metabolites, HVA or DOPAC, likely due to the relative few number of dopamine neurons in the zebrafish brain. It therefore remains unknown if expression of wildtype or TorsinA[ΔE] changes the level of dopamine metabolites.

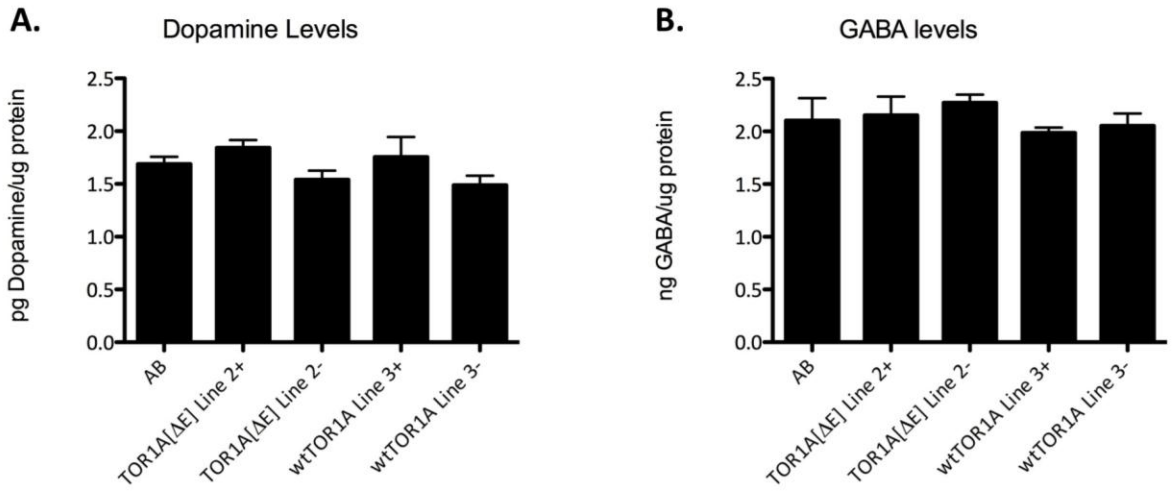

Figure 6.2 Dopamine and GABA content of zebrafish expressing either wildtype or TorsinA[ΔE].

Whole brain levels for of dopamine **(A)** or GABA **(B)** were measured using HPLC followed by electrochemical detection, and neurotransmitter levels were normalized to protein concentration. Each bar represents the mean +/- SE for each group (n=3 for all groups). No significant differences were detected using one-way ANOVA.

6.4 SPONTANEOUS LOCOMOTION OF TRANSGENIC ZEBRAFISH

Because onset of DYT1 dystonia occurs primarily during adolescent development, I next decided to examine the spontaneous locomotion during larval and adolescent development of the transgenic lines described in Chapter 5. To measure spontaneous motion in larval and adolescent zebrafish (14 to 90dpf), individual fish, followed throughout development, were placed in single wells of a multiwell plate (96-well for 14dpf, 48well for 21-45dpf, and 6-well for 60-90dpf) and

recorded for 2-3 hours in the morning or afternoon. Videos were tracked using the Viewpoint system, and the total amount of movement (in mm) during the recording period was divided by the total recording time (in seconds) to calculate the mean velocity (Vm) of individual zebrafish. Each recording contained two controls: non-transgenic clutchmates, to confirm that an effect is the result of the transgene, and wildtype AB strain zebrafish, to confirm that outcrosses did not harbor mutations affecting spontaneous locomotion. A preliminary set of experiments revealed a significant reduction in Vm in one of the TOR1A[ΔE] lines at 35dpf and a non-significant trend in the other two lines. After three replicates for each line, all three TOR1A[ΔE] lines showed a significant reduction of approximately 20% in Vm of transgenic animals, compared to both nontransgenic clutchmates and wildtype AB strain zebrafish, at 35dpf (Figure 6.3A). No change in the spontaneous locomoter activity was observed at any of the other time points tested (Figure 6.3B shows results at 35dpf). Because no differences were observed during preliminary experiments at 28 dpf or 45 dpf in any TOR1A[ΔE] lines, I decided to include additional time points in the analysis of the TOR1A[ΔE] lines (Line 1) to determine the exact timing of the reduction in Vm observed at 35dpf (Figure 6.3C). Beginning at 30dpf, a non-significant trend ($p=.0503$) in Vm reduction was observed, and by 33 dpf this reduction reached significance between transgenic and both nontransgenic clutchmates and wildtype AB strain zebrafish. A significant reduction in Vm was observed at 33 dpf, 35 dpf, 37 dpf, and 40dpf when TOR1A[ΔE] Line 1 transgenics were compared to both nontransgenic clutchmates and wildtype AB strain zebrafish. No significant differences were detected at earlier or later timepoints in any of the TOR1A[ΔE] or wtTOR1A transgenic zebrafish. These data suggest that expression of TorsinA[ΔE] in the zebrafish CNS produces a transient decrease in spontaneous locomotion beginning after one month of development and lasting for approximately one week.

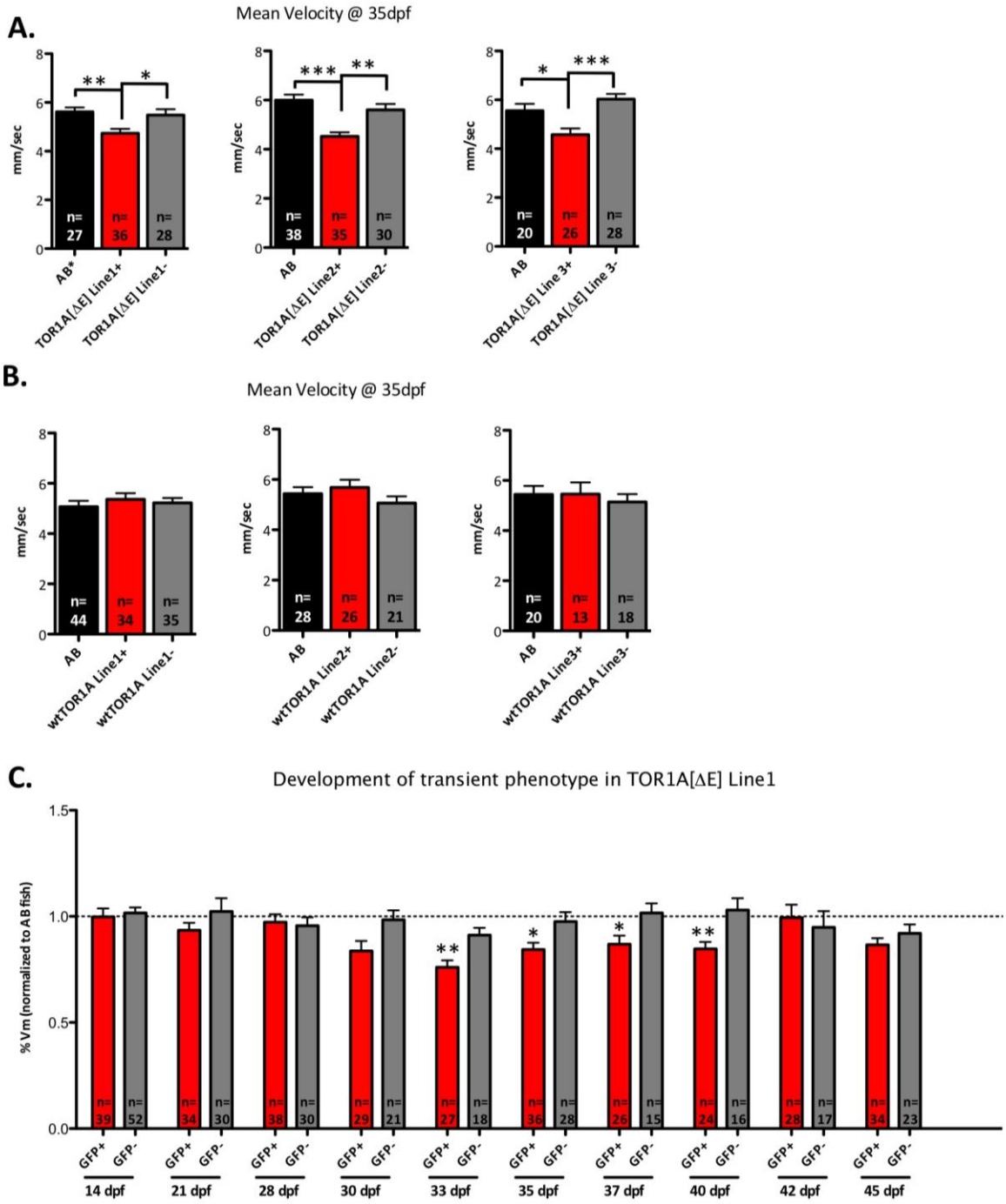

Figure 6.3 Spontaneous Locomotion during Adolescent Development of Transgenic Zebrafish.

(A) Graphs depict the average Vm (in mm/sec) at 35 dpf for the three TorsinA[ΔE] transgenic lines, non-transgenic clutchmates, and wildtype AB strain zebrafish. (B) Graphs depict the

average Vm (in mm/sec) at 35 dpf for the three wtTorsinA transgenic lines, non-transgenic clutchmates, and wildtype AB strain zebrafish. (C) Graph presents the Vm, normalized to AB strain zebrafish (dashed line), of TorsinA[ΔE] Line 1 (GFP+), and nontransgenic cluchmates (GFP-) at varying developmental time points. Because all groups passed D'Agostino and Pearson omnibus normality test, the bars on all graphs represent mean +/- SE and the number of animals in each group is labeled at the base of each bar. Astericks indicate the degree of statistical significance (*=p<.05, **=p<.01, ***=p<.001) using ANOVA followed by Bonferroni's Mutliple Comparison Test.

6.5 ACOUSTIC STARTLE OF TRANSGENIC ZEBRAFSIH

In order to address the mechanism by which TOR1A[ΔE] lines showed a significant reduction in spontaneous locomotion, I decided to more closely examine the kinesis of adolescent transgenic fish at 35dpf. Larval stage zebrafish exhibit a rapid, stereotyped startle response to acoustic stimuli, starting with a "C-bend" of the body. This response occurs within 12 ms of the stimulus, and is dependent upon Mauthner cells in the hindbrain (Burgess and Granato, 2007). A set of preliminary experiments, executed with the assistance of Dr. Harold Burgess (NIH), revealed that at 35dpf, adolescent fish exhibited a "C-bend" response to acoustic stimuli with a similar latency, duration and angular velocities to larval fish. I therefore decided to test all the transgenic lines in this assay to see if any changes in this reflex behavior could be detected. Zebrafish, in groups of nine, were placed in individual wells mounted to a vibration device and filmed with a high-speed camera (1000 frames/sec) immediately following a 6ms, 500 Hz

waveform stimuli. Each group of fish were tested for 20 trials, separated by 15 ms to avoid habituation, and the videos were analyzed using the Flote software package (Burgess and Granato, 2007). There was no difference in the responsivity of different transgenic lines to this stimulus (data no shown). Therefore, only trials where individual fish initiated movement within 20 msec of the stimulus were further analyzed. Because there was a large variation in fish size, which could be a confounding factor, as some of which were the diagonal length of the recording well, I first checked for a correlation between size and response metrics. A significant, negative correlation was found between the size of the fish and the angular velocity of the response. Removal of the 24 largest fish from analysis abolished the correlation between size and angular velocity, however this also resulted in the loss of fish from TOR1A[ΔE] line 2. The data for the remaining 189 fish was further analyzed and is presented in Figure 6.4. No differences were observed between any of the groups in terms of latency or duration of the C-bend response (Figure 6.4A,B). Next, the Flote software was able to segment the body of the zebrafish into head (Figure 6.4C,D), trunk (Figure 6.4E,F), and tail (Figure 6.4G,H) regions, and analyze the change in orientation of these body regions before and after the acoustic stimulus, as well as the maximal angular velocity of each of these segments during the C-bend response. Again, no differences were detected between any group in the degrees of orientation change or maximal angular velocity of the head, trunk, or tail. These data suggest that expression of either wildtype or TorsinA[ΔE] does not disrupt the reflexive movements of zebrafish to acoustic stimuli, and therefore, likely does not disrupt the functioning of reticulospinal system.

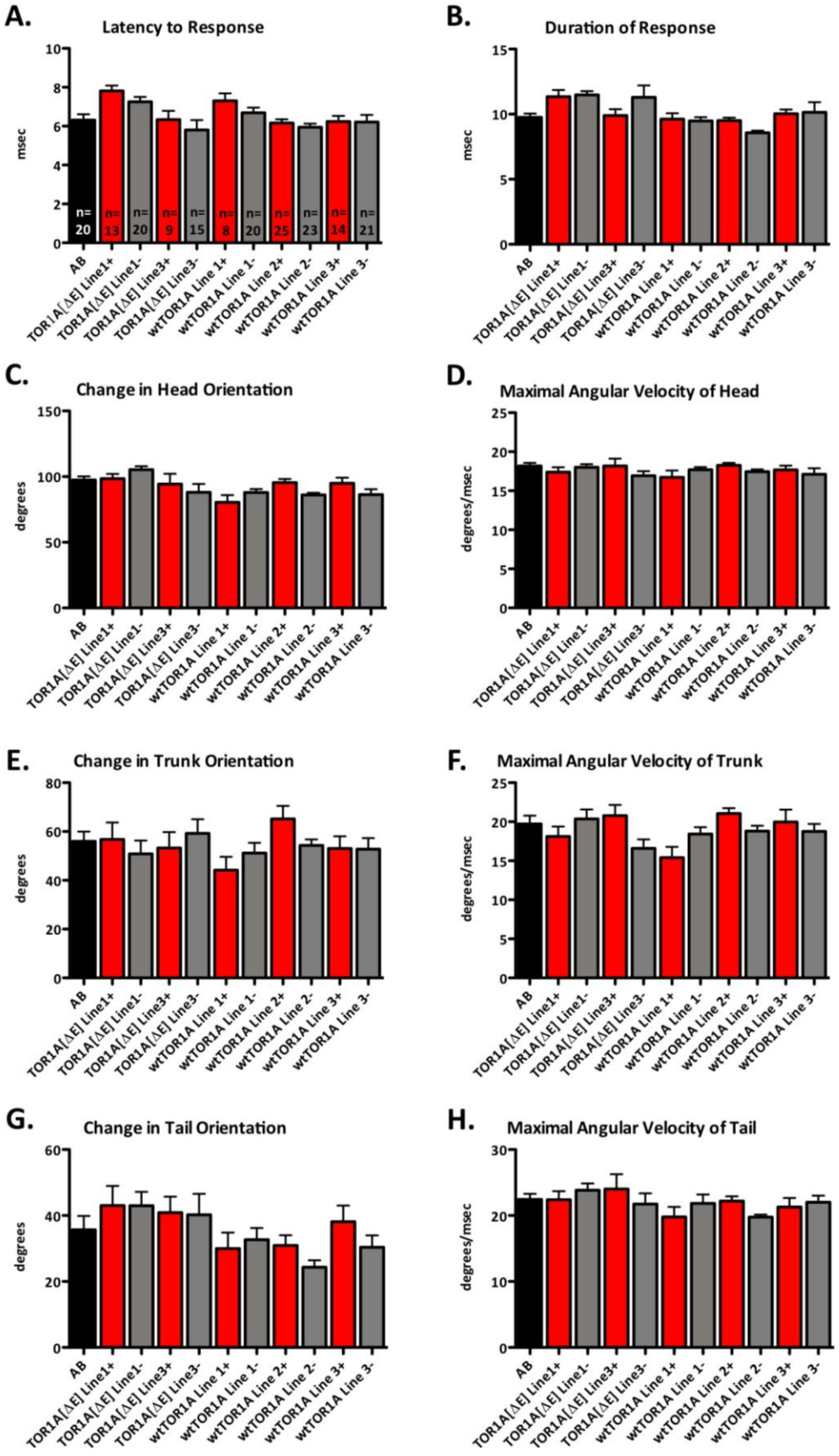
A.
Latency to Response
msec
n= 20
n= 13
n= 20
n= 9
n= 15
n= 8
n= 20
n= 25
n= 23
n= 14
n= 21
B.
Duration of Response
msec
C.
Change in Head Orientation
degrees
D.
Maximal Angular Velocity of Head
degrees/msec
E.
Change in Trunk Orientation
degrees
F.
Maximal Angular Velocity of Trunk
degrees/msec
G.
Change in Tail Orientation
degrees
H.
Maximal Angular Velocity of Tail
degrees/msec
AB
TOR1A[ΔE] Line1+
TOR1A[ΔE] Line1-
TOR1A[ΔE] Line3+
TOR1A[ΔE] Line3-
wtTOR1A Line 1+
wtTOR1A Line 1-
wtTOR1A Line 2+
wtTOR1A Line 2-
wtTOR1A Line 3+
wtTOR1A Line 3-

Figure 6.4 Acoustic startle response of zebrafish overexpressing wildtype and TorsinA[ΔE]

C-bend startle responses were analyzed in by the following metrics: **(A)** latency to respond, **(B)** duration of response, **(C)** change in head orientation, **(D)** maximal angular velocity of the head, **(E)** change in trunk orientation, **(F)** maximal angular velocity of the trunk, **(G)** change in orientation of the tail, and **(H)** maximal angular velocity of the tail. For all graphs, bars represent the mean +/- SE of the group.

6.6 DISCUSSION

The data presented in this chapter reveal two primary phenotypes of TorsinA[ΔE] expression in the zebrafish nervous system: a localization of the TorsinA[ΔE] protein to perinuclear puncta and a transient decrease in spontaneous movement at one month post fertilization. This punctated nuclear envelope ring, observed in zebrafish neurons, is similar to the localization of TorsinA[ΔE] in transgenic rats overexpressing the protein (Grundmann et al., 2012). As discussed in Chapter 5, TorsinA[ΔE] localization differs between cell types, ranging from cytoplasmic aggregates to being primarily localized to the lumen of the nuclear envelope. The reasons for these different localization patterns are unknown, but possibilities include expression levels and differences in the complement of interacting proteins between species and cell types.

The significant decrease in spontaneous locomotion observed in all three TOR1A[ΔE] transgenic lines around 35dpf raises several interesting questions. First, why is the phenotype

observed at this time point? A clear comparison between zebrafish and mammalian developmental time points is complicated by the different body morphologies. Despite similar lifespans, embryonic patterning occurs much more rapidly in zebrafish compared to mice. Interestingly, zebrafish are typically considered to be in larval stages until one month of development, and the following two months, until adulthood, are considered to be a juvenile phase. The switch from larval to juvenile is not characterized by metamorphic changes, but is more defined by the appearance of an adult fin pattern, the development of scales, and the completion of skull ossification (Nüsslein-Volhard and Dahm, 2002). Little is known about the development of the zebrafish nervous system at this time point, although it has been found that motorneurons continue to be born until the juvenile phase of development (Nüsslein-Volhard and Dahm, 2002). In line with this observation, one possibility is that TorsinA[ΔE] expression disrupts the plasticity of descending inputs to the spinal cord, after motorneurons have innervated their target muscle group.

A second question raised by these findings regard the transient nature of the spontaneous locomoter phenotype. One possibility is that the transgenic fish are able to recruit new neurons or rewire neuronal circuits to compensate for the effect of TorsinA[ΔE] expression. Unlike mammals, zebrafish constitutively produce new neurons throughout life and exhibit a remarkable ability to regenerate the nervous system following injury. It is unknown when, or if, the *eno2* promoter would drive expression of the transgene in later-born neurons. An alternate possibility could be an upregulation of the endogenous *tor1* gene in zebrafish. Because TorsinA is believed to function as a hexamer, and the human TorsinA is able to interact with the zebrafish Torsin1, it is possible that an increase in of the number of Torsin1 monomers in Torsin1:TorsinA[ΔE] hexamers could mitigate the effects of TorsinA[ΔE] expression. In support of this hypothesis,

the antibody directed against Torsin1, characterized in Chapter 4, was not able to detect the presence of Torsin1 in embryonic and larval zebrafish (up to 28dpf), despite detectable *tor1* transcription, and the earliest reliable timepoint at which the antibody could detect the putative Torsin1 bands in the zebrafish brain was around 2 months post fertilization.

The circuit controlling the "C-bend" startle response in zebrafish has been well studied, and is thought to involve only three bilateral pairs of reticulospinal neurons, without modulation by more rostral brain regions (Burgess and Granato, 2007). The lack of a detectable change in the kinesis of the in this startle reflex was not necessarily surprising. Although abnormalities can be detected in the electrical recordings during later phases of brainstem reflexes in patients with dystonia, the latency and initial activation patterns largely appear normal (Berardelli et al., 1998). This has lead to the hypothesis that descending inputs from cortical regions to the brainstem are the cause of these altered responses, and not dysfunction of the brainstem or spinal cord circuits (Berardelli et al., 1998). Because the "C-bend" reflex is not modulated by descending inputs to the brainstem, it is therefore unlikely that expression of TorsinA[ΔE] in zebrafish disrupts the function of hindbrain or spinal cord neurons directly, and further suggests that the observed decrease in spontaneous locomotion is more likely the result of dysregulation of descending influences during slow swimming.

Taken together, the data presented in this chapter provide a basic characterization of the transgenic lines described in chapter 5, and identify a transient, behavioral phenotype occurring around the beginning of the zebrafish juvenile phase. The following chapter will discuss future directions for the use of zebrafish as a model system for DYT1 dystonia.

7.0 GENERAL DISCUSSION

The data presented in chapters 3-6 of this thesis provide a detailed characterization of the zebrafish homolog of the human TorsinA protein and the development of a potential zebrafish model for DYT1 dystonia. The findings demonstrate that the zebrafish genome contains a single homolog of the human TOR1A, *tor1*, and a gene duplication event, likely occurring during the rise of the tetrapod lineage, resulting in two distinct *tor1* homologs, *tor1a* and *tor1b*, in the genomes of later diverging species. Sequence homology at the amino acid level reveals a high degree of conservation, especially surrounding the conserved ATP binding and hydrolysis domains. Despite more significant divergence at the amino termini, both TorsinA and Torsin1 encode a protein with predicted cleavable ER retention signal, followed by a hydrophobic, putatively membrane-spanning, domain. The zebrafish Torsin1 protein localizes similarly to the human TorsinA protein in cell culture, and mutations in the Walker B, ATP hydolysis, domain of Torsin1 results in the accumulation of Torsin1 at the nuclear envelope, similar to the relocalization observed after mutation of the ATP hydrolysis domain of human TorsinA. Furthermore, Torsin1 accumulates at the NE when co-expressed with TorsinA[ΔE], strongly suggesting that the human and zebrafish proteins interact *in vitro*.

At the behavioral level, overexpression of TorsinA[ΔE] in zebrafish caused a transient decrease in spontaneous locomotor activity starting around 33 dpf and lasting for approximately one-week, after which time Tg[*eno2:TOR1A[ΔE]*) zebrafish resumed wildtype levels of

spontaneous swimming. In this chapter, I will further discuss these key findings and propose several experiments that would aid in the understanding of the evolution of Torsin1 function and help define the mechanistic basis for the phenotype observed in the transgenic animals described in chapters 5 and 6.

7.1 UTILITY OF A *TOR1* NULL ALLELE

Since transient knockdown of zebrafish *tor1* did not result in a phenotype before gene expression recovered, a clear assessment for the role of *tor1* in zebrafish awaits the generation of stable *tor1* null-allele mutants. However, the lack of a zebrafish embryonic stem cell line has prevented the use of targeted genetic approaches based on homologous recombination. Until recently, the generation of null-alleles in zebrafish has relied upon forward genetic mutational screens. Over the past couple of years, however, two different techniques have emerged that are able to overcome this shortcoming: zinc-finger nucleases (ZFNs) (Doyon et al., 2008) and transcription activator-like effector nucleases (TALENs) (Huang et al., 2011; Sander et al., 2011). Both of these techniques utilize the catalytic domain of the *Fok*I restriction endonuclease to induce double stranded breaks in genomic DNA, and these double stranded breaks are repaired by non-homologous end-joining, often resulting in small deletions or insertions that results in frame-shift mutations that are transmissible through the germline as null alleles (Caroll and Zhang, 2011).

Given that homozygous knockout of the *C. elegans*, Drosophila, and mouse homologs of TorsinA are all lethal, it seems likely that a zebrafish *tor1* null-allele will also result in arrested development. It would be of interest, therefore, to determine whether *tor1* null zebrafish would be viable, and if not at what developmental stage death occurs, as death occurs at different

developmental stages in each of the model systems lacking the human TOR1A homolog. Loss of *C. elegans* ooc-5 arrested development at the 2-cell stage (Basham and Rose, 1999), loss of *dtorsin* in *Drosophila* resulted in the majority of animals dying at the pre-pupal stage (Wakabayashi-Ito et al., 2011), and loss of the mouse *tor1a* caused perinatal lethality due to lack of feeding (Goodchild et al., 2005). The degree of divergence in ontogeny between these model systems makes it difficult to speculate when knocking out *tor1* would become essential for continued development in zebrafish. One possibility would be that zebrafish lacking *tor1* would die when they begin actively feeding, around 5dpf. Conversely, overexpression of TorsinA[ΔE] did not produce a behavioral effect until approximately one month post fertilization, and it is possible that zebrafish lacking *tor1* would survive until this larval to juvenile transition. Depending upon the age at death, it may also be possible to perform large-scale novel compound screens to identify molecules capable of preventing death by loss of functional Torsin1 protein.

7.1.1 Validation of the Torsin1 antibody

Beyond determining whether *tor1* is necessary for survival, the generation of a zebrafish *tor1* null allele would also allow for a definitive demonstration of the specificity of the antibody described in chapter 4. At this point in time, it remains unclear whether the antibody is truly recognizing the zebrafish Torsin1 protein. Although the antibody can detect Torsin1 in transfected cells, and the detection of two putative Torsin1 bands in zebrafish whole brain lysate can be blocked by pre-incubation with the cognate peptide, these experiments only demonstrate that the antibody is capable of recognizing the peptide sequence (Saper, 2005). Although BLAST searches did not reveal other proteins with a similar peptide sequence, and other zebrafish Torsin family members are highly divergent at the aligned amino acid sequence, these

observations do not nullify the hypothesis that the antibody is able to recognize more than one protein. Lack of immunoreactive signal in tissue harboring a genetic knockout for the target protein is generally considered the "gold standard" for demonstrating antibody specificity (Saper, 2005). Therefore, in order to unambiguously demonstrate the specificity of the antibody, zebrafish *tor1* null-allele tissue is necessary.

7.1.2 Evaluation of the evolution of Torsin1 function

Lastly, the generation of a zebrafish *tor1* null-allele would allow for a set of experiments to examine the evolutionary conservation, or divergence, of TorsinA and TorsinB function. Assuming that loss of *tor1* results in an observable phenotype, it would be of interest to introduce either TOR1A or TOR1B into the *tor1* null background to see if the phenotype could be reversed by expression of either protein. Several outcomes could be expected, each revealing information regarding the evolutionary consequences of the *tor1* gene duplication. If either expression of TOR1A or TOR1B were able to compensate for loss of *tor1*, it would suggest that both TorsinA and TorsinB retain the ancestral function of Torsin1 and that lethality in *tor1a* knockout mice may be due to the lack (Augood et al., 1999), or reduced expression (Kim et al., 2010) of TorsinB in neurons. Alternatively, if only one protein was able to compensate for loss of *tor1* it would suggest that one protein would have retained the ancestral function (the compensatory protein), while the other protein has lost the ancestral, and possibly gained new, functions. Conversely, expression of both TorsinA and TorsinB may be necessary to compensate for the loss of Torsin1, suggesting a segregation of ancestral function between the duplicated genes, which could potentially result from the complementary expression patterns (Kim et al., 2010) if the function of Torsin1 differs between cell types. In line with this set of experiments, it

would also be of interest to express the zebrafish Torsin1 protein in the mouse *tor1a* knockout to see if the Torsin1 protein is able to compensate for the loss of TorsinA. Very little information is known about the function of TorsinB in tetrapods, and the identification of a vertebrate animal lacking distinct *tor1a* and *tor1b* genes provides the opportunity to explore the degree of redundancy between TorsinA and TorsinB function.

7.2 ROLE OF TORSIN DURING JUVENILLE DEVELOPMENT

Because DYT1 dystonia is a developmental disorder, with clinical manifestations most commonly occurring during juvenile development, the observation that expression of TorsinA[ΔE] resulted in a motor phenotype during the larval to juvenile transition in zebrafish merits further investigation. It remains unknown why expression of TorsinA[ΔE] in the neurons of the zebrafish CNS results in a reduction of spontaneous locomoter activity. The degree to which this phenotype shares physiologic commonalities with DYT1 dystonia is also uncertain. However, several experiments could be conducted to examine these unknowns.

7.2.1 Electrophysiological ramifications of the TorsinA[ΔE] overexpression in zebrafish

To further examine the relevance of the observed decrease in spontaneous locomotion to DYT1 dystonia, it would be interesting to examine the pattern of muscle activity in zebrafish overexpressing TorsinA[ΔE] at the phenotypic timepoint. EMG recordings during voluntary movements in human patients with dystonia often show prolonged activation of agonist muscle groups, lasting several seconds, resulting in an overlap in muscle activity in agonist and

antagonist muscle groups (Berardelli et al., 1998). Similarly, EMG recordings in one of the mouse models for DYT1 dystonia revealed that sharp burst of muscle activity in the biceps and triceps of transgenic animals was sometimes synchronized during voluntary forelimb movement (Chiken et al., 2008). Although EMG recordings in this model did not reveal sustained contraction of either the bicep or tricep muscle groups during movement, sustained muscle activity (>10sec) was frequently observed when animals were at rest, and was sometimes present in both bicep and triceps simultaneously. EMG recordings in teleosts during unrestrained (Zottoli, 1977) and *in vitro* preparations reveal a left-right alternation of muscle activity within a single body segment, and a temporal wave of activation between different segments that proceed in a rostral to caudal direction (Gabriel et al., 2008). It would be of interest to examine the pattern of muscle activity in the transgenic zebrafish overexpressing TorsinA[ΔE] during the 5th week of development to see if this pattern of muscle activity is disrupted and if sustained muscle contractions and co-contraction of agonist and antagonist muscle groups are present. Furthermore, EMG recordings in adult zebrafish are able to distinguish between activity of primary and secondary motoneurons, which control different aspect of zebrafish behavior (fast reflexes vs slow swimming, respectively), allowing for a more detailed characterization of the observed phenotype (Liu and Westerfield, 1988).

7.2.2 Onset of the phenotype caused by overexpression of TorsinA[ΔE]

Another set of questions raised by the observed decrease in spontaneous locomotor activity in TorsinA[ΔE] overexpressing zebrafish regard the timing of the phenotype, both in terms of onset and recovery. Because the onset of the phenotype is at the larval to juvenile transition, it is possible that this phenotype correlates to the onset of DYT1 dystonia in humans. Several

observation suggest that dystonia is related to abnormal neuronal connectivity or plasticity within motor circuits; although there is no obvious neurodegeneration or changes in the positioning of neuronal nuclei in post-mortem studies of brain tissue from patients with DYT1 dystonia, positron emission tomography of both dystonia-manifesting and non-manifesting carriers of the DYT1 allele show increased metabolic activity in the lentiform nucleus, cerebellum and supplementary motor areas (Eidelberg et al., 1998). The adolescent age of onset, combined with the level of plasticity in motor circuits at this time in development, makes it plausible that loss of TorsinA in regions of the motor system disrupts important processes during developmental circuit refinement. Although plasticity is less well characterized in motor circuits, several key principles have emerged regarding developmental critical periods, which are applicable across circuits, despite modality (Hensch, 2004). Two of these principles are of particular interest to DYT1 dystonia: i) critical period plasticity progresses sequentially through circuit nodes, beginning at either the input (sensory neurons) or output (motoneurons), and ii) the onset of critical periods can be largely regulated by experience, not solely age. Combining these principles with the observation that, in zebrafish, motor neurons cease to be born after one month of development (Nüsslein-Volhard and Dahm, 2002), suggests that refinement of the descending circuits with control over motor neurons may be occurring around this time. To examine if there is a phenotype in the refinement of motor circuit connectivity, one could use retrograde labeling techniques to examine the number of neurons in higher order motor processing areas that are able to influence activity of a single motor unit.

7.2.3 Recovery of the phenotype caused by TorsinA[ΔE] expression in zebrafish

One hypothesis for why TorsinA[ΔE] overexpressing zebrafish are able to recover wildtype levels of spontaneous locomotion could be that expression of the endogenous zebrafish Torsin1 protein is upregulated during this period of development and is able to compensate for expression of TorsinA[ΔE]. This hypothesis is supported by preliminary data using the antibody described in chapter 4; the two bands detected in adult zebrafish brain are not present at 28dpf, but can be detected at 2 months post fertilization. One set of experiments to address this hypothesis would be to knockdown the endogenous *tor1* at this time point. Although RNAi technologies have not been used successfully to target endogenous genes in zebrafish, different delivery methods of morpholino antisense oligonucleotides have been developed to extend their use past early development, including electroporation (Cerda et al., 2006) and conjugation of the morpholino to an octa-guanidine dendrimer, delivery moiety (Kizil and Brand, 2011). It would be interesting to use one of these techniques during the phenotypic time windows to knockdown expression of *tor1*. If the recovery from the motor phenotype observed in zebrafish overexpressing TorsinA[ΔE] is caused by increased expression of the endogenous *tor1*, it would be expected that knock down of *tor1* at this time would either exacerbate or prolong the phenotype observed in these animals. Similarly, if the phenotype is caused by a dominant-negative effect of TorsinA[ΔE] on the zebrafish Torsin1, it would be expected that knockdown of *tor1* in wildtype zebrafish at this time point would produce a similar behavioral phenotype to overexpression of TorsinA[ΔE]. A similar technique could be used to test the hypothesis that later-born neurons are able to compensate for the expression of TorsinA[ΔE]; cerebroventricular microinjection of *pcna* directed morpholinos results in decreased neurogenesis (Kizil and Brand,

2011). By abrogating neurogenesis at this time point, the phenotypic abnormalities in transgenic zebrafish would be expected to persist until neurogenesis recovers, if the birth of new neurons was responsible for recovery of the motor phenotype.

7.3 FINAL CONCLUSIONS

The data presented in this thesis present a detailed characterization of the endogenous zebrafish *tor1* gene, the homolog of the human *TOR1A* gene, and the generation of novel transgenic zebrafish overexpressing the dystonia-associated mutant form of TorsinA. Although these transgenic animals did not exhibit overt involuntary movements resembling dystonia clinically, a transient, juvenile-onset decrease in spontaneous locomotor activity was observed. The mechanisms underlying this phenotype will be resolved by further experimentation. Further examination of the abnormal physiology responsible for this phenotype will help to establish its relevance to DYT1 dystonia. In addition, the zebrafish offers an opportunity to examine the evolution of the tetrapod *tor1a* and *tor1b* genes, and could potentially yield insights into novel functions of TorsinA in later stages of neural circuit development.

BIBLIOGRAPHY

Airhart, M.J., Lee, D.H., Wilson, T.D., Miller, B.E., Miller, M.N., and Skalko, R.G. (2007). Movement disorders and neurochemical changes in zebrafish larvae after bath exposure to fluoxetine (PROZAC). Neurotoxicol Teratol *29*, 652–664.

Amsterdam, A., Burgess, S., Golling, G., Chen, W., Sun, Z., Townsend, K., Farrington, S., Haldi, M., and Hopkins, N. (1999). A large-scale insertional mutagenesis screen in zebrafish. Genes Dev. *13*, 2713–2724.

Anichtchik, O., Diekmann, H., Fleming, A., Roach, A., Goldsmith, P., and Rubinsztein, D.C. (2008). Loss of PINK1 function affects development and results in neurodegeneration in zebrafish. J Neurosci *28*, 8199–8207.

Anichtchik, O.V., Kaslin, J., Peitsaro, N., Scheinin, M., and Panula, P. (2004). Neurochemical and behavioural changes in zebrafish Danio rerio after systemic administration of 6-hydroxydopamine and 1-methyl-4-phenyl-1,2,3,6-tetrahydropyridine. J Neurochem *88*, 443–453.

Augood, S.J., Martin, D.M., Ozelius, L.J., Breakefield, X.O., Penney, J.B., and Standaert, D.G. (1999). Distribution of the mRNAs encoding torsinA and torsinB in the normal adult human brain. Ann Neurol *46*, 761–769.

Augood, S.J., Penney, J.B., Friberg, I.K., Breakefield, X.O., Young, A.B., Ozelius, L.J., and Standaert, D.G. (1998). Expression of the early-onset torsion dystonia gene (DYT1) in human brain. Ann Neurol *43*, 669–673.

Babst, M. (1998). The Vps4p AAA ATPase regulates membrane association of a Vps protein complex required for normal endosome function. Embo J. *17*, 2982–2993.

Bae, Y.-K., Kani, S., Shimizu, T., Tanabe, K., Nojima, H., Kimura, Y., Higashijima, S.-I., and Hibi, M. (2009). Anatomy of zebrafish cerebellum and screen for mutations affecting its development. Dev Biol *330*, 406–426.

Bai, Q., and Burton, E.A. (2009). Cis-acting elements responsible for dopaminergic neuron-specific expression of zebrafish slc6a3 (dopamine transporter) in vivo are located remote from the transcriptional start site. Neuroscience *164*, 1138–1151.

Bai, Q., Garver, J.A., Hukriede, N.A., and Burton, E.A. (2007). Generation of a transgenic

zebrafish model of Tauopathy using a novel promoter element derived from the zebrafish eno2 gene. Nucleic Acids Res. *35*, 6501–6516.

Bai, Q., Mullett, S.J., Garver, J.A., Hinkle, D.A., and Burton, E.A. (2006). Zebrafish DJ-1 is evolutionarily conserved and expressed in dopaminergic neurons. Brain Res *1113*, 33–44.

Bai, Q., Wei, X., and Burton, E.A. (2009). Expression of a 12-kb promoter element derived from the zebrafish enolase-2 gene in the zebrafish visual system. Neurosci Lett *449*, 252–257.

Balcioglu, A., Kim, M.-O., Sharma, N., Cha, J.-H., Breakefield, X.O., and Standaert, D.G. (2007). Dopamine release is impaired in a mouse model of DYT1 dystonia. J Neurochem *102*, 783–788.

Basham, S.E., and Rose, L.S. (1999). Mutations in ooc-5 and ooc-3 disrupt oocyte formation and the reestablishment of asymmetric PAR protein localization in two-cell Caenorhabditis elegans embryos. Dev Biol *215*, 253–263.

Becker, C.G., and Becker, T. (2008). Adult zebrafish as a model for successful central nervous system regeneration. Restor. Neurol. Neurosci. *26*, 71–80.

Berardelli, A., Rothwell, J.C., Hallett, M., Thompson, P.D., Manfredi, M., and Marsden, C.D. (1998). The pathophysiology of primary dystonia. Brain *121 (Pt 7)*, 1195–1212.

Best, J.D., Berghmans, S., Hunt, J.J.F.G., Clarke, S.C., Fleming, A., Goldsmith, P., and Roach, A.G. (2008). Non-associative learning in larval zebrafish. Neuropsychopharmacology *33*, 1206–1215.

Boehmler, W., Carr, T., Thisse, C., Thisse, B., Canfield, V.A., and Levenson, R. (2007). D4 Dopamine receptor genes of zebrafish and effects of the antipsychotic clozapine on larval swimming behaviour. Genes Brain Behav. *6*, 155–166.

Boehmler, W., Obrecht-Pflumio, S., Canfield, V., Thisse, C., Thisse, B., and Levenson, R. (2004). Evolution and expression of D2 and D3 dopamine receptor genes in zebrafish. Dev. Dyn. *230*, 481–493.

Bragg, D.C., Camp, S.M., Kaufman, C.A., Wilbur, J.D., Boston, H., Schuback, D.E., Hanson, P.I., Sena-Esteves, M., and Breakefield, X.O. (2004). Perinuclear biogenesis of mutant torsin-A inclusions in cultured cells infected with tetracycline-regulated herpes simplex virus type 1 amplicon vectors. Neuroscience *125*, 651–661.

Breakefield, X.O., Blood, A.J., Li, Y., Hallett, M., Hanson, P.I., and Standaert, D.G. (2008). The pathophysiological basis of dystonias. Nat Rev Neurosci *9*, 222–234.

Breakefield, X.O., Kamm, C., and Hanson, P.I. (2001). TorsinA: movement at many levels. Neuron *31*, 9–12.

Bretaud, S., Lee, S., and Guo, S. (2004). Sensitivity of zebrafish to environmental toxins implicated in Parkinson's disease. Neurotoxicol Teratol *26*, 857–864.

Brockerhoff, S.E. (2006). Measuring the optokinetic response of zebrafish larvae. Nat Protoc *1*, 2448–2451.

Brockerhoff, S.E., Hurley, J.B., Janssen-Bienhold, U., Neuhauss, S.C., Driever, W., and Dowling, J.E. (1995). A behavioral screen for isolating zebrafish mutants with visual system defects. Proc Natl Acad Sci USA *92*, 10545–10549.

Brustein, E., Chong, M., Holmqvist, B., and Drapeau, P. (2003). Serotonin patterns locomotor network activity in the developing zebrafish by modulating quiescent periods. J Neurobiol *57*, 303–322.

Burgess, H.A., and Granato, M. (2007). Sensorimotor gating in larval zebrafish. J Neurosci *27*, 4984–4994.

Buss, R.R., and Drapeau, P. (2001). Synaptic drive to motoneurons during fictive swimming in the developing zebrafish. J. Neurophysiol. *86*, 197–210.

Cahill, G.M. (2007). Automated video image analysis of larval zebrafish locomotor rhythms. Methods Mol. Biol. *362*, 83–94.

Calakos, N., Patel, V.D., Gottron, M., Wang, G., Tran-Viet, K.-N., Brewington, D., Beyer, J.L., Steffens, D.C., Krishnan, R.R., and Züchner, S. (2010). Functional evidence implicating a novel TOR1A mutation in idiopathic, late-onset focal dystonia. J. Med. Genet. *47*, 646–650.

Callan, A.C., Bunning, S., Jones, O.T., High, S., and Swanton, E. (2007). Biosynthesis of the dystonia-associated AAA+ ATPase torsinA at the endoplasmic reticulum. Biochem J *401*, 607–612.

Camargos, S., Scholz, S., Simón-Sánchez, J., Paisán-Ruiz, C., Lewis, P., Hernandez, D., Ding, J., Gibbs, J.R., Cookson, M.R., Bras, J., et al. (2008). DYT16, a novel young-onset dystonia-parkinsonism disorder: identification of a segregating mutation in the stress-response protein PRKRA. Lancet Neurol *7*, 207–215.

Candy, J., and Collet, C. (2005). Two tyrosine hydroxylase genes in teleosts. Biochim. Biophys. Acta *1727*, 35–44.

Cannon, S.C. (2004). Paying the price at the pump: dystonia from mutations in a Na+/K+ -ATPase. Neuron *43*, 153–154.

Cario, C.L., Farrell, T.C., Milanese, C., and Burton, E.A. (2011). Automated measurement of zebrafish larval movement. J. Physiol. (Lond.) *589*, 3703–3708.

Caroll, D., and Zhang, B. (2011). Primer and interviews: advances in targeted gene modification. Interview by Julie C. Kiefer. Dev. Dyn. *240*, 2688–2696.

Cerda, G.A., Thomas, J.E., Allende, M.L., Karlstrom, R.O., and Palma, V. (2006). Electroporation of DNA, RNA, and morpholinos into zebrafish embryos. Methods *39*, 207–

211.

Chen, Y.-C., Priyadarshini, M., and Panula, P. (2009). Complementary developmental expression of the two tyrosine hydroxylase transcripts in zebrafish. Histochem. Cell Biol. *132*, 375–381.

Chiken, S., Shashidharan, P., and Nambu, A. (2008). Cortically evoked long-lasting inhibition of pallidal neurons in a transgenic mouse model of dystonia. J Neurosci *28*, 13967–13977.

Choi, H.K., Won, L.A., Kontur, P.J., Hammond, D.N., Fox, A.P., Wainer, B.H., Hoffmann, P.C., and Heller, A. (1991). Immortalization of embryonic mesencephalic dopaminergic neurons by somatic cell fusion. Brain Res *552*, 67–76.

Creton, R. (2009). Automated analysis of behavior in zebrafish larvae. Behav Brain Res *203*, 127–136.

Dang, M.T., Yokoi, F., McNaught, K.S.P., Jengelley, T.-A., Jackson, T., Li, J., and Li, Y. (2005). Generation and characterization of Dyt1 DeltaGAG knock-in mouse as a model for early-onset dystonia. Exp Neurol *196*, 452–463.

Dang, M.T., Yokoi, F., Pence, M.A., and Li, Y. (2006). Motor deficits and hyperactivity in Dyt1 knockdown mice. Neurosci Res *56*, 470–474.

Deng, H.X., Hentati, A., Tainer, J.A., Iqbal, Z., Cayabyab, A., Hung, W.Y., Getzoff, E.D., Hu, P., Herzfeldt, B., and Roos, R.P. (1993). Amyotrophic lateral sclerosis and structural defects in Cu,Zn superoxide dismutase. Science *261*, 1047–1051.

Doyon, Y., McCammon, J.M., Miller, J.C., Faraji, F., Ngo, C., Katibah, G.E., Amora, R., Hocking, T.D., Zhang, L., Rebar, E.J., et al. (2008). Heritable targeted gene disruption in zebrafish using designed zinc-finger nucleases. Nat. Biotechnol. *26*, 702–708.

Driever, W., Solnica-Krezel, L., Schier, A.F., Neuhauss, S.C., Malicki, J., Stemple, D.L., Stainier, D.Y., Zwartkruis, F., Abdelilah, S., Rangini, Z., et al. (1996). A genetic screen for mutations affecting embryogenesis in zebrafish. Development *123*, 37–46.

Drummond, A.J., and Rambaut, A. (2007). BEAST: Bayesian evolutionary analysis by sampling trees. BMC Evol. Biol. *7*, 214.

Eidelberg, D., Moeller, J.R., Antonini, A., Kazumata, K., Nakamura, T., Dhawan, V., Spetsieris, P., DeLeon, D., Bressman, S.B., and Fahn, S. (1998). Functional brain networks in DYT1 dystonia. Ann Neurol *44*, 303–312.

Epidemiological Study of Dystonia in Europe (ESDE) Collaborative Group (2000). A prevalence study of primary dystonia in eight European countries. J. Neurol. *247*, 787–792.

Farrell, T.C., Cario, C.L., Milanese, C., Vogt, A., Jeong, J.-H., and Burton, E.A. (2011). Evaluation of spontaneous propulsive movement as a screening tool to detect rescue of Parkinsonism phenotypes in zebrafish models. Neurobiol Dis *44*, 9–18.

Flinn, L., Mortiboys, H., Volkmann, K., Köster, R.W., Ingham, P.W., and Bandmann, O. (2009). Complex I deficiency and dopaminergic neuronal cell loss in parkin-deficient zebrafish (Danio rerio). Brain *132*, 1613–1623.

Fuchs, T., and Ozelius, L.J. (2011). Genetics of dystonia. Semin Neurol *31*, 441–448.

Fuchs, T., Gavarini, S., Saunders-Pullman, R., Raymond, D., Ehrlich, M.E., Bressman, S.B., and Ozelius, L.J. (2009). Mutations in the THAP1 gene are responsible for DYT6 primary torsion dystonia. Nat Genet *41*, 286–288.

Gabriel, J.P., Mahmood, R., Walter, A.M., Kyriakatos, A., Hauptmann, G., Calabrese, R.L., and Manira, El, A. (2008). Locomotor pattern in the adult zebrafish spinal cord in vitro. *99*, 37–48.

Gavarini, S., Cayrol, C., Fuchs, T., Lyons, N., Ehrlich, M.E., Girard, J.-P., and Ozelius, L.J. (2010). Direct interaction between causative genes of DYT1 and DYT6 primary dystonia. Ann Neurol *68*, 549–553.

Geyer, H.L., and Bressman, S.B. (2006). The diagnosis of dystonia. Lancet Neurol *5*, 780–790.

Giacomini, N.J., Rose, B., Kobayashi, K., and Guo, S. (2006). Antipsychotics produce locomotor impairment in larval zebrafish. Neurotoxicol Teratol *28*, 245–250.

Giles, L.M., Li, L., and Chin, L.-S. (2009). Printor, a novel torsinA-interacting protein implicated in dystonia pathogenesis. J Biol Chem *284*, 21765–21775.

Goedert, M., Spillantini, M.G., Jakes, R., Rutherford, D., and Crowther, R.A. (1989). Multiple isoforms of human microtubule-associated protein tau: sequences and localization in neurofibrillary tangles of Alzheimer's disease. Neuron *3*, 519–526.

Goodchild, R.E., and Dauer, W.T. (2004). Mislocalization to the nuclear envelope: an effect of the dystonia-causing torsinA mutation. Proc Natl Acad Sci USA *101*, 847–852.

Goodchild, R.E., and Dauer, W.T. (2005). The AAA+ protein torsinA interacts with a conserved domain present in LAP1 and a novel ER protein. J Cell Biol *168*, 855–862.

Goodchild, R.E., Kim, C.E., and Dauer, W.T. (2005). Loss of the dystonia-associated protein torsinA selectively disrupts the neuronal nuclear envelope. Neuron *48*, 923–932.

Grabher, C., and Wittbrodt, J. (2008). Recent advances in meganuclease-and transposon-mediated transgenesis of medaka and zebrafish. Methods Mol. Biol. *461*, 521–539.

Granata, A., Watson, R., Collinson, L.M., Schiavo, G., and Warner, T.T. (2008). The dystonia-associated protein torsinA modulates synaptic vesicle recycling. J Biol Chem *283*, 7568–7579.

Grundmann, K., Glöckle, N., Martella, G., Sciamanna, G., Hauser, T.-K., Yu, L., Castaneda, S., Pichler, B., Fehrenbacher, B., Schaller, M., et al. (2012). Generation of a novel rodent

model for DYT1 dystonia. Neurobiol Dis *47*, 61–74.

Grundmann, K., Reischmann, B., Vanhoutte, G., Hübener, J., Teismann, P., Hauser, T.-K., Bonin, M., Wilbertz, J., Horn, S., Nguyen, H.P., et al. (2007). Overexpression of human wildtype torsinA and human DeltaGAG torsinA in a transgenic mouse model causes phenotypic abnormalities. Neurobiol Dis *27*, 190–206.

Guo, S., Wilson, S.W., Cooke, S., Chitnis, A.B., Driever, W., and Rosenthal, A. (1999). Mutations in the zebrafish unmask shared regulatory pathways controlling the development of catecholaminergic neurons. Dev Biol *208*, 473–487.

Hanson, P.I., and Whiteheart, S.W. (2005). AAA+ proteins: have engine, will work. Nat Rev Mol Cell Biol *6*, 519–529.

HDCRG (1993). A novel gene containing a trinucleotide repeat that is expanded and unstable on Huntington"s disease chromosomes. The Huntington"s Disease Collaborative Research Group. Cell *72*, 971–983.

Hensch, T.K. (2004). Critical period regulation. Annu. Rev. Neurosci. *27*, 549–579.

Hewett, J., Gonzalez-Agosti, C., Slater, D., Ziefer, P., Li, S., Bergeron, D., Jacoby, D.J., Ozelius, L.J., Ramesh, V., and Breakefield, X.O. (2000). Mutant torsinA, responsible for early-onset torsion dystonia, forms membrane inclusions in cultured neural cells. Hum Mol Genet *9*, 1403–1413.

Hewett, J., Johanson, P., Sharma, N., Standaert, D., and Balcioglu, A. (2010). Function of dopamine transporter is compromised in DYT1 transgenic animal model in vivo. J Neurochem *113*, 228–235.

Hewett, J.W., Tannous, B., Niland, B.P., Nery, F.C., Zeng, J., Li, Y., and Breakefield, X.O. (2007). Mutant torsinA interferes with protein processing through the secretory pathway in DYT1 dystonia cells. Proc Natl Acad Sci USA *104*, 7271–7276.

Hewett, J.W., Zeng, J., Niland, B.P., Bragg, D.C., and Breakefield, X.O. (2006). Dystonia-causing mutant torsinA inhibits cell adhesion and neurite extension through interference with cytoskeletal dynamics. Neurobiol Dis *22*, 98–111.

Higashijima, S., Okamoto, H., Ueno, N., Hotta, Y., and Eguchi, G. (1997). High-frequency generation of transgenic zebrafish which reliably express GFP in whole muscles or the whole body by using promoters of zebrafish origin. Dev Biol *192*, 289–299.

Holzschuh, J., Ryu, S., Aberger, F., and Driever, W. (2001). Dopamine transporter expression distinguishes dopaminergic neurons from other catecholaminergic neurons in the developing zebrafish embryo. Mech. Dev. *101*, 237–243.

Huang, P., Xiao, A., Zhou, M., Zhu, Z., Lin, S., and Zhang, B. (2011). Heritable gene targeting in zebrafish using customized TALENs. Nat. Biotechnol. *29*, 699–700.

Hutton, M., Lendon, C.L., Rizzu, P., Baker, M., Froelich, S., Houlden, H., Pickering-Brown, S., Chakraverty, S., Isaacs, A., Grover, A., et al. (1998). Association of missense and 5'-splice-site mutations in tau with the inherited dementia FTDP-17. Nature *393*, 702–705.

Imbert, G., Saudou, F., Yvert, G., Devys, D., Trottier, Y., Garnier, J.M., Weber, C., Mandel, J.L., Cancel, G., Abbas, N., et al. (1996). Cloning of the gene for spinocerebellar ataxia 2 reveals a locus with high sensitivity to expanded CAG/glutamine repeats. Nat Genet *14*, 285–291.

Jacquier, A., and Dujon, B. (1985). An intron-encoded protein is active in a gene conversion process that spreads an intron into a mitochondrial gene. Cell *41*, 383–394.

Jensen, P.J., Gitlin, J.D., and Carayannopoulos, M.O. (2006). GLUT1 deficiency links nutrient availability and apoptosis during embryonic development. J Biol Chem *281*, 13382–13387.

Kafri, R., Springer, M., and Pilpel, Y. (2009). Genetic redundancy: new tricks for old genes. Cell *136*, 389–392.

Kaiser, F.J., Osmanoric, A., Rakovic, A., Erogullari, A., Uflacker, N., Braunholz, D., Lohnau, T., Orolicki, S., Albrecht, M., Gillessen-Kaesbach, G., et al. (2010). The dystonia gene DYT1 is repressed by the transcription factor THAP1 (DYT6). Ann Neurol *68*, 554–559.

Kamm, C., Boston, H., Hewett, J., Wilbur, J., Corey, D.P., Hanson, P.I., Ramesh, V., and Breakefield, X.O. (2004). The early onset dystonia protein torsinA interacts with kinesin light chain 1. J Biol Chem *279*, 19882–19892.

Kapsimali, M., Vidal, B., Gonzalez, A., Dufour, S., and Vernier, P. (2000). Distribution of the mRNA encoding the four dopamine D(1) receptor subtypes in the brain of the european eel (Anguilla anguilla): comparative approach to the function of D(1) receptors in vertebrates. J. Comp. Neurol. *419*, 320–343.

Kawaguchi, Y., Okamoto, T., Taniwaki, M., Aizawa, M., Inoue, M., Katayama, S., Kawakami, H., Nakamura, S., Nishimura, M., and Akiguchi, I. (1994). CAG expansions in a novel gene for Machado-Joseph disease at chromosome 14q32.1. Nat Genet *8*, 221–228.

Kawakami, K. (2004). Transgenesis and gene trap methods in zebrafish by using the Tol2 transposable element. Methods Cell Biol. *77*, 201–222.

Kawakami, K., Shima, A., and Kawakami, N. (2000). Identification of a functional transposase of the Tol2 element, an Ac-like element from the Japanese medaka fish, and its transposition in the zebrafish germ lineage. Proc Natl Acad Sci USA *97*, 11403–11408.

Kim, C.E., Perez, A., Perkins, G., Ellisman, M.H., and Dauer, W.T. (2010). A molecular mechanism underlying the neural-specific defect in torsinA mutant mice. Proc Natl Acad Sci USA *107*, 9861–9866.

Kim, C.H., Ueshima, E., Muraoka, O., Tanaka, H., Yeo, S.Y., Huh, T.L., and Miki, N. (1996). Zebrafish elav/HuC homologue as a very early neuronal marker. Neurosci Lett *216*, 109–

112.

Kimmel, C.B. (1993). Patterning the brain of the zebrafish embryo. Annu. Rev. Neurosci. *16*, 707–732.

Kinugawa, K., Vidailhet, M., Clot, F., Apartis, E., Grabli, D., and Roze, E. (2009). Myoclonus-dystonia: an update. Mov Disord *24*, 479–489.

Kizil, C., and Brand, M. (2011). Cerebroventricular microinjection (CVMI) into adult zebrafish brain is an efficient misexpression method for forebrain ventricular cells. PloS ONE *6*, e27395.

Koga, A., Suzuki, M., Inagaki, H., Bessho, Y., and Hori, H. (1996). Transposable element in fish. Nature *383*, 30.

Kramer, P.L., Heiman, G.A., Gasser, T., Ozelius, L.J., de Leon, D., Brin, M.F., Burke, R.E., Hewett, J., Hunt, A.L., and Moskowitz, C. (1994). The DYT1 gene on 9q34 is responsible for most cases of early limb-onset idiopathic torsion dystonia in non-Jews. American Journal of Human Genetics *55*, 468–475.

Lam, C.S., Korzh, V., and Strahle, U. (2005). Zebrafish embryos are susceptible to the dopaminergic neurotoxin MPTP. Eur. J. Neurosci. *21*, 1758–1762.

Landles, C., and Bates, G.P. (2004). Huntingtin and the molecular pathogenesis of Huntington's disease. Fourth in molecular medicine review series. EMBO Rep. *5*, 958–963.

Larkin, M.A., Blackshields, G., Brown, N.P., Chenna, R., McGettigan, P.A., McWilliam, H., Valentin, F., Wallace, I.M., Wilm, A., Lopez, R., et al. (2007). Clustal W and Clustal X version 2.0. Bioinformatics *23*, 2947–2948.

Lee, H.-Y., Xu, Y., Huang, Y., Ahn, A.H., Auburger, G.W.J., Pandolfo, M., Kwiecinski, H., Grimes, D.A., Lang, A.E., Nielsen, J.E., et al. (2004). The gene for paroxysmal non-kinesigenic dyskinesia encodes an enzyme in a stress response pathway. Hum Mol Genet *13*, 3161–3170.

Lee, V.M., Goedert, M., and Trojanowski, J.Q. (2001). Neurodegenerative tauopathies. Annu. Rev. Neurosci. *24*, 1121–1159.

Lemmens, R., Van Hoecke, A., Hersmus, N., Geelen, V., D'Hollander, I., Thijs, V., Van Den Bosch, L., Carmeliet, P., and Robberecht, W. (2007). Overexpression of mutant superoxide dismutase 1 causes a motor axonopathy in the zebrafish. Hum Mol Genet *16*, 2359–2365.

Leung, J.C., Klein, C., Friedman, J., Vieregge, P., Jacobs, H., Doheny, D., Kamm, C., DeLeon, D., Pramstaller, P.P., Penney, J.B., et al. (2001). Novel mutation in the TOR1A (DYT1) gene in atypical early onset dystonia and polymorphisms in dystonia and early onset parkinsonism. Neurogenetics *3*, 133–143.

Levy, L.M., and Hallett, M. (2002). Impaired brain GABA in focal dystonia. Ann Neurol *51*, 93–

101.

Liu, D.W., and Westerfield, M. (1988). Function of identified motoneurones and co-ordination of primary and secondary motor systems during zebra fish swimming. J. Physiol. (Lond.) *403*, 73–89.

Long, Q., Meng, A., Wang, H., Jessen, J.R., Farrell, M.J., and Lin, S. (1997). GATA-1 expression pattern can be recapitulated in living transgenic zebrafish using GFP reporter gene. Development *124*, 4105–4111.

Ma, P.M. (2003). Catecholaminergic systems in the zebrafish. IV. Organization and projection pattern of dopaminergic neurons in the diencephalon. J. Comp. Neurol. *460*, 13–37.

MacPhail, R.C., Brooks, J., Hunter, D.L., Padnos, B., Irons, T.D., and Padilla, S. (2009). Locomotion in larval zebrafish: Influence of time of day, lighting and ethanol. Neurotoxicology *30*, 52–58.

Makino, S., Kaji, R., Ando, S., Tomizawa, M., Yasuno, K., Goto, S., Matsumoto, S., Tabuena, M.D., Maranon, E., Dantes, M., et al. (2007). Reduced neuron-specific expression of the TAF1 gene is associated with X-linked dystonia-parkinsonism. American Journal of Human Genetics *80*, 393–406.

Malicki, J., Neuhauss, S.C., Schier, A.F., Solnica-Krezel, L., Stemple, D.L., Stainier, D.Y., Abdelilah, S., Zwartkruis, F., Rangini, Z., and Driever, W. (1996). Mutations affecting development of the zebrafish retina. Development *123*, 263–273.

McKinley, E.T., Baranowski, T.C., Blavo, D.O., Cato, C., Doan, T.N., and Rubinstein, A.L. (2005). Neuroprotection of MPTP-induced toxicity in zebrafish dopaminergic neurons. Brain Res Mol Brain Res *141*, 128–137.

McNaught, K.S.P., Kapustin, A., Jackson, T., Jengelley, T.-A., Jnobaptiste, R., Shashidharan, P., Perl, D.P., Pasik, P., and Olanow, C.W. (2004). Brainstem pathology in DYT1 primary torsion dystonia. Ann Neurol *56*, 540–547.

Meng, A., Tang, H., Ong, B.A., Farrell, M.J., and Lin, S. (1997). Promoter analysis in living zebrafish embryos identifies a cis-acting motif required for neuronal expression of GATA-2. Proc Natl Acad Sci USA *94*, 6267–6272.

Milanese, C., Sager, J.J., Bai, Q., Farrell, T.C., Cannon, J.R., Greenamyre, J.T., and Burton, E.A. (2012). Hypokinesia and Reduced Dopamine Levels in Zebrafish Lacking β- and γ1-Synucleins. J Biol Chem *287*, 2971–2983.

Miller, V.M., Nelson, R.F., Gouvion, C.M., Williams, A., Rodriguez-Lebron, E., Harper, S.Q., Davidson, B.L., Rebagliati, M.R., and Paulson, H.L. (2005). CHIP suppresses polyglutamine aggregation and toxicity in vitro and in vivo. J Neurosci *25*, 9152–9161.

Misbahuddin, A., and Warner, T.T. (2001). Dystonia: an update on genetics and treatment. Curr Opin Neurol *14*, 471–475.

Molina, G., Vogt, A., Bakan, A., Dai, W., Queiroz de Oliveira, P., Znosko, W., Smithgall, T.E., Bahar, I., Lazo, J.S., Day, B.W., et al. (2009). Zebrafish chemical screening reveals an inhibitor of Dusp6 that expands cardiac cell lineages. Nat. Chem. Biol. *5*, 680–687.

Mueller, T., Vernier, P., and Wullimann, M.F. (2004). The adult central nervous cholinergic system of a neurogenetic model animal, the zebrafish Danio rerio. Brain Res *1011*, 156–169.

Muraro, N.I., and Moffat, K.G. (2006). Down-regulation of torp4a, encoding the Drosophila homologue of torsinA, results in increased neuronal degeneration. J Neurobiol *66*, 1338–1353.

Naismith, T.V., Dalal, S., and Hanson, P.I. (2009). Interaction of torsinA with its major binding partners is impaired by the dystonia-associated DeltaGAG deletion. J Biol Chem *284*, 27866–27874.

Naismith, T.V., Heuser, J.E., Breakefield, X.O., and Hanson, P.I. (2004). TorsinA in the nuclear envelope. Proc Natl Acad Sci USA *101*, 7612–7617.

Nasevicius, A., and Ekker, S.C. (2000). Effective targeted gene "knockdown" in zebrafish. Nat Genet *26*, 216–220.

Noriko Wakabayashi-Ito, O.M.D.H.M.X.O.B.J.F.G.J.M.O.N.I. (2011). dtorsin, the Drosophila Ortholog of the Early-Onset Dystonia TOR1A (DYT1), Plays a Novel Role in Dopamine Metabolism. PloS ONE *6*.

Nutt, J.G., Muenter, M.D., Aronson, A., Kurland, L.T., and Melton, L.J. (1988). Epidemiology of focal and generalized dystonia in Rochester, Minnesota. Mov Disord *3*, 188–194.

Nüsslein-Volhard, C., and Dahm, R. (2002). Zebrafish (Oxford University Press, USA).

Orr, H.T., Chung, M.Y., Banfi, S., Kwiatkowski, T.J., Servadio, A., Beaudet, A.L., McCall, A.E., Duvick, L.A., Ranum, L.P., and Zoghbi, H.Y. (1993). Expansion of an unstable trinucleotide CAG repeat in spinocerebellar ataxia type 1. Nat Genet *4*, 221–226.

Ozelius, L.J., and Bressman, S.B. (2011). Genetic and clinical features of primary torsion dystonia. Neurobiol Dis *42*, 127–135.

Ozelius, L.J., Hewett, J.W., Page, C.E., Bressman, S.B., Kramer, P.L., Shalish, C., de Leon, D., Brin, M.F., Raymond, D., Corey, D.P., et al. (1997). The early-onset torsion dystonia gene (DYT1) encodes an ATP-binding protein. Nat Genet *17*, 40–48.

Page, M.E., Bao, L., Andre, P., Pelta-Heller, J., Sluzas, E., Gonzalez-Alegre, P., Bogush, A., Khan, L.E., Iacovitti, L., Rice, M.E., et al. (2010). Cell-autonomous alteration of dopaminergic transmission by wild type and mutant (DeltaE) TorsinA in transgenic mice. Neurobiol Dis *39*, 318–326.

Paquet, D., Bhat, R., Sydow, A., Mandelkow, E.-M., Berg, S., Hellberg, S., Fälting, J., Distel,

M., Köster, R.W., Schmid, B., et al. (2009). A zebrafish model of tauopathy allows in vivo imaging of neuronal cell death and drug evaluation. J. Clin. Invest. *119*, 1382–1395.

Park, H.C., Kim, C.H., Bae, Y.K., Yeo, S.Y., Kim, S.H., Hong, S.K., Shin, J., Yoo, K.W., Hibi, M., Hirano, T., et al. (2000). Analysis of upstream elements in the HuC promoter leads to the establishment of transgenic zebrafish with fluorescent neurons. Dev Biol *227*, 279–293.

Rainier, S., Thomas, D., Tokarz, D., Ming, L., Bui, M., Plein, E., Zhao, X., Lemons, R., Albin, R., Delaney, C., et al. (2004). Myofibrillogenesis regulator 1 gene mutations cause paroxysmal dystonic choreoathetosis. Arch. Neurol. *61*, 1025–1029.

Reiner, A., and Northcutt, R.G. (1992). An immunohistochemical study of the telencephalon of the senegal bichir (Polypterus senegalus). J. Comp. Neurol. *319*, 359–386.

Rink, E., and Wullimann, M.F. (2001). The teleostean (zebrafish) dopaminergic system ascending to the subpallium (striatum) is located in the basal diencephalon (posterior tuberculum). Brain Res *889*, 316–330.

Rink, E., and Wullimann, M.F. (2002). Development of the catecholaminergic system in the early zebrafish brain: an immunohistochemical study. Brain Res Dev Brain Res *137*, 89–100.

Rink, E., and Wullimann, M.F. (2004). Connections of the ventral telencephalon (subpallium) in the zebrafish (Danio rerio). Brain Res *1011*, 206–220.

Roeser, T., and Baier, H. (2003). Visuomotor behaviors in larval zebrafish after GFP-guided laser ablation of the optic tectum. J Neurosci *23*, 3726–3734.

Rosen, D.R., Siddique, T., Patterson, D., Figlewicz, D.A., Sapp, P., Hentati, A., Donaldson, D., Goto, J., O'Regan, J.P., and Deng, H.X. (1993). Mutations in Cu/Zn superoxide dismutase gene are associated with familial amyotrophic lateral sclerosis. Nature *362*, 59–62.

Ryu, S., Holzschuh, J., Mahler, J., and Driever, W. (2006). Genetic analysis of dopaminergic system development in zebrafish. J. Neural Transm. Suppl. 61–66.

Sager, J.J., Bai, Q., and Burton, E.A. (2010). Transgenic zebrafish models of neurodegenerative diseases. Brain Struct Funct *214*, 285–302.

Saint-Amant, L., and Drapeau, P. (1998). Time course of the development of motor behaviors in the zebrafish embryo. J Neurobiol *37*, 622–632.

Sallinen, V., Sundvik, M., Reenilä, I., Peitsaro, N., Khrustalyov, D., Anichtchik, O., Toleikyte, G., Kaslin, J., and Panula, P. (2009a). Hyperserotonergic phenotype after monoamine oxidase inhibition in larval zebrafish. J Neurochem *109*, 403–415.

Sallinen, V., Torkko, V., Sundvik, M., Reenilä, I., Khrustalyov, D., Kaslin, J., and Panula, P. (2009b). MPTP and MPP+ target specific aminergic cell populations in larval zebrafish. J Neurochem *108*, 719–731.

Sander, J.D., Cade, L., Khayter, C., Reyon, D., Peterson, R.T., Joung, J.K., and Yeh, J.-R.J. (2011). Targeted gene disruption in somatic zebrafish cells using engineered TALENs. Nat. Biotechnol. *29*, 697–698.

Saper, C.B. (2005). An open letter to our readers on the use of antibodies. J. Comp. Neurol. *493*, 477–478.

Schiffer, N.W., Broadley, S.A., Hirschberger, T., Tavan, P., Kretzschmar, H.A., Giese, A., Haass, C., Hartl, F.U., and Schmid, B. (2007). Identification of anti-prion compounds as efficient inhibitors of polyglutamine protein aggregation in a zebrafish model. J Biol Chem *282*, 9195–9203.

Schug, J., Schuller, W.-P., Kappen, C., Salbaum, J.M., Bucan, M., and Stoeckert, C.J. (2005). Promoter features related to tissue specificity as measured by Shannon entropy. Genome Biol. *6*, R33.

Sharma, N., Baxter, M.G., Petravicz, J., Bragg, D.C., Schienda, A., Standaert, D.G., and Breakefield, X.O. (2005). Impaired motor learning in mice expressing torsinA with the DYT1 dystonia mutation. J Neurosci *25*, 5351–5355.

Sharma, S.C., Berthoud, V.M., and Breckwoldt, R. (1989). Distribution of substance P-like immunoreactivity in the goldfish brain. J. Comp. Neurol. *279*, 104–116.

Shashidharan, P., Kramer, B.C., Walker, R.H., Olanow, C.W., and Brin, M.F. (2000). Immunohistochemical localization and distribution of torsinA in normal human and rat brain. Brain Res *853*, 197–206.

Shashidharan, P., Sandu, D., Potla, U., Armata, I.A., Walker, R.H., McNaught, K.S., Weisz, D., Sreenath, T., Brin, M.F., and Olanow, C.W. (2005). Transgenic mouse model of early-onset DYT1 dystonia. Hum Mol Genet *14*, 125–133.

Solnica-Krezel, L., Schier, A.F., and Driever, W. (1994). Efficient recovery of ENU-induced mutations from the zebrafish germline. Genetics *136*, 1401–1420.

Soroldoni, D., Hogan, B.M., and Oates, A.C. (2009). Simple and efficient transgenesis with meganuclease constructs in zebrafish. Methods Mol. Biol. *546*, 117–130.

Stuart, G.W., McMurray, J.V., and Westerfield, M. (1988). Replication, integration and stable germ-line transmission of foreign sequences injected into early zebrafish embryos. Development *103*, 403–412.

Suls, A., Dedeken, P., Goffin, K., Van Esch, H., Dupont, P., Cassiman, D., Kempfle, J., Wuttke, T.V., Weber, Y., Lerche, H., et al. (2008). Paroxysmal exercise-induced dyskinesia and epilepsy is due to mutations in SLC2A1, encoding the glucose transporter GLUT1. Brain *131*, 1831–1844.

Sun, Y., Dong, Z., Khodabakhsh, H., Chatterjee, S., and Guo, S. (2012). Zebrafish chemical screening reveals the impairment of dopaminergic neuronal survival by cardiac glycosides.

PloS ONE *7*, e35645.

Thermes, V., Grabher, C., Ristoratore, F., Bourrat, F., Choulika, A., Wittbrodt, J., and Joly, J.-S. (2002). I-SceI meganuclease mediates highly efficient transgenesis in fish. Mech. Dev. *118*, 91–98.

Thirumalai, V., and Cline, H.T. (2008). Endogenous dopamine suppresses initiation of swimming in prefeeding zebrafish larvae. J. Neurophysiol. *100*, 1635–1648.

Tomasiewicz, H.G., Flaherty, D.B., Soria, J.P., and Wood, J.G. (2002). Transgenic zebrafish model of neurodegeneration. J Neurosci Res *70*, 734–745.

Torres, G.E., Sweeney, A.L., Beaulieu, J.-M., Shashidharan, P., and Caron, M.G. (2004). Effect of torsinA on membrane proteins reveals a loss of function and a dominant-negative phenotype of the dystonia-associated DeltaE-torsinA mutant. Proc Natl Acad Sci USA *101*, 15650–15655.

Turner, B.J., and Talbot, K. (2008). Transgenics, toxicity and therapeutics in rodent models of mutant SOD1-mediated familial ALS. Prog. Neurobiol. *85*, 94–134.

Wakabayashi-Ito, N., Doherty, O.M., Moriyama, H., Breakefield, X.O., Gusella, J.F., O'Donnell, J.M., and Ito, N. (2011). Dtorsin, the Drosophila ortholog of the early-onset dystonia TOR1A (DYT1), plays a novel role in dopamine metabolism. PloS ONE *6*, e26183.

Watts, R., and Koller, W. (2004). Movement Disorders: Neurologic Principles & Practice, Second Edition (McGraw-Hill Professional).

Weibezahn, J. (2003). Characterization of a Trap Mutant of the AAA+ Chaperone ClpB. Journal of Biological Chemistry *278*, 32608–32617.

Whiteheart, S.W., Rossnagel, K., Buhrow, S.A., Brunner, M., Jaenicke, R., and Rothman, J.E. (1994). N-ethylmaleimide-sensitive fusion protein: a trimeric ATPase whose hydrolysis of ATP is required for membrane fusion. J Cell Biol *126*, 945–954.

Williams, A., Sarkar, S., Cuddon, P., Ttofi, E.K., Saiki, S., Siddiqi, F.H., Jahreiss, L., Fleming, A., Pask, D., Goldsmith, P., et al. (2008). Novel targets for Huntington's disease in an mTOR-independent autophagy pathway. Nat. Chem. Biol. *4*, 295–305.

Wullimann, M.F., Rupp, B., and Reichert, H. (1996). Neuroanatomy of the zebrafish brain (Birkhäuser).

Yokoi, F., Dang, M.T., Miller, C.A., Marshall, A.G., Campbell, S.L., Sweatt, J.D., and Li, Y. (2009). Increased c-fos expression in the central nucleus of the amygdala and enhancement of cued fear memory in Dyt1 DeltaGAG knock-in mice. Neurosci Res *65*, 228–235.

Yokoi, F., Dang, M.T., Mitsui, S., Li, J., and Li, Y. (2007). Motor Deficits and Hyperactivity in Cerebral Cortex-specific Dyt1 Conditional Knockout Mice. J Biochem *143*, 39–47.

Zeddies, D.G., and Fay, R.R. (2005). Development of the acoustically evoked behavioral response in zebrafish to pure tones. J. Exp. Biol. *208*, 1363–1372.

Zhao, Y., DeCuypere, M., and LeDoux, M.S. (2008). Abnormal motor function and dopamine neurotransmission in DYT1 DeltaGAG transgenic mice. Exp Neurol *210*, 719–730.

Zheng, P.-P., Romme, E., van der Spek, P.J., Dirven, C.M.F., Willemsen, R., and Kros, J.M. (2010). Glut1/SLC2A1 is crucial for the development of the blood-brain barrier in vivo. Ann Neurol *68*, 835–844.

Zheng, P.-P., van der Spek, P.J., Dirven, C.M.F., Willemsen, R., and Kros, J.M. (2012). Sinus venosus defect (SVD) identified in zebrafish Glut1 morphants by video imaging. Int. J. Cardiol. *154*, e60–e61.

Zirn, B., Grundmann, K., Huppke, P., Puthenparampil, J., Wolburg, H., Riess, O., and Müller, U. (2008). Novel TOR1A mutation p.Arg288Gln in early-onset dystonia (DYT1). J. Neurol. Neurosurg. Psychiatr. *79*, 1327–1330.

Zoghbi, H.Y., and Orr, H.T. (2009). Pathogenic mechanisms of a polyglutamine-mediated neurodegenerative disease, spinocerebellar ataxia type 1. J Biol Chem *284*, 7425–7429.

Zon, L.I., and Peterson, R.T. (2005). In vivo drug discovery in the zebrafish. Nat Rev Drug Discov *4*, 35–44.

Zottoli, S.J. (1977). Correlation of the startle reflex and Mauthner cell auditory responses in unrestrained goldfish. J. Exp. Biol. *66*, 243–254.